



UNIVERSITY OF  
**TEXAS**  
ARLINGTON

TxDOT Implementation Report 5-6957-01-1

## **Slope Repair and Maintenance Management System Final Report**

Mohsen Shahandashti, Ph.D., P.E.

Sahadat Hossain, Ph.D., P.E.

Anil Baral

Isha Adhikari

Pouria Pourmand

Bahram Abediniangerabi, Ph.D.

---

Report Publication Date: Submitted: August 2020

Published: March 2022

Project: 5-6957-01

Project Title: Slope Repair and Maintenance Management System

Technical Report Documentation Page

1. Report No. FHWA/TX-20/5-6957-01-1		2. Government Accession No.		3. Recipient's Catalog No.	
4. Title and Subtitle Slope Repair and Maintenance Management System Final Report				5. Report Date August 2020 Published: March 2022	
				6. Performing Organization Code	
7. Author(s) Mohsen Shahandashti ( <a href="https://orcid.org/0000-0002-2373-7596">https://orcid.org/0000-0002-2373-7596</a> ), Sahadat Hossain, Anil Baral, Isha Adhikari, Pouria Pourmand, Bahram Abediniangerabi				8. Performing Organization Report No. 5-6957-01-1	
9. Performing Organization Name and Address The University of Texas at Arlington Department of Civil Engineering P.O. Box 19308 Arlington, TX 76019				10. Work Unit No. (TRAIS)	
				11. Contract or Grant No. 5-6957-01	
12. Sponsoring Agency Name and Address Texas Department of Transportation Research and Technology Implementation Division 125 E. 11th Street Austin, TX 78701				13. Type of Report and Period Covered Technical Report January 2019- August 2020	
				14. Sponsoring Agency Code	
15. Supplementary Notes Project performed in cooperation with the Texas Department of Transportation and the Federal Highway Administration.					
16. Abstract <p>Recurring slope failures are common in Texas due to the extreme weather and soil conditions. TxDOT spends millions of dollars annually to repair embankment slope failures along state roads and highways. The proactive maintenance of highway embankments and cut slopes can significantly reduce the cost of emergency stabilization and improve highway operations. This project aims to develop a Slope Repair Maintenance and Management System (SRMMS) to identify the highly critical highway slopes to facilitate proactive slope maintenance. The objectives of this implementation project were to (1) collect data and create layers of an existing TxDOT ArcGIS database for assessing conditions of slopes and slope repairs, (2) develop slope failure predictive models, (3) monitor slope failures, calibrate slope failure predictive models, and update the location of critical segments of the corridors, (4) recommend rapid, resilient, and sustainable repair methods to prevent recurring failures, and (5) develop a repair and maintenance master plan.</p> <p>SRMMS will help TxDOT personnel identify critical slope segments and facilitate proactive slope maintenance decisions. The implementation of the system will minimize slope failures and enhance safety, road-user satisfaction, infrastructure service life, environmental sustainability, and transportation system reliability.</p>					
17. Key Words Rainfall-induced slope failures, Clayey soils, Slope failure susceptibility analysis			18. Distribution Statement No restrictions. This document is available to the public through the National Technical Information Service, Alexandria, Virginia 22312; <a href="https://www.ntis.gov/">https://www.ntis.gov/</a> .		
19. Security Classif. (of report) Unclassified		20. Security Classif. (of this page) Unclassified		21. No. of pages 182	
				22. Price	

**SLOPE REPAIR AND MAINTENANCE MANAGEMENT SYSTEM  
FINAL REPORT**

by:

Mohsen Shahandashti, Ph.D., P.E.

Sahadat Hossain, Ph.D., P.E.

Anil Baral

Isha Adhikari

Pouria Pourmand

Bahram Abediniangerabi, Ph.D.

The University of Texas at Arlington

**Report 5-6957-01-1**

Project 5-6957-01

Project Title: Slope Repair and Maintenance Management System

Performed in cooperation with  
the Texas Department of Transportation and the Federal Highway Administration

August 31, 2020  
Published March 2022



425 Nedderman Dr., 416 Yates St.  
Box 19308, Arlington, TX 76019

## **DISCLAIMER**

The contents of this report reflect the views of the authors, who are responsible for the facts and the accuracy of the data presented herein. The contents do not necessarily reflect the official view or policies of the Federal Highway Administration (FHWA) or the Texas Department of Transportation (TxDOT). This report does not constitute a standard, specification, or regulation.

This report is not intended for construction, bidding, or permit purposes.

The United States Government and the State of Texas do not endorse products or manufacturers. Trade or manufacturers' names appear herein solely because they are considered essential to the object of this report.

## **ACKNOWLEDGMENT**

This project was conducted in cooperation with TxDOT. The authors are grateful for the support and guidance provided by Ms. Shelley Pridgen, Project Manager of Research and Technology Implementation (RTI). The authors are thankful for the technical guidance provided by the TxDOT Paris District representatives Sydney Newman, Chad Ingram, and Noel Paramanantham. Their prompt assistance and advice have been central to the successful completion of this project.

## TABLE OF CONTENTS

EXECUTIVE SUMMARY .....	x
CHAPTER 1 INTRODUCTION .....	1
CHAPTER 2 SPATIAL DATA COLLECTION AND PROCESSING.....	3
2.1. Introduction .....	3
2.2. Data Collection.....	3
2.2.1. Soil Type and Properties .....	3
2.2.2. Slope Angle .....	4
2.2.3. Precipitation.....	6
2.2.4. Vegetation .....	7
2.2.5. General Features .....	11
CHAPTER 3 DATA MODEL DEVELOPMENT FOR SRMMS .....	15
3.1. Introduction .....	15
3.2. Conceptual Data Model.....	15
3.2.1. Data Dictionary.....	16
3.3. Logical Data Model.....	17
3.3.1. Data Dictionary.....	18
CHAPTER 4 SLOPE REPAIR AND MAINTENANCE MANAGEMENT GEODATABASE AND METADATA .....	31
4.1. Introduction .....	31
4.2. Slope Repair and Maintenance Management Geodatabase .....	31
4.3. Metadata Development .....	34
CHAPTER 5 MAP-BASED ARCGIS INTERFACE FOR UPDATING AND VISUALIZING DATA .....	36
5.1. Introduction .....	36

---

5.2. Map-based Interface.....	36
5.3. Entities In Map-Based Interface.....	38
5.4. Use Cases .....	38
CHAPTER 6 SLOPE FAILURE PREDICTIVE MODELING.....	47
6.1. Introduction .....	47
6.2. Literature Review.....	47
6.2.1. Slope Susceptibility Analysis Methods .....	47
6.2.2. Causative Factor for Slope Instability .....	49
6.3. Development of Slope Failure Predictive Model.....	51
6.3.1. Steps for Determining Highway Slopes Susceptibility .....	51
6.3.2. Failure Susceptibility Indicator Scheme.....	58
6.4. Slope Failure Susceptibility Maps.....	59
6.5. Map-based Interface to Visualize Critical Slope.....	62
6.5.1. Steps for Visualizing a Slope Failure Susceptibility Map.....	63
CHAPTER 7 CALIBRATING SLOPE FAILURE PREDICTIVE MODEL .....	65
7.1. Introduction .....	65
7.2. The Effect of Land Cover on Slope Failure Predictive Modeling .....	65
7.2.1. Land Cover Categories .....	65
7.3. Calibrating Slope Failure Predictive Model Using Land Cover Data.....	69
7.3.1. Collecting Land Cover Data .....	69
7.3.2. Validating Land Cover Data.....	71
7.3.3. Calibrating Susceptibility Maps .....	71
CHAPTER 8 RECOMMEND REPAIR METHODS TO PREVENT RECURRING SLOPE FAILURES .....	73
8.1. Introduction .....	73

8.2. Multi-criteria Decision Support System For Generating A Ranked List of Repair and Maintenance Methods .....	73
8.2.1. Identification of Slope Repair Methods and Development of Ranking Criteria .....	75
8.2.2. Elimination of Irrelevant Slope Repair Methods.....	76
8.2.3. Creation of Slope Repair Decision Matrix .....	78
8.2.4. Determination of Weights of Slope Repair Criteria Using The Entropy Method.....	79
8.2.5. Ranking of Slope Repair Methods Using Technique for Order Preference by Similarity of Ideal Solution (TOPSIS) Method.....	81
8.3. Map-based Interface For Providing a List of Ranked Slope Repair Methods .....	83
CHAPTER 9 SLOPE REPAIR AND MAINTENANCE MASTER PLAN .....	85
9.1. Master Plan Vision.....	85
9.2. Investigated Corridors .....	86
9.3. Critical Segments in The Corridor .....	87
9.3.1. Maps of Critical Slope Segments .....	87
9.3.2. Google Street View Images of Critical Slope Segments.....	119
9.4. Maintenance Schedule.....	139
9.5. List of Repair Methods And Their Order of Magnitude Costs .....	143
CHAPTER 10 SUMMARY AND CONCLUSION .....	157
REFERENCES .....	159



## LIST OF FIGURES

<b>Figure 2.1</b> LiDAR data available in the TxDOT Paris district area.....	5
<b>Figure 2.2</b> NLCD 2016 land cover for the TxDOT Paris district area.....	8
<b>Figure 2.3</b> NLCD 2016 imperviousness for the TxDOT Paris district area .....	10
<b>Figure 2.4</b> NLCD 2016 tree canopy for the TxDOT Paris district area.....	11
<b>Figure 2.5</b> Past slope failure GIS feature layer .....	13
<b>Figure 3.1</b> Conceptual data model .....	15
<b>Figure 3.2</b> Slope repair and maintenance management data categories .....	17
<b>Figure 4.1</b> Metadata visualization in ArcCatalog .....	35
<b>Figure 5.1</b> Slope Repair and Maintenance Management System (SRMMS) .....	36
<b>Figure 5.2</b> SRMSS interface showing different widgets.....	37
<b>Figure 5.3</b> SRMSS interface displaying failure attributes .....	37
<b>Figure 5.4</b> Use Case Diagram .....	39
<b>Figure 6.1</b> Drained fully softened frictional angle correlation between for CFs 25-45% and CF $\geq$ 50% (Gamez and Stark, 2014).....	53
<b>Figure 6.2</b> Slope failure parallel to surface showing the model parameters .....	53
<b>Figure 6.3</b> Graph of peak response duration, $tp^*$ , for a wide range of normalized rainfall duration $T^*$ (Iverson, 2000) .....	57
<b>Figure 6.4</b> Graphs of pressure head $\Psi p^*(t^*)$ versus normalized rainfall duration $T^*$ for different return periods .....	58
<b>Figure 6.5</b> Corridors with the availability of LiDAR data.....	59
<b>Figure 6.6</b> Slope failure susceptibility map of Grayson county at US 75 and Randall Lake Rd intersection using LiDAR-derived slope angles .....	60
<b>Figure 6.7</b> Slope failure susceptibility map of Grayson county at US 75 and Randall Lake Rd intersection using NED derived slope angles .....	61
<b>Figure 6.8</b> Map-Interface displaying the slope failure susceptibility map of the TxDOT Paris district .....	62
<b>Figure 6.9</b> Map-based interface displaying slope susceptibility levels for embankments along the TxDOT Paris district highway corridors.....	63

<b>Figure 7.1</b> Mechanically stabilized slopes (a) Intersection of SE Loop 286 and old Clarksville Rd., Lamar Co. (b) Intersection of State Highway 24 and FM 499, Hunt Co. (c) Intersection of NE Loop 286 and Pine mill Rd., Lamar Co. (d) Intersection of IH-30 and State Highway 24, Hunt Co. ....	66
<b>Figure 7.2</b> Vegetated slopes (a) Along US 271, near the intersection of SE Loop 286 and Old Clarksville road, Lamar Co. (b) Intersection of State Highway 11 and Golden Rd intersection, Grayson Co. (c) Intersection of Tx-503 SPUR-E and Theresa Dr. Grayson Co. (d) Intersection of US 75 and FM 121, Grayson Co.....	67
<b>Figure 7.3</b> Mechanically stabilized slopes at the intersection of SW Loop 286 and Farm Road 137 in Lamar Co. (a) Polygon shapefiles showing mechanically stabilized slope segments (b) images of mechanically stabilized slopes obtained from google earth. ....	70
<b>Figure 7.4</b> Validation of land cover (left image: validation point at the intersection of SE Loop 286 and old Clarksville Rd., Lamar Co.; top-right image: Google Earth image associated with the shown validation point; bottom-right image: Photo taken at the site for validating the Google Earth image) .....	71
<b>Figure 7.5</b> Calibration of slope failure susceptibility map (Intersection of NE Loop 286 and Pine mill Rd., Lamar Co); (a) Slope susceptibility map developed using the physically-based model; (b) Stable slope identified from Google Earth; (c) Slopes classified as non-critical in calibrated susceptibility map .....	72
<b>Figure 8.1</b> Components of the multi-criteria decision support system to propose a ranked list of slope repair methods .....	74
<b>Figure 8.2</b> Classification of Slope Repair Methods (Shahandashti et al., 2019) .....	75
<b>Figure 8.3</b> Process of accessing the list of slope repair methods and recommended implementation practices for avoiding recurring failures using the map-based interface .....	84
<b>Figure 9.1</b> Slope failure at the intersection of SE Loop 286 and Clarksville St, Paris, Texas.....	85
<b>Figure 9.2</b> Location of selected corridors for the development of the master plan .....	86
<b>Figure 9.3</b> A large-scale map of the first strip of US 75 starting at intersection of US 75 and SH 91, Denison, Texas.....	88
<b>Figure 9.4</b> US 75 corridor in Paris district.....	119
<b>Figure 9.5</b> Map showing the southern segment of Loop 286 corridor in Paris district .....	133

## LIST OF TABLES

<b>Table 2.1</b> Land cover classification description (MRLC, 2019).....	8
<b>Table 2.2</b> Past Slope Failures .....	12
<b>Table 3.1</b> Conceptual data model terms description .....	16
<b>Table 3.2</b> Slope repair and maintenance management entities description.....	18
<b>Table 3.3</b> Attribute description of vector entities.....	21
<b>Table 3.4</b> Description of raster layers' attribute (cell value).....	28
<b>Table 4.1</b> List of Entities in Slope Repair Management Geodatabase.....	31
<b>Table 4.2</b> Attributes of feature entities in slope repair and maintenance management geodatabase .....	33
<b>Table 5.1</b> Description of Widgets in the map-based interface .....	38
<b>Table 5.2</b> UC1: Login.....	40
<b>Table 5.3</b> UC2: Sign Up.....	40
<b>Table 5.4</b> UC3: Search .....	40
<b>Table 5.5</b> UC4: Return to initial map view extent .....	41
<b>Table 5.6</b> UC5: Zoom in and zoom out of the map view.....	41
<b>Table 5.7</b> UC6: Find the user location .....	41
<b>Table 5.8</b> UC7: Change basemap.....	41
<b>Table 5.9</b> UC8: Display spatial data entity .....	42
<b>Table 5.10</b> UC9: Display the legend of the data entity .....	42
<b>Table 5.11</b> UC10: Display the user manual .....	42
<b>Table 5.12</b> UC11: Update existing slope failure feature.....	43
<b>Table 5.13</b> UC12: Delete a slope failure feature.....	44
<b>Table 5.14</b> UC13: Add new slope failure feature.....	45
<b>Table 5.15</b> UC14: Display slope susceptibility map.....	46
<b>Table 5.16</b> UC15: Logout.....	46
<b>Table 6.1</b> Ratio of Volumetric water content versus pressure head at saturation .....	55
<b>Table 6.2</b> Display slope failure susceptibility map .....	63
<b>Table 6.3</b> Display the legend for slope failure susceptibility map.....	64
<b>Table 8.1</b> Applicability of slope repair method based on soil and failure type.....	77

**Table 8.2** Base matrix for representing expert evaluations ..... 78

**Table 9.1** Maintenance schedule of critical slope segments along US 75 highway corridor..... 140

**Table 9.2** Maintenance schedule of critical slope segments along Loop 286 ..... 142

**Table 9.3** Order of magnitude cost estimate for repair and maintenance of critical slope segments in US 75 Corridor..... 144

**Table 9.4** Order of magnitude cost estimate for repair and maintenance of critical slope segments in Loop 286..... 154

## EXECUTIVE SUMMARY

Recurring slope failures are common in Texas due to the extreme weather and soil conditions. The Texas Department of Transportation (TxDOT) annually spends millions of dollars to repair embankment slope failures along the state roads and highways. The proactive maintenance of highway embankments and cut slopes can significantly reduce the cost of emergency stabilization and improve highway operations. This project aims to develop a Slope Repair Maintenance and Management System (SRMMS) to identify the highly critical highway slopes to facilitate proactive slope maintenance. The objectives of this implementation project were to (1) collect data and create layers of an existing Receiving Agency ArcGIS database for assessing conditions of slopes and slope repairs, (2) develop slope failure predictive models, (3) monitor slope failures, calibrate slope failure predictive models and update the location of critical segments of the corridors, (4) recommend rapid, resilient, and sustainable repair methods to prevent recurring failures, and (5) develop a repair and maintenance master plan.

The geospatial data on soil properties, precipitation, historical slope failures, slope geometry, and landcover in the TxDOT Paris district slopes were collected and integrated into a geodatabase. The geospatial data were used as inputs to a physically-based geotechnical model to assess the stability of the slopes along the highway corridors. Based on the minimum duration of rainfall required to trigger the slope instabilities, color-coded slope failure susceptibility maps were prepared: Highly critical (< 3 days), Critical (3-10 days), Moderately critical (10-45 days), and Non-critical (>45 days). A map-based interface was developed to visualize the collected geospatial data entities and color-coded slope failure susceptibility maps. The slope failure susceptibility maps were calibrated to consider the effect of landcover on slope stability. The validation of the susceptibility maps was carried out using the ten past slope failures that were located in the corridors for which the susceptibility maps were developed. Nine slope failures were located in highly critical regions, which require rainfall duration of fewer than 3 days to trigger slope instability, and one slope failure was located in the critical region, which requires less than 7 days rainfall to trigger slope instability. The validation results showed that slope failure susceptibility maps could effectively identify the slope segments highly susceptible to slope failures. A multi-criteria decision support system was developed to recommend a list of methods for maintenance and repair of critical slope segments. Finally, a repair and maintenance master plan was prepared for critical slope segments

along US 75 and Loop 286 corridors in the TxDOT Paris district. The order of magnitude cost estimate and maintenance schedule were prepared for the proactive maintenance of the critical slope segments.

The slope repair and maintenance management system (SRMMS) helps the TxDOT personnel to identify the critical slopes and facilitate proactive slope maintenance decisions. The implementation of the system helps to minimize the slope failures and also enhance safety, customer satisfaction, infrastructure conditions and service life, environmental sustainability, and transportation system reliability.

## CHAPTER 1 INTRODUCTION

Slope failures cause significant economic and casualty losses in the U.S. (White et al., 2005). According to the U.S. Geological Survey (2003), the United States is experiencing an excess cost of \$1 billion in damages and about 50 deaths annually due to slope failures. Shallow slope failures along the highway corridors cause damages to the existing structures, shoulders, road surfaces, utility poles, bridges, and drainage facilities. They severely limit the flow of workforce, goods, and resources (Miller et al., 2012; Khan et al., 2017; Shahandashti et al., 2019). Recurring slope failures happen frequently in Texas due to the extreme weather and soil conditions (Hossain et al. 2017). The Texas Department of Transportation (TxDOT) annually spends millions of dollars to repair embankment slope failures along the state roads and highways. The proactive maintenance of the critical slope segments can help to minimize the slope failures in highway embankments and cut slopes. This research aims to identify highly critical slopes to facilitate proactive slope maintenance decisions. To support the proactive maintenance decisions, a Slope Repair and Maintenance System (SRMMS) is developed for the TxDOT Paris district.

The objectives of this implementation project are to (1) collect data and create layers of an existing Receiving Agency ArcGIS database for assessing conditions of slopes and slope repairs, (2) develop slope failure predictive models, (3) monitor slope failures, calibrate slope failure predictive models and update the location of critical segments of the corridors, (4) recommend rapid, resilient, and sustainable repair methods to prevent recurring failures, and (5) develop a repair and maintenance master plan.

This technical report explains all the Tasks performed in the development of the Slope Repair and Maintenance Management System (SRMMS) for the TxDOT Paris District. The report is organized as follows:

**Chapter 1** is this introductory chapter.

**Chapter 2** explains data collection procedures and data sources.

**Chapter 3** explains data model development for the slope repair and management system.

**Chapter 4** describes the geodatabase developed for the slope repair and management system.

**Chapter 5** explains the Map-based ArcGIS Interface.

**Chapter 6** explains the slope failure predictive modeling.

**Chapter 7** explains the calibration of the slope failure predictive model.

**Chapter 8** explains the multi-criteria decision support system to rank the list of slope repair methods.

**Chapter 9** includes the master plan developed for the two major corridors in the TxDOT Paris district.



## CHAPTER 2 SPATIAL DATA COLLECTION AND PROCESSING

### 2.1. INTRODUCTION

The spatial data on soil properties, slope angle, precipitation, and vegetation are required to assess the condition of highway embankments and cut slopes. Also, some general spatial data, such as past slope failures, Paris district boundary, and Paris district connectivity corridors are required for visualization, data cleaning, and data organization. This chapter explains the data collection and processing of different spatial data entities.

### 2.2. DATA COLLECTION

#### 2.2.1. Soil Type and Properties

Several soil properties, such as bulk density, saturated hydraulic conductivity, liquid limit, percent clay, plasticity index, water content, and soil type (based on Unified soil classification system (USCS)), are required to assess the condition of slopes adjacent to highway corridors. Soil Survey Geographic (SSURGO) database provides the data on the distribution of soil properties on the landscape. The SSURGO database is developed by the National Cooperative soil survey, an agency of the United States Department of Agriculture (USDA). Web Soil Survey (WSS) operated by the Natural Resource conservation system makes the SSURGO dataset publicly available. The SSURGO dataset provides the soil properties up to a depth of 7 feet from the surface. These data provide an approximation of soil type and properties. First, soil properties for seven different soil depths, each at an interval of 1 foot in the TxDOT Paris district was extracted from the SSURGO datasets. Then, an automated data processing was designed and implemented to convert all raw soil data into one final GIS feature (polygon) layer. So, the final product became a GIS polygon feature that contained bulk density, saturated hydraulic conductivity, liquid limit, percent clay, plasticity index and water content for all depth ranges from 0 to 7 ft with a 1 ft interval (0 ft-1 ft, 1 ft-2 ft, ..., 6 ft-7 ft) and the soil type data based on the Unified Soil Classification System.

The information about raw soil data used to create the TxDOT Paris district soil properties GIS feature (polygon) layer is as follows:

- **Data source:** Soil Survey Geographic Database (SSURGO) which provides soil data and information collected by the National Cooperative Soil Survey (NCSS). SSURGO was accessed through the Web Soil Survey (WSS) website which is operated by the United States Department of Agriculture (USDA) National Resource Conservation System (NRCS).
- **Data format:** feature (polygon), which can be derived from Microsoft Access datasets using the USDA's Soil Data Viewer tool in ESRI ArcMap platform.
- **Datasets:** soil data for seven counties including Grayson, Fannin, Lamar, Red River, Franklin, Hunt, and Hopkins were collected to cover all the TxDOT Paris district area (Lamar county soil dataset included soil data for Delta county area and Hopkins county soil dataset included soil data for Rain county).

### 2.2.2. Slope Angle

The slope angle is one of the major causative factors for slope instability. The slope angles can be derived from ground elevation data sets. Light Detection and Ranging (LiDAR) data were found as the most suitable spatial elevation data for creating slope angle spatial data because of its high granularity and accuracy. Figure 2.1 shows the availability of LiDAR data in the TxDOT Paris district area based on the Texas Natural Resources Information System (TNRIS) website. This figure shows that LiDAR data are available for almost half of the TxDOT Paris district area. For the areas in Paris district with no LiDAR data, the National Elevation Datasets (NEDs) provided by the United States Geological Survey (USGS) were used to create slope angle spatial data. Information about data collection and processing to convert LiDAR and National Elevation Datasets into slope angle GIS raster layers are provided in the following subsections.

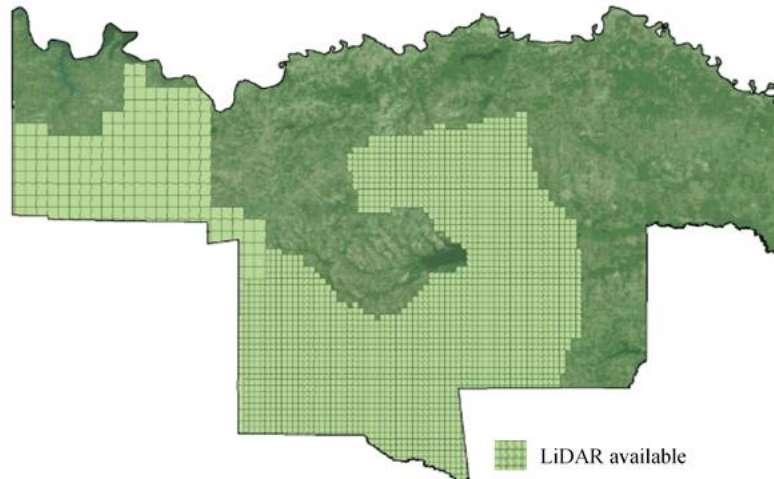


**Figure 2.1** LiDAR data available in the TxDOT Paris district area

### *Creating Slope Angle GIS Raster Layer Using Lidar Data*

LiDAR data were collected from Texas Strategic Mapping (StratMap) datasets available in the TNRIS Online DataHub. StratMap 2009, 2010, 2011, 2014, and 2017 were used to collect LiDAR data for the TxDOT Paris district area. Then, an automated process was designed and implemented to integrate all LiDAR data in the TxDOT Paris district area and convert them into elevation data sets. Then, the elevation data sets were converted to the final slope angle raster layer. The final slope angle raster layer derived from LiDAR data shows the slope angle in degree in every 3 m by 3 m pixel.

The information about raw LiDAR data that was used to create the TxDOT Paris district slope angle GIS raster layer is as follows:

**Data source:** Texas Natural Resources Information System (TNRIS)

**Data format:** compressed point clouds (LAZ)

**Data quality:** at least 4 laser points per square meters

**Data accuracy:** 50-75 Centimeters horizontally and 15 centimeters vertically based on Quality Assurance (QA)/Quality Control (QC) reports of StartMap LiDAR acquisition projects

**Data granularity:** a maximum 75 centimeters according to horizontal accuracy (3-meter granularity were found the most suitable to create slope angle GIS raster layer)

### *Creating Slope Angle GIS Raster Layer Using National Elevation Dataset (NED)*

National Elevation Datasets (NEDs) are raster obtained from United States Geological Survey (USGS) Digital Elevation Models (DEMs). Each dataset covers a rectangular-shaped area. Five NEDs are needed to cover all the TxDOT Paris district area. First, NEDs were collected from the United States Geological Survey (USGS) database through The National Map (TNM). Then, data processing was conducted to integrate all NEDs into one GIS raster elevation layer. The elevation layer was finally converted to the slope angle raster layer. The final slope angle raster layer derived from National Elevation Datasets (NEDs) shows the slope angle in degree in every 10 m by 10 m pixel of the TxDOT Paris district area.

The information about NED data that was used to create the TxDOT Paris district slope angle GIS raster layer are as follows:

**Data source:** United States Geological Survey – The National Map (NEDs of Texas can also be collected from the Texas Natural Resources Information System (TNRIS) online DataHub)

**Data format:** raster

**Data granularity:** approximately 10 m for Paris district area

### **2.2.3. Precipitation**

The National Oceanic and Atmospheric Administration (NOAA) database was used to collect data for precipitation. NOAA Atlas 14, Volume 11 (NOAA, 2018) includes updated precipitation frequency estimates and rainfall data (frequency-duration-intensity relation). Precipitation Frequency Data Server (PFDS) provides access to NOAA Atlas 14 precipitation frequency estimates. Raw precipitation data were collected from NOAA Precipitation Frequency Data Server (PFDS) were processed to become GIS raster layers that represent the estimated precipitation intensity based on different frequencies and durations. NOAA Atlas 14, Volume 11 provides precipitation intensity based on 10 different frequencies (1, 2, 5, 10, 25, 50, 100, 200, 500, 1000 years) and 19 different durations (5 minutes, 10 minutes, 15 minutes, 20 minutes, 30 minutes, 45 minutes, 60 minutes, 2 hours, 3 hours, 6 hours, 12 hours, 24 hours, 48 hours, 3 days, 4 days, 7 days, 10 days, 20 days, 30 days, 45 days, and 60 days). All 190 data sets were collected to be processed into 190 precipitation GIS raster layers covering the TxDOT Paris district area.

The information about the raw precipitation data used to create final precipitation raster layers is as follows:

**Data source:** NOAA's National Weather Service, Hydrometeorological Design Studies Center, Precipitation Frequency Data Server (PFDS)

**Data format:** American Standard Code (ASCII)

**Data type:** precipitation intensity based on the precipitation frequency and duration, including upper bound of the 90% confidence interval, lower bound of the 90% confidence interval, and precipitation frequency estimates.

**Data accuracy:** 90% confidence interval

**Data granularity:** 750 meters by 750 meters

#### 2.2.4. Vegetation

The National Land Cover Database (NLCD) was used to collect land cover spatial data. Three types of spatial data were found for the conterminous U.S. in MRLC (Multi-Resolution Land Characteristics): land cover, surface imperviousness, and tree canopy. First, the raw data that covered all the conterminous United States were collected from the National Land Cover Database (NLCD). Then, data for the TxDOT Paris district area were retrieved from the raw data.

NLCD 2016 is the most recent land cover and surface imperviousness data (published in May 2019), and NLCD 2011 is the most recent tree canopy data published by U.S. Geological Survey (tree canopy 2016 has not been released to date). The information about all three types of land cover data are as follows:

**Data source:** United States Geological Survey (USGS)

**Data format:** raster

**Data accuracy:**

- 83% level 2, 89% level 1 for NLCD 2011(Wickham et al., 2017)
- An overall agreement ranging from 71% to 97% between land cover classification and reference data for NLCD 2016 (Yang et al., 2018)

**Data granularity:** 30 meters

More details about the land cover, surface imperviousness, and tree canopy GIS raster data are provided in the following subsections.

*Land Cover*

NLCD 2016 land cover is a nationwide data on land cover and land cover change at a 30m resolution with a 16-class legend based on a modified Anderson Level II classification system (MRLC, June 2019). The land cover data (raster image) for the TxDOT Paris district area was retrieved from the NLCD 2016. Figure 2.2 illustrates the land coverage for the TxDOT Paris district. Grid values of NLCD land cover 2011 raster layer are classified as shown in Table 2.1.

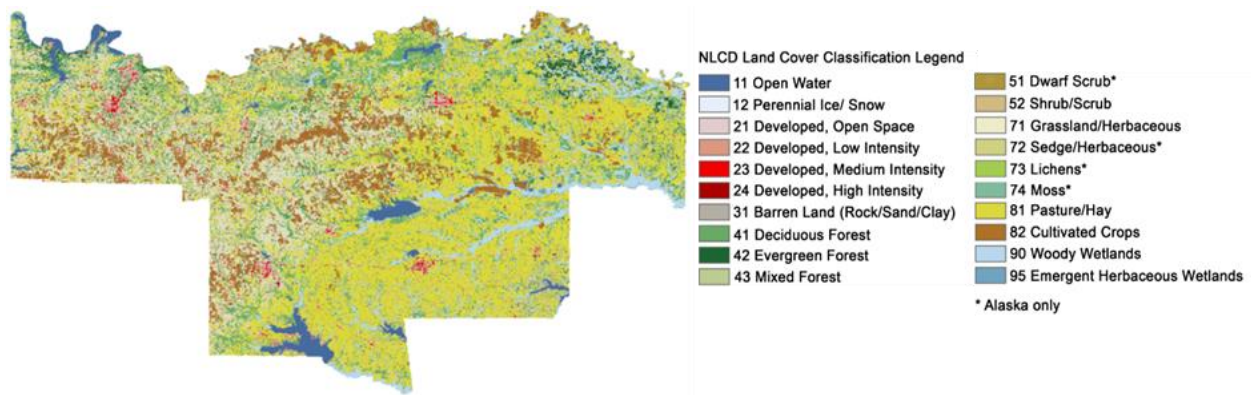


**Figure 2.2** NLCD 2016 land cover for the TxDOT Paris district area

**Table 2.1** Land cover classification description (MRLC, 2019)

Class\ Value	Classification Description
<b>Water</b>	
11	<b>Open Water</b> - areas of open water, generally with less than 25% cover of vegetation or soil.
12	<b>Perennial Ice/Snow</b> - areas characterized by a perennial cover of ice and/or snow, generally greater than 25% of total cover.
<b>Developed</b>	
21	<b>Developed, Open Space</b> - areas with a mixture of some constructed materials, but mostly vegetation in the form of lawn grasses. Impervious surfaces account for less than 20% of the total cover. These areas most commonly include large-lot single-family housing units, parks, golf courses, and vegetation planted in developed settings for recreation, erosion control, or aesthetic purposes.
22	<b>Developed, Low Intensity</b> - areas with a mixture of constructed materials and vegetation. Impervious surfaces account for 20% to 49% percent of total cover. These areas most commonly include single-family housing units.
23	<b>Developed, Medium Intensity</b> -areas with a mixture of constructed materials and vegetation. Impervious surfaces account for 50% to 79% of the total cover. These areas most commonly include single-family housing units.

Class\ Value	Classification Description
24	<b>Developed High Intensity</b> -highly developed areas where people reside or work in high numbers. Examples include apartment complexes, row houses, and commercial/industrial. Impervious surfaces account for 80% to 100% of the total cover.
<b>Barren</b>	
31	<b>Barren Land (Rock/Sand/Clay)</b> - areas of bedrock, desert pavement, scarps, talus, slides, volcanic material, glacial debris, sand dunes, strip mines, gravel pits and other accumulations of earthen material. Generally, vegetation accounts for less than 15% of the total cover.
<b>Forest</b>	
41	<b>Deciduous Forest</b> - areas dominated by trees generally greater than 5 meters tall, and greater than 20% of total vegetation cover. More than 75% of the tree species shed foliage simultaneously in response to seasonal change.
42	<b>Evergreen Forest</b> - areas dominated by trees generally greater than 5 meters tall, and greater than 20% of total vegetation cover. More than 75% of the tree species maintain their leaves all year. Canopy is never without green foliage.
43	<b>Mixed Forest</b> - areas dominated by trees generally greater than 5 meters tall, and greater than 20% of total vegetation cover. Neither deciduous nor evergreen species are greater than 75% of total tree cover.
<b>Shrubland</b>	
51	<b>Dwarf Scrub</b> - Alaska only areas dominated by shrubs less than 20 centimeters tall with shrub canopy typically greater than 20% of total vegetation. This type is often co-associated with grasses, sedges, herbs, and non-vascular vegetation.
52	<b>Shrub/Scrub</b> - areas dominated by shrubs; less than 5 meters tall with shrub canopy typically greater than 20% of total vegetation. This class includes true shrubs, young trees in an early successional stage or trees stunted from environmental conditions.
<b>Herbaceous</b>	
71	<b>Grassland/Herbaceous</b> - areas dominated by graminoid or herbaceous vegetation, generally greater than 80% of total vegetation. These areas are not subject to intensive management, such as tilling but can be utilized for grazing.
72	<b>Sedge/Herbaceous</b> - Alaska only areas dominated by sedges and forbs, generally greater than 80% of total vegetation. This type can occur with significant other grasses or other grass-like plants and includes sedge tundra, and sedge tussock tundra.
73	<b>Lichens</b> - Alaska only areas dominated by fruticose or foliose lichens generally greater than 80% of total vegetation.
74	<b>Moss</b> - Alaska only areas dominated by mosses, generally greater than 80% of total vegetation.
<b>Planted/Cultivated</b>	
81	<b>Pasture/Hay</b> -areas of grasses, legumes, or grass-legume mixtures planted for livestock grazing or the production of seed or hay crops, typically on a perennial cycle. Pasture/hay vegetation accounts for greater than 20% of total vegetation.
82	<b>Cultivated Crops</b> -areas used for the production of annual crops, such as corn, soybeans, vegetables, tobacco, and cotton, and also perennial woody crops such as orchards and vineyards. Crop vegetation accounts for greater than 20% of total vegetation. This class also includes all land being actively tilled.
<b>Wetlands</b>	
90	<b>Woody Wetlands</b> - areas where forest or shrubland vegetation accounts for greater than 20% of vegetative cover and the soil or substrate is periodically saturated with or covered with water.
95	<b>Emergent Herbaceous Wetlands</b> - Areas where perennial herbaceous vegetation accounts for greater than 80% of vegetative cover and the soil or substrate is periodically saturated with or covered with water.

### *Surface Imperviousness*

Imperviousness data collected from the National Land Cover Database (NLCD) represents urban impervious surfaces as a percentage of the developed surface over every 30-meter pixel of the conterminous U.S. (MRLC, 2019). The imperviousness data (raster image) was retrieved for the TxDOT Paris district area from NLCD 2016. The result is shown in Figure 2.3.

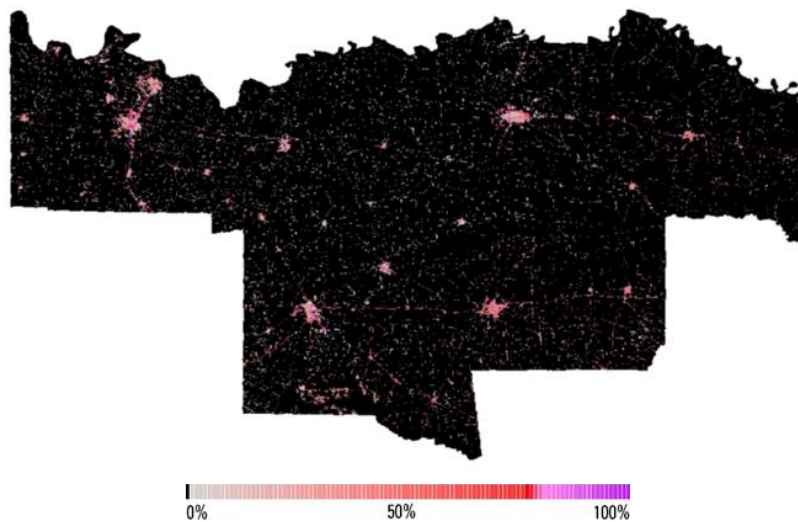


**Figure 2.3** NLCD 2016 imperviousness for the TxDOT Paris district area

### *Tree Canopy*

NLCD 2011 tree canopy data contain percent tree canopy estimates, as a continuous variable, for each pixel (30m by 30m) across all land covers generated by the United States Forest Service (MRLC, 2019). The tree canopy data (raster image) were retrieved for the TxDOT Paris district area from NLCD 2016. The result is shown in Figure 2.4.



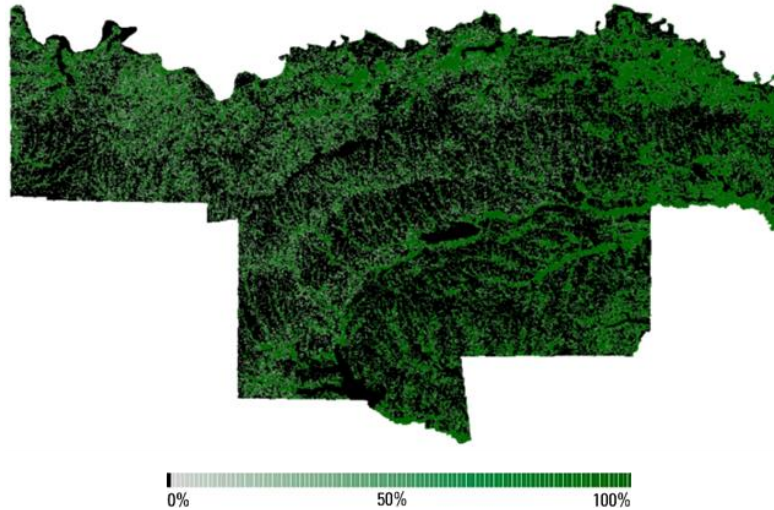


**Figure 2.4** NLCD 2016 tree canopy for the TxDOT Paris district area

### **2.2.5. General Features**

General features include GIS feature layers, such as Paris district past slope failures, Paris district boundary, Paris district connectivity corridors, and Paris district stabilized slopes. Data collection and processing of these GIS feature layers are explained in the following subsections.

#### *Paris District Past Slope Failures*

Information about past slope failures was collected from the TxDOT Paris district. Table 2.2 shows the information about the past slope failures collected from the TxDOT Paris district. A feature layer was created to show the past slope failures on the GIS map. Furthermore, four more fields (slope failure type, failure depth, failure year, and the number of failure recurrences) were added to the slope failure GIS feature layer for adding more information about slope failures.

**Table 2.2** Past Slope Failures

<b>Grayson County Slope Failure Sites</b>							
<b>City</b>	<b>Highway Affected</b>	<b>Intersecting Road</b>	<b>Intersection Quarter</b>	<b>Type of Slope</b>	<b>Soil Classification</b>	<b>Geotechnical Data Available</b>	<b>Number of Sites</b>
Denison	US 75	Randall Lake Rd	NE & NW	Excavated	CH	YES	2
Sherman	US 82	FM 1417	SE	Embankment	CL	YES	1
Sherman	US 82	US 75	SW	Excavated	CL	YES	1
Sherman	SH 56	FM 1417	SW	Embankment	CL/CH	NO	1
<b>Fannin County Slope Failure Sites</b>							
<b>City</b>	<b>Highway Affected</b>	<b>Intersecting Road</b>	<b>Intersection Quarter</b>	<b>Type of slope</b>	<b>Soil Classification</b>	<b>Geotechnical Data Available</b>	<b>Number of Sites</b>
Lannius	US 82	FM 897	SE	Embankment	CH	YES	1
Lannius	US 82	CR 2975	SE	Excavated	CH	YES	1
<b>Lamar County Slope Failure Sites</b>							
<b>City</b>	<b>Highway Affected</b>	<b>Intersecting Road</b>	<b>Intersection Quarter</b>	<b>Type of slope</b>	<b>Soil Classification</b>	<b>Geotechnical Data Available</b>	<b>Number of Sites</b>
Paris	US 82 (NW loop)	FM 79	NE, SE, SW, NW	Embankment	CL/ML	(not sure)	4
Paris	US 82 (NW loop)	BU 271	SW	Embankment	CL/ML	(not sure)	1
Paris	US 271 (NE loop)	FM 195	NW	Embankment	ML	(not sure)	1
Paris	US 271 (SE loop)	BU 271/LP 286	SW & W	Embankment	CL	(not sure)	4
<b>Hopkins County Slope Failure Sites</b>							
<b>City</b>	<b>Highway Affected</b>	<b>Intersecting Road</b>	<b>Intersection Quarter</b>	<b>Type of slope</b>	<b>Soil Classification</b>	<b>Geotechnical Data Available</b>	<b>Number of Sites</b>
Brashear	IH 30	FM 2653	SE	Excavated	CL	NO	1
White Oak Junction	IH 30	CR 3341	NE	Excavated	CL	NO	1

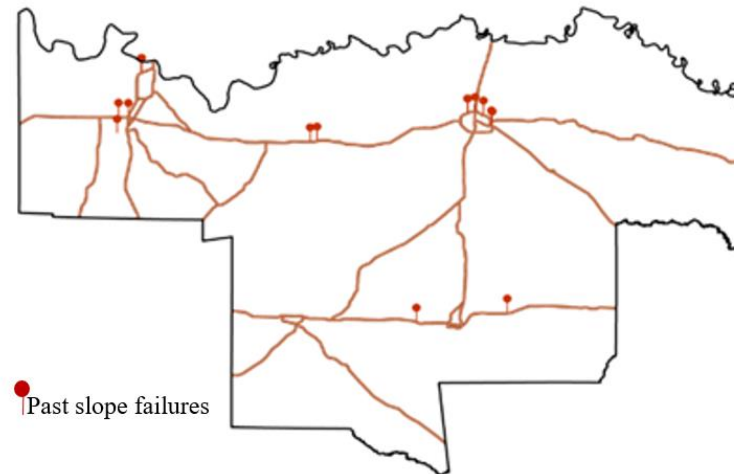


**Figure 2.5** Past slope failure GIS feature layer

### *Paris District Boundary*

The GIS feature layer representing the boundary of the TxDOT Paris district was obtained from TxDOT's online open data portal. Because the study area of this research project is limited to the TxDOT Paris district, a GIS feature layer indicating the TxDOT Paris district boundary was used to remove data outside the TxDOT Paris district area. For example, the shape of National Elevation Datasets (NEDs) collected from USGS was rectangular and included a large amount of data outside the TxDOT Paris district area. Therefore, using the TxDOT Paris district boundary layer, the NED layers were clipped, and all data outside the TxDOT Paris district area were removed.

### *Paris District Connectivity Corridors*

Based on the proposal, only 2 corridors were initially selected for developing the slope repair and maintenance management system (SRMMS). However, the approach for collecting data (covering all Paris district area) enabled researchers to select 22 corridors. Corridors were selected considering the importance of corridors and locations of the past slope failures collected from the TxDOT Paris district. The corridors on this network represent the Texas Transportation Commission approved corridors under the Unified Transportation Program's Category 4 funding category (TxDOT, 2018). This network is composed of:

- Texas Trunk System
- National Highway System (NHS)

- Connections from the Texas Trunk System or the NHS to major ports on international borders or Texas water ports
- National Freight Network
- Texas Freight Network
- Hurricane Evacuation Routes

Eighteen out of 19 past slope failures were along the TxDOT's Statewide Connectivity Corridors. Therefore, the TxDOT's Statewide Connectivity Corridors GIS layer was used to create the TxDOT Paris district connectivity corridors layer by removing corridors outside the TxDOT Paris district area. Paris district connectivity corridors GIS feature layer consists of lines approximately on the centerlines of Paris district connectivity corridors.

#### *Paris District Stabilized Slopes*

A GIS polygon feature layer was created to represent the stabilized slopes along the connectivity corridors of the TxDOT Paris district. Currently, this layer represents the mechanically stabilized slopes along the connectivity corridors in the TxDOT Paris district.

## CHAPTER 3 DATA MODEL DEVELOPMENT FOR SRMMS

### 3.1. INTRODUCTION

The development of a prototype data model for slope repair and maintenance management system (SRMMS) has been summarized in this chapter. The most recent TxDOT Data Architecture (TxDOT, 2010) was used to create a logical data model based on the data obtained from different sources, as described in Chapter 2. This chapter includes two sections: a conceptual data model that represents the general idea of the SRMMS and a logical data model that provides detailed information about entities and attributes used in the SRMMS.

### 3.2. CONCEPTUAL DATA MODEL

Figure 3.1 shows the conceptual data model of SRMMS. All the data entities (see Chapter 2) will be imported to the slope repair and maintenance management geodatabase and will be spatially matched. Data can be imported into the geodatabase as well as exported out of the geodatabase. Data inside the geodatabase can be accessed by the slope failure predictive model which uses the data layers as the inputs and provides slope failure predictions. Verified users can access and use spatial data by a map-based interface (created and designed to be used in SRMMS) through their computers and phones, as well as contributing to the database by updating slope failures records. An administrator is needed to manage and verify data and users.

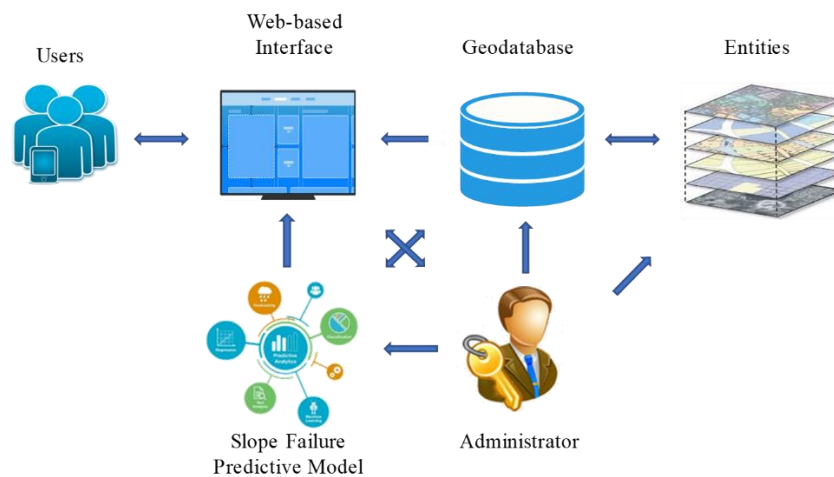


**Figure 3.1** Conceptual data model

### 3.2.1. Data Dictionary

Conceptual data model terms are described in Table 3.1.

**Table 3.1** Conceptual data model terms description

Term	Description
Entity	<b>Definition:</b> an entity is the detailed representation of an object of interest (e.g. the TxDOT Paris district corridors entity consists of lines that represent the TxDOT connectivity corridors within the administrative boundary of Paris district). In this study, entities are categorized into five main categories (general features, soil properties, slope angle, precipitation, vegetation) which are explained in the next section.
Slope repair and maintenance geodatabase	<b>Definition:</b> a slope repair and maintenance geodatabase is a georeferenced database created using ESRI ArcGIS Pro that was used to store and organize GIS-based entities. Geodatabases use an efficient data structure that is optimized for performance and storage.
Slope failure predictive model	<b>Definition:</b> a slope failure predictive model is a model that uses causative factors data for slope instability as well as other general data as its inputs and provides slope failure predictions and represents them in the map-based interface.
SRMMS map-based interface	<b>Definition:</b> a SRMMS map-based interface is a map-based interface that is based on ESRI ArcGIS online that uses the data entities from geodatabase that are hosted in ArcGIS Online.
User	<b>Definition:</b> a user is a TxDOT employee who has been granted the authority to interact with the SRMMS map-based interface.
Administrator	<b>Definition:</b> an administrator is a TxDOT employee or a person authorized by TxDOT who has knowledge about slope repair and maintenance management system (SRMMS) and is in charge of managing and organizing the system as well as updating data and verifying data and users.

### 3.3. LOGICAL DATA MODEL

A logical data model based on the TxDOT Data Architecture document (TxDOT, 2010) was developed to represent the collected spatial data entities. Entities are classified into different categories to improve their organization and readability. Figure 3.2 illustrates different categories and their associated entities within the geodatabase. All the collected spatial entities can be classified into vector or raster data. A vector data represents real-world features (e.g., streets, sewer lines, soil types) using point, line, or polygon and is also known as a feature class. A raster consists of a grid of cells (or pixels) organized as row and columns. For raster layers data is stored in each cell to represent a geographic feature. The definitions of entities and their associated attributes are provided in the following subsections.

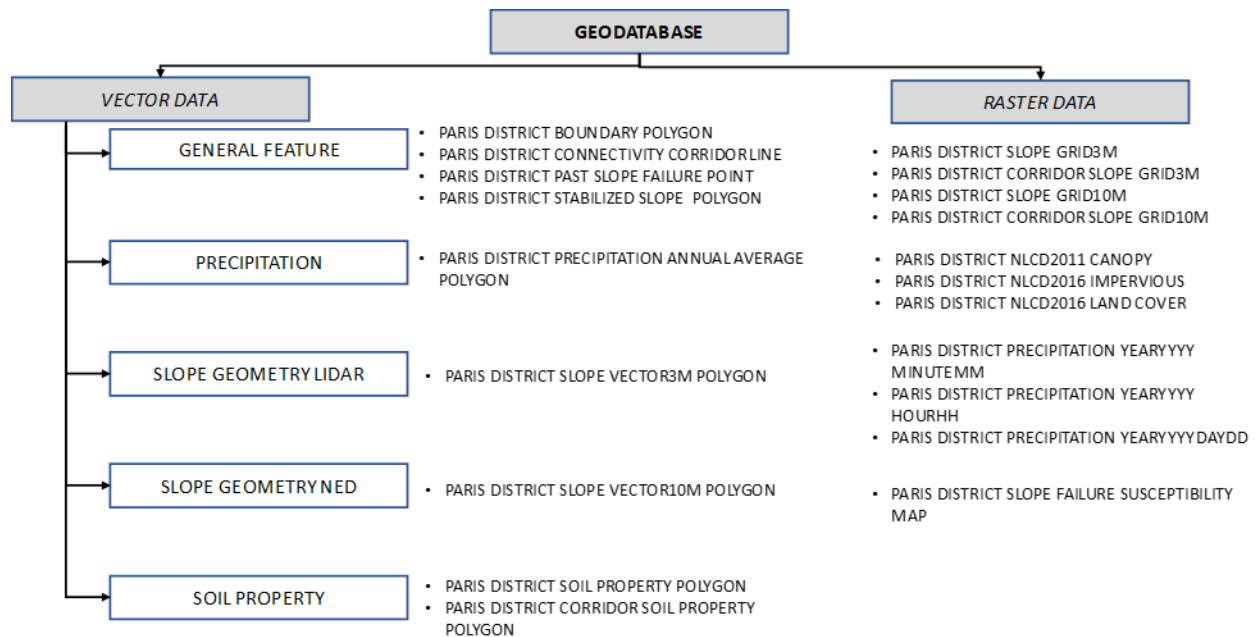


**Figure 3.2** Slope repair and maintenance management data categories

### 3.3.1. Data Dictionary

All entities shown in Figure 3.2 are described in Table 3.2. The data dictionary is developed based on the latest TxDOT Data Architecture recommendations.

**Table 3.2** Slope repair and maintenance management entities description

Category	Entity	Description
Vector Data: <i>General Feature</i>	PARIS DISTRICT BOUNDARY POLYGON	<b>Definition:</b> a PARIS DISTRICT BOUNDARY POLYGON is the administrative boundary of the TxDOT Paris district as one of TxDOT's 25 Districts, which are geographic subdivisions of the state.
Vector Data: <i>General Feature</i>	PARIS DISTRICT CONNECTIVITY CORRIDOR LINE	<b>Definition:</b> a PARIS DISTRICT CONNECTIVITY CORRIDOR is a network of corridors of Paris district that represent the Texas Transportation Commission approved corridors for the TxDOT Paris district under the Unified Transportation Program's Category 4 funding category (TxDOT 2018).
Vector Data: <i>General Feature</i>	PARIS DISTRICT PAST SLOPE FAILURE POINT	<b>Definition:</b> a PARIS DISTRICT PAST SLOPE FAILURE POINT is a set of slope failure locations in the TxDOT Paris district area. Currently, PARIS DISTRICT PAST SLOPE FAILURE includes 19 slope failure locations.
Vector Data: <i>General Feature</i>	PARIS DISTRICT STABILIZED SLOPE POLYGON	<b>Definition:</b> a PARIS DISTRICT STABILIZED SLOPE POLYGON is an entity that represents the stabilized slopes as polygons along the TxDOT Paris district corridors. Currently, PARIS DISTRICT STABILIZED SLOPE POLYGON represents the mechanically stabilized slopes along the corridors of the TxDOT Paris district. This data is developed by visualizing the stabilized slopes in Paris district corridors on Google earth.
Vector Data: <i>Precipitation</i>	PARIS DISTRICT PRECIPITATION ANNUAL AVERAGE POLYGON	<b>Definition:</b> a PARIS DISTRICT PRECIPITATION ANNUAL AVERAGE is an entity that provides derived average annual precipitation according to a model using point precipitation and elevation data for the 30 years of 1981-2010 (USDA/NRCS, 2011)
Vector Data: <i>Slope Geometry Lidar</i>	PARIS DISTRICT SLOPE VECTOR3M POLYGON	<b>Definition:</b> a PARIS DISTRICT SLOPE VECTOR3M POLYGON is an entity of ground slope angle derived from ground LiDAR points. This feature entity is created using a raster with the granularity of 3 meters, which is derived from LiDAR data collected from the Texas Natural Resources Information System (TNRIS) database. This feature layer only represents the slopes along the corridors represented by PARIS DISTRICT CONNECTIVITY CORRIDOR LINE.
Vector Data: <i>Slope Geometry NED</i>	PARIS DISTRICT SLOPE VECTOR10M POLYGON	<b>Definition:</b> a PARIS DISTRICT SLOPE VECTOR10M POLYGON is a feature layer of ground slope angle derived from National Elevation Datasets (NEDs). This feature layer is derived from a raster format with the granularity of 10 meters, which is created using NEDs collected from the United States Geographical Survey (USGS) database (NEDs of Texas also can be collected from TNRIS database). This feature layer only represents the slopes along the corridors represented by PARIS DISTRICT CONNECTIVITY CORRIDOR LINE.



Category	Entity	Description
Vector Data: <i>Soil Property</i>	PARIS DISTRICT SOIL PROPERTY POLYGON	<b>Definition:</b> a PARIS DISTRICT SOIL PROPERTY is an entity that represents soil properties (bulk density, saturated hydraulic conductivity, liquid limit, percent clay, plasticity index, water content and soil type based on Unified Soil Classification System (USCS)) for different depths ranges (from 0 to 7 feet) in the TxDOT Paris district area.
Vector Data: <i>Soil Property</i>	PARIS DISTRICT CORRIDOR SOIL PROPERTY POLYGON	<b>Definition:</b> a PARIS DISTRICT CORRIDOR SOIL PROPERTY is an entity that represents soil properties (bulk density, saturated hydraulic conductivity, liquid limit, percent clay, plasticity index, water content and soil type based on Unified Soil Classification System (USCS)) for different depth ranges (from 0 to 7 feet) in a 300-foot wide buffer area around the center lines of Paris district connectivity corridors.
Raster Data	PARIS DISTRICT SLOPE GRID3M	<b>Definition:</b> a PARIS DISTRICT SLOPE GRID3M is a raster data set of ground slope angle derived from ground LiDAR points. PARIS DISTRICT SLOPE GRID3M granularity is 3 meters and is created using LiDAR data collected from the Texas Natural Resources Information System (TNRIS) database. According to LiDAR data availability, this entity covers almost half of the TxDOT Paris district area.
Raster Data	PARIS DISTRICT CORRIDOR SLOPE GRID3M	<b>Definition:</b> a PARIS DISTRICT CORRIDOR SLOPE GRID3M is a raster data set of ground slope angle derived from ground LiDAR points. PARIS DISTRICT CORRIDORS SLOPE GRID3M granularity is 3 meters and is created using LiDAR data from the Texas Natural Resources Information System (TNRIS) database. The coverage area of this entity is limited to a 300-foot wide buffer area around connectivity corridors in the TxDOT Paris district. Based on the LiDAR data availability, this entity covers almost half of the TxDOT Paris district's connectivity corridors represented by PARIS DISTRICT CONNECTIVITY CORRIDOR LINE.
Raster Data	PARIS DISTRICT SLOPE GRID10M	<b>Definition:</b> a PARIS DISTRICT SLOPE GRID10M is a raster data set of ground slope angle derived from National Elevation Datasets (NEDs). PARIS DISTRICT SLOPE GRID10M granularity is 3 meters and is created using NEDs collected from United States Geological Survey (USGS) database (NEDs also can be collected from TNRIS online data portal). PARIS DISTRICT SLOPE GRID10M covers all Paris district area.
Raster Data	PARIS DISTRICT CORRIDOR SLOPE GRID10M	<b>Definition:</b> a PARIS DISTRICT CORRIDOR SLOPE GRID10M is a raster data set of ground slope angle derived from National Elevation Datasets (NEDs). PARIS DISTRICT SLOPE GRID10M granularity is 10 meters and is created using NEDs collected from United States Geological Survey (USGS) database (NEDs also can be collected from TNRIS online data portal). PARIS DISTRICT CORRIDORS SLOPE GRID10M coverage area is limited to a 300-foot wide buffer area around Paris district's connectivity corridors. This raster entity only represents the slopes along the corridors

Category	Entity	Description
		represented by PARIS DISTRICT CONNECTIVITY CORRIDOR LINE.
Raster Data	PARIS DISTRICT NLCD2011 CANOPY	<b>Definition:</b> a PARIS DISTRICT NLCD2011 CANOPY is a 30m raster data set covering the TxDOT Paris district area and contains percent tree canopy estimates for each pixel (MRLC, 2019).
Raster Data	PARIS DISTRICT NLCD2016 IMPERVIOUS	<b>Definition:</b> a PARIS DISTRICT NLCD2016 IMPERVIOUS represents urban impervious surfaces as a percentage of developed surfaces over every 30-meter pixel in the TxDOT Paris district area.
Raster Data	PARIS DISTRICT NLCD2016 LAND COVER	<b>Definition:</b> a PARIS DISTRICT NLCD2016 LAND COVER is a district-wide data on the land cover at a 30m resolution with a 16-class legend based on a modified Anderson Level II classification system.
Raster Data	PARIS DISTRICT PRECIPITATION YEARYYYY MINUTEMM	<b>Definition:</b> a PARIS DISTRICT PRECIPITATION YEARYYYY MINUTEMM is a GIS grid atlas that contains precipitation intensity estimates for the TxDOT Paris district based on the precipitation data collected between 1833-2017 (NOAA, 2018). <ul style="list-style-type: none"> <li>• YYYY: frequency year (0001, 0002, 0005, 0010, 0025, 0050, 0100, 0200, 0500, 1000)</li> <li>• MM: Duration in minute (05, 10, 15, 30, 60)</li> </ul> Example: PARIS DISTRICT PRECIPITATION YEAR0500 MINUTE15 Number of Entities: 50
Raster Data	PARIS DISTRICT PRECIPITATION YEARYYYY HOURHH	<b>Definition:</b> a PARIS DISTRICT PRECIPITATION YEARYYYY HOURHH is a GIS grid atlas contains precipitation intensity estimates for the TxDOT Paris district based on precipitation data collected between 1833-2017 (NOAA, 2018). <ul style="list-style-type: none"> <li>• YYYY: frequency year (0001, 0002, 0005, 0010, 0025, 0050, 0100, 0200, 0500, 1000)</li> <li>• HH: Duration in hour (02, 03, 06, 12, 24, 48)</li> </ul> Example: PARIS DISTRICT PRECIPITATION YEAR0025 HOUR03 Number of Entities: 60
Raster Data	PARIS DISTRICT PRECIPITATION YEARYYYY DAYDD	<b>Definition:</b> a PARIS DISTRICT PRECIPITATION YEARYYYY HOURHH is a GIS grid atlas contains precipitation intensity estimates for the TxDOT Paris district based on precipitation data collected between 1833-2017 (NOAA, 2018). <ul style="list-style-type: none"> <li>• YYYY: frequency year (0001, 0002, 0005, 0010, 0025, 0050, 0100, 0200, 0500, 1000)</li> <li>• DD: Duration in days (03, 04, 07, 10, 20, 30, 45, 60)</li> </ul> Example: PARIS DISTRICT PRECIPITATION YEAR1000 DAY45 Number of Entities: 80
Raster Data	PARIS DISTRICT SLOPE	<b>Definition:</b> a PARIS DISTRICT SLOPE SUSCEPTIBILITY MAP is raster data that represent the minimum duration of rainfall required to trigger slope instability along the corridor of the TxDOT Paris district.

Category	Entity	Description
	SUSCEPTIBILITY MAP	

### Attributes Description

Attributes of raster and vector data entities are described in two tables. Table 3.3 contains descriptions of the attributes of GIS vector entities. Table 3.4 contains descriptions of cell values of raster entities (as there was no instruction about raster format entities in the TxDOT Data Architecture manual, cell value in a raster format entity was considered to be the attribute of raster format entity).

**Table 3.3** Attribute description of vector entities

Entity	Attribute	Description
PARIS DISTRICT PAST SLOPE FAILURE POINT	FAILURE TYPE	<b>Definition:</b> a FAILURE TYPE is a word that defines failure type based on the depth of failure <b>Purpose:</b> FAILURE TYPE categorizes failure into two categories based on the depth of failure. <b>Example:</b> N/A <b>Valid Values:</b> 'shallow' and 'deep' <b>Format:</b> string
PARIS DISTRICT PAST SLOPE FAILURE POINT	FAILURE DEPTH	<b>Definition:</b> a FAILURE DEPTH is an integer number that defines the depth of slope failure in feet. <b>Purpose:</b> FAILURE DEPTH indicates the depth of failure <b>Example:</b> N/A <b>Valid Values:</b> 1 through 7 <b>Format:</b> number
PARIS DISTRICT PAST SLOPE FAILURE POINT	FAILURE OCCURRENCE	<b>Definition:</b> a FAILURE OCCURRENCE is a word that provides information about the recurrence of failure. <b>Purpose:</b> FAILURE OCCURRENCE provides information about the recurrence of failure. <b>Example:</b> N/A <b>Valid Values:</b> 'First Time Failure' and 'Recurring Failure' <b>Format:</b> string
PARIS DISTRICT PAST SLOPE FAILURE POINT	FAILURE YEAR	<b>Definition:</b> a FAILURE YEAR is an integer number that defines the year in which the slope failure occurred. <b>Purpose:</b> FAILURE YEAR determines the year of failure occurrence. <b>Example:</b> N/A <b>Valid Values:</b> N/A <b>Format:</b> DateTime

Entity	Attribute	Description
PARIS DISTRICT PAST SLOPE FAILURE POINT	FAILURE EDITOR	<p><b>Definition:</b> a FAILURE EDITOR is a word or phrase that provides the information on the name of the TxDOT staff who reported the slope failure.</p> <p><b>Purpose:</b> FAILURE EDITOR provides the name of a person who reported the failure.</p> <p><b>Example:</b> N/A</p> <p><b>Valid Values:</b> N/A</p> <p><b>Format:</b> string</p>
PARIS DISTRICT BOUNDARY POLYGON	DISTRICT NAME	<p><b>Definition:</b> a DISTRICT NAME is a word that defines the name of the District</p> <p><b>Purpose:</b> DISTRICT NAME identifies the district by its name</p> <p><b>Example:</b> N/A</p> <p><b>Valid Values:</b> N/A</p> <p><b>Format:</b> string</p>
PARIS DISTRICT CONNECTIVITY CORRIDOR LINE	ROUTE NAME	<p><b>Definition:</b> a ROUTE NAME is a word that defines the name of the route based on TxDOT road naming convention</p> <p><b>Purpose:</b> ROUTE NAME identifies road by a unique designated name</p> <p><b>Example:</b> SH0056-RG</p> <p><b>Valid Values:</b> N/A</p> <p><b>Format:</b> string</p>
PARIS DISTRICT STABILIZED SLOPE POLYGON	STABILIZED SLOPE DESCRIPTION	<p><b>Definition:</b> a STABILIZED SLOPE DESCRIPTION is a word or phrase that defines the approach used to stabilize the slope.</p> <p><b>Purpose:</b> STABILIZED SLOPE DESCRIPTION identifies the methods that were used in stabilizing the slope.</p> <p><b>Example:</b> gabion with vegetation</p> <p><b>Valid Values:</b> N/A</p> <p><b>Format:</b> string</p>
PARIS DISTRICT STABILIZED SLOPE POLYGON	STABILIZED SLOPE YEAR	<p><b>Definition:</b> a STABILIZED SLOPE YEAR is a date that helps to determine the year the slope was stabilized</p> <p><b>Purpose:</b> STABILIZED SLOPE YEAR identifies the year of stabilization</p> <p><b>Example:</b> 2019</p> <p><b>Valid Values:</b> N/A</p> <p><b>Format:</b> Date</p>
PARIS DISTRICT STABILIZED SLOPE POLYGON	STABILIZED SLOPE EDITOR	<p><b>Definition:</b> a STABILIZED SLOPE EDITOR is the name of the person who added the information about slope stabilization.</p> <p><b>Purpose:</b> STABILIZED SLOPE EDITOR identifies the name of the person who updated information on slope repair.</p> <p><b>Example:</b> N/A</p> <p><b>Valid Values:</b> N/A</p> <p><b>Format:</b> string</p>

Entity	Attribute	Description
PARIS DISTRICT SOIL PROPERTY POLYGON	BULK DENSITY DDFT	<p><b>Definition:</b> a BULK DENSITY DDFT is a number that defines bulk density, which is the oven-dry weight of the soil material less than 2 millimeters in size per unit volume of soil at water tension of 1/3 bar, expressed in grams per cubic centimeter (USDA, 2015). DD is an integer number from 01 to 07 and addresses the depth in which the bulk density is measured (e.g., BULK DENSITY 03FT is an attribute that provides the bulk density of soil between the depth of 2 feet and 3 feet). These 7 attributes cover all Paris district area.</p> <p><b>Purpose:</b> BULK DENSITY DDFT shows the bulk density of soil at a specific depth range.</p> <p><b>Example:</b> N/A</p> <p><b>Valid Values:</b> N/A</p> <p><b>Format:</b> number</p>
PARIS DISTRICT SOIL PROPERTY POLYGON	SATURATED HYDRAULIC CONDUCTIVITY DDFT	<p><b>Definition:</b> a SATURATED HYDRAULIC CONDUCTIVITY DDFT is a number that defines saturated hydraulic conductivity of soil, which refers to the ease with which pores in a saturated soil transmit water in terms of micrometers per second (USDA, 2015). The estimates are expressed. DD is an integer number from 01 to 07 and addresses the depth in which saturated hydraulic conductivity is measured (e.g., SATURATED HYDRAULIC CONDUCTIVITY 03FT, provides saturated hydraulic conductivity of soil between the depth of 2 feet and 3 feet). These 7 attributes cover all Paris district area.</p> <p><b>Purpose:</b> SATURATED HYDRAULIC CONDUCTIVITY DDFT shows saturated hydraulic conductivity of soil at a specific depth range.</p> <p><b>Example:</b> N/A</p> <p><b>Valid Values:</b> N/A</p> <p><b>Format:</b> number</p>
PARIS DISTRICT SOIL PROPERTY POLYGON	LIQUID LIMIT DDFT	<p><b>Definition:</b> a LIQUID LIMIT DDFT is a number that defines liquid limit (LL) of soil, which is one of the standard Atterberg limits used to indicate the plasticity characteristics of a soil. It is the water content, on a percent by weight basis, of the soil (passing #40 sieve) at which the soil changes from a plastic to a liquid state (USDA, 2015). DD is an integer number from 01 to 07 and addresses the depth in which liquid limit is measured (e.g., LIQUID LIMIT 03FT, provides the liquid limit of soil between the depth of 2 feet and 3 feet). These 7 attributes cover all Paris district area.</p> <p><b>Purpose:</b> LIQUID LIMIT DDFT shows liquid of soil at a specific depth range.</p> <p><b>Example:</b> N/A</p> <p><b>Valid Values:</b> N/A</p> <p><b>Format:</b> number</p>

Entity	Attribute	Description
PARIS DISTRICT SOIL PROPERTY POLYGON	PERCENT CLAY DDFT	<p><b>Definition:</b> a PERCENT CLAY DDFT is a number that defines the estimated clay content of each soil layer given as a percentage, by weight, of the soil material that is less than 2 millimeters in diameter (USDA, 2015). DD is an integer number from 01 to 07 and addresses the depth in which percent clay is measured (e.g., PERCENT CLAY 03FT, provides percent clay of soil between the depth of 2 feet and 3 feet). These 7 attributes cover all Paris district area.</p> <p><b>Purpose:</b> PERCENT CLAY DDFT shows percent clay of soil at a specific depth range.</p> <p><b>Example:</b> N/A</p> <p><b>Valid Values:</b> N/A</p> <p><b>Format:</b> number</p>
PARIS DISTRICT SOIL PROPERTY POLYGON	PLASTICITY INDEX DDFT	<p><b>Definition:</b> a PLASTICITY INDEX DDFT is a number that defines the plasticity index (PI), which is the standard Atterberg limits used to indicate the plasticity characteristics of soil (USDA, 2015). It is defined as the numerical difference between the liquid limit and the plasticity limit of the soil. It is the range of water content in which a soil exhibits the characteristics of a plastic solid. DD is an integer number from 01 to 07 and addresses the depth in which the plasticity index is measured (e.g., PLASTICITY INDEX 03FT, provides plasticity index of soil between the depth of 2 feet and 3 feet). These 7 attributes cover all Paris district area.</p> <p><b>Purpose:</b> PLASTICITY INDEX DDFT shows the plasticity index of soil at a specific depth range.</p> <p><b>Example:</b> N/A</p> <p><b>Valid Values:</b> N/A</p> <p><b>Format:</b> number</p>
PARIS DISTRICT SOIL PROPERTY POLYGON	WATER CONTENT DDFT	<p><b>Definition:</b> a WATER CONTENT DDFT is a number that defines water content, which is the amount of soil water retained at a tension of 1/3 bar, expressed as a volumetric percentage of the whole soil (USDA, 2015). DD is an integer number from 01 to 07 and addresses the depth in which water content is measured (e.g., WATER CONTENT 03FT, provides water content of soil between the depth of 2 feet and 3 feet). These 7 attributes cover all Paris district area.</p> <p><b>Purpose:</b> WATER CONTENT DDFT shows the water content of the soil at a specific depth range.</p> <p><b>Example:</b> N/A</p> <p><b>Valid Values:</b> N/A</p> <p><b>Format:</b> number</p>
PARIS DISTRICT SOIL PROPERTY POLYGON	SOIL TYPE	<p><b>Definition:</b> a SOIL TYPE is a word that defines the Unified soil classification system classifies mineral and organic mineral soils for engineering purposes based on particle-size characteristics, liquid limit, and plasticity index (USDA, 2015). This attribute covers all Paris district area.</p>

Entity	Attribute	Description
		<p><b>Purpose:</b> SOIL TYPE shows soil classification based on the Unified soil classification system.</p> <p><b>Example:</b> CL</p> <p><b>Valid Values:</b> CH, CL, SC-SM, SM, CL-ML, GC, ML, SC</p> <p><b>Format:</b> string</p>
PARIS DISTRICT CORRIDOR SOIL PROPERTY POLYGON	BULK DENSITY DDFT	<p><b>Definition:</b> a BULK DENSITY DDFT is a number that defines the bulk density of soil, which is the oven-dry weight of the soil material less than 2 millimeters in size per unit volume of soil at water tension of 1/3 bar, expressed in grams per cubic centimeter (USDA, 2015). DD is an integer number from 01 to 07 and addresses the depth in which the bulk density is measured (e.g., BULK DENSITY 03FT is an attribute that provides the bulk density of soil between the depth of 2 feet and 3 feet). These 7 attributes cover a 300-ft wide buffer around the TxDOT Paris district connectivity corridors.</p> <p><b>Purpose:</b> BULK DENSITY DDFT shows the bulk density of soil at a specific depth range.</p> <p><b>Example:</b> N/A</p> <p><b>Valid Values:</b> N/A</p> <p><b>Format:</b> number</p>
PARIS DISTRICT CORRIDOR SOIL PROPERTY POLYGON	SATURATED HYDRAULIC CONDUCTIVITY DDFT	<p><b>Definition:</b> a SATURATED HYDRAULIC CONDUCTIVITY DDFT is a number that defines saturated hydraulic conductivity of soil that refers to the ease with which pores in a saturated soil transmit water. The estimates are expressed in terms of micrometers per second (USDA, 2015). DD is an integer number from 01 to 07 and addresses the depth in which saturated hydraulic conductivity is measured (e.g., SATURATED HYDRAULIC CONDUCTIVITY 03FT, provides saturated hydraulic conductivity of soil between the depth of 2 feet and 3 feet). These 7 attributes cover a 300-ft wide buffer around the connectivity corridors of the TxDOT Paris district.</p> <p><b>Purpose:</b> SATURATED HYDRAULIC CONDUCTIVITY DDFT shows the saturated hydraulic conductivity of soil at a specific depth range.</p> <p><b>Example:</b> N/A</p> <p><b>Valid Values:</b> N/A</p> <p><b>Format:</b> number</p>
PARIS DISTRICT CORRIDOR SOIL PROPERTY POLYGON	LIQUID LIMIT DDFT	<p><b>Definition:</b> a LIQUID LIMIT DDFT is a number that defines liquid limit (LL) of soil, which is one of the standard Atterberg limits used to indicate the plasticity characteristics of a soil. It is the water content, on a percent by weight basis, of the soil (passing #40 sieve) at which the soil changes from a plastic to a liquid state (USDA, 2015). DD is an integer number from 01 to 07 and addresses the depth in which liquid limit is measured (e.g., LIQUID LIMIT 03FT, provides a</p>

Entity	Attribute	Description
		<p>liquid limit of soil between the depth of 2 feet and 3 feet). These 7 attributes cover a 300-ft wide buffer around the TxDOT Paris district connectivity corridors.</p> <p><b>Purpose:</b> LIQUID LIMIT DDFT shows the liquid limit of soil at a specific depth range.</p> <p><b>Example:</b> N/A</p> <p><b>Valid Values:</b> N/A</p> <p><b>Format:</b> number</p>
<p>PARIS DISTRICT CORRIDOR SOIL PROPERTY POLYGON</p>	<p>PERCENT CLAY DDFT</p>	<p><b>Definition:</b> a PERCENT CLAY DDFT is a number that defines the estimated clay content of each soil layer given as a percentage, by weight, of the soil material that is less than 2 millimeters in diameter (USDA, 2015). DD is an integer number from 01 to 07 and addresses the depth in which percent clay is measured (e.g., PERCENT CLAY 03FT, provides percent clay of soil between the depth of 2 feet and 3 feet). These 7 attributes cover a 600-ft wide buffer around the connectivity corridors of the TxDOT Paris district.</p> <p><b>Purpose:</b> PERCENT CLAY DDFT shows percent clay of soil at a specific depth range.</p> <p><b>Example:</b> N/A</p> <p><b>Valid Values:</b> N/A</p> <p><b>Format:</b> number</p>
<p>PARIS DISTRICT CORRIDOR SOIL PROPERTY POLYGON</p>	<p>PLASTICITY INDEX DDFT</p>	<p><b>Definition:</b> a PLASTICITY INDEX DDFT is a number that defines plasticity index (PI), which is one of the standard Atterberg limits used to indicate the plasticity characteristics of a soil. It is defined as the numerical difference between the liquid limit and the plasticity limit of the soil (USDA, 2015). It is the range of water content in which a soil exhibits the characteristics of a plastic solid. DD is an integer number from 01 to 07 and addresses the depth in which the plasticity index is measured (e.g., PLASTICITY INDEX 03FT, provides plasticity index of soil between the depth of 2 feet and 3 feet). These 7 attributes cover a 300-ft wide buffer around the TxDOT Paris district connectivity corridors.</p> <p><b>Purpose:</b> PLASTICITY INDEX DDFT shows the plasticity index of soil at a specific depth range.</p> <p><b>Example:</b> N/A</p> <p><b>Valid Values:</b> N/A</p> <p><b>Format:</b> number</p>
<p>PARIS DISTRICT CORRIDOR SOIL PROPERTY POLYGON</p>	<p>WATER CONTENT DDFT</p>	<p><b>Definition:</b> a WATER CONTENT DDFT is a number that defines water content, which is the amount of soil water retained at a tension of 1/3 bar, expressed as a volumetric percentage of the whole soil. DD is an integer number from 01 to 07 and addresses the depth in which water content is measured (e.g., WATER CONTENT 03FT, provides water content of soil between the depth of 2 feet and 3 feet). These</p>



Entity	Attribute	Description
		<p>7 attributes cover a 300-ft wide buffer around the TxDOT Paris district connectivity corridors.</p> <p><b>Purpose:</b> WATER CONTENT DDFT shows the water content of the soil at a specific depth range.</p> <p><b>Example:</b> N/A</p> <p><b>Valid Values:</b> N/A</p> <p><b>Format:</b> number</p>
<p>PARIS DISTRICT CORRIDOR SOIL PROPERTY POLYGON</p>	<p>SOIL TYPE</p>	<p><b>Definition:</b> a SOIL TYPE is a word that defines soil type based on the Unified Soil Classification System (USCS). This attribute covers a 300-ft wide buffer around the TxDOT Paris district connectivity corridors.</p> <p><b>Purpose:</b> SOIL TYPE shows the soil type based on the Unified Soil Classification System</p> <p><b>Example:</b> CL</p> <p><b>Valid Values:</b> CH, CL, SC-SM, SM, CL-ML, GC, ML, SC (only for the TxDOT Paris district area)</p> <p><b>Format:</b> string</p>
<p>PARIS DISTRICT CORRIDORS SLOPE VECTOR3M POLYGON</p>	<p>SLOPE ANGLE</p>	<p><b>Definition:</b> a SLOPE ANGLE is a number that provides the ground slope angle (in degree) in every 3m grid in the area of 300ft wide buffer around the TxDOT Paris district connectivity corridors.</p> <p><b>Purpose:</b> SLOPE ANGLE shows the slope angle information.</p> <p><b>Example:</b> N/A</p> <p><b>Valid Values:</b> N/A</p> <p><b>Format:</b> number</p>
<p>PARIS DISTRICT CORRIDORS SLOPE VECTOR10M POLYGON</p>	<p>SLOPE ANGLE</p>	<p><b>Definition:</b> a SLOPE ANGLE is a number that provides the ground slope angle in degrees.</p> <p><b>Purpose:</b> SLOPE ANGLE provides slope geometry information.</p> <p><b>Example:</b> N/A</p> <p><b>Valid Values:</b> N/A</p> <p><b>Format:</b> number</p>
<p>PARIS DISTRICT PRECIPITATION ANNUAL AVERAGE POLYGON</p>	<p>ANNUAL AVERAGE</p>	<p><b>Definition:</b> an ANNUAL AVERAGE is a number that provides derived annual average precipitation in inches according to data for 30 years from 1981-2010 (USDA/NRCS, 2011)</p> <p><b>Purpose:</b> ANNUAL AVERAGE shows the annual average precipitation intensity of a location.</p> <p><b>Example:</b> N/A</p> <p><b>Valid Values:</b> N/A</p> <p><b>Format:</b> number</p>

**Table 3.4** Description of raster layers’ attribute (cell value)

Entity	Attribute (Cell Value) Description
<p>PARIS DISTRICT SLOPE GRID3M</p>	<p><b>Definition:</b> the cell value of this raster entity is a number that defines the slope angle of that 3m cell. 3m Cell values are available for almost half of the TxDOT Paris district area (according to LiDAR data availability).</p> <p><b>Purpose:</b> cell value of this entity shows the slope angle of soil in almost half of the TxDOT Paris district area.</p> <p><b>Example:</b> N/A</p> <p><b>Valid Values:</b> 0 through 90</p> <p><b>Format:</b> number</p> <p><b>Cell Size:</b> 3 meters by 3 meters</p>
<p>PARIS DISTRICT CORRIDOR SLOPE GRID3M</p>	<p><b>Definition:</b> the cell value of this raster entity is a number that defines the slope angle of that 3m cell. The slope angle is calculated using LiDAR data available for the area of a 300-ft wide buffer around the connectivity corridors of the TxDOT Paris district. Therefore, cell values are available for almost half of the 300-wide buffer area around the connectivity corridors of the TxDOT Paris district.</p> <p><b>Purpose:</b> cell value of this entity shows the slope angle of soil around connectivity corridors of the TxDOT Paris district.</p> <p><b>Example:</b> N/A</p> <p><b>Valid Values:</b> 0 to 90</p> <p><b>Format:</b> number</p> <p><b>Cell Size:</b> 3 meters</p>
<p>PARIS DISTRICT SLOPE GRID10M</p>	<p><b>Definition:</b> the cell value of this raster entity is a number that defines the slope angle of that 10m cell. The slope angle is processed using National Elevation Datasets available for all Paris district area. Therefore, cell values are available for the whole Paris district area.</p> <p><b>Purpose:</b> cell value of this entity shows the slope angle of soil.</p> <p><b>Example:</b> N/A</p> <p><b>Valid Values:</b> 0 to 90</p> <p><b>Format:</b> number</p> <p><b>Cell Size:</b> 10 meters</p>
<p>PARIS DISTRICT CORRIDOR SLOPE GRID10M</p>	<p><b>Definition:</b> the cell value of this raster entity is a number that defines the slope angle of that 10m cell. The slope angle is calculated using National Elevation Datasets available for the area of a 300-ft wide buffer around the connectivity corridors of the TxDOT Paris district. Therefore, cell values are available for all the 300-wide buffer area around the connectivity corridors of the TxDOT Paris district.</p> <p><b>Purpose:</b> cell value of this entity shows the slope angle of soil.</p> <p><b>Example:</b> N/A</p> <p><b>Valid Values:</b> 0 to 90</p> <p><b>Format:</b> number</p> <p><b>Cell Size:</b> 10 meters</p>
<p>PARIS DISTRICT PRECIPITATION YEARYYYY MINUTEMM</p>	<p><b>Definition:</b> the cell value of this raster entity is a number that estimates the intensity of precipitation for a specified return period (YYYY year) and rainfall duration (MM minutes) in microinches within a 90% confidence interval range. (e.g., the cell value of PARIS DIST PRECIPITATION YEAR0050 MINUTE15 estimates the maximum intensity of 15-minute precipitation for a return period of 50 years.)</p> <p><b>Purpose:</b> cell value of this entity estimates future precipitation intensity in a specific duration and frequency</p>

Entity	Attribute (Cell Value) Description
	<p><b>Example:</b> N/A  <b>Valid Values:</b> N/A  <b>Format:</b> number  <b>Cell Size:</b> 750 meters</p>
<p>PARIS DISTRICT  PRECIPITATION  YEARYYYY  HOURHH</p>	<p><b>Definition:</b> the cell value of this raster entity is a number that estimates the intensity of precipitation for a specified return period (YYYY year) and rainfall duration (HH hour) in microinches within a 90% confidence interval range. (e.g., the cell value of PARIS DIST PRECIPITATION YEAR0050 HOUR24 estimates the maximum intensity of 24-hour precipitation for a return period of 50 years.)  <b>Purpose:</b> cell value of this entity estimates future precipitation intensity in a specific duration and frequency  <b>Example:</b> N/A  <b>Valid Values:</b> N/A  <b>Format:</b> number  <b>Cell Size:</b> 750 meters</p>
<p>PARIS DISTRICT  PRECIPITATION  YEARYYYY DAYDD</p>	<p><b>Definition:</b> the cell value of this raster entity is a number that estimates the intensity of precipitation for a specified return period (YYYY year) and rainfall duration (DD day) in microinches within a 90% confidence interval range. (e.g., the cell value of PARIS DIST PRECIPITATION YEAR0050 DD03 estimates the maximum intensity of 3-day precipitation for a return period of 50 years.)  <b>Purpose:</b> cell value of this entity estimates future precipitation intensity in a specific duration and frequency  <b>Example:</b> N/A  <b>Valid Values:</b> N/A  <b>Format:</b> number  <b>Cell Size:</b> 750 meters</p>
<p>PARIS DISTRICT  NLCD2011 TREE  CANOPY</p>	<p><b>Definition:</b> the cell value of this raster entity is a number that represents percent tree canopy  <b>Purpose:</b> cell value of this entity shows the percent of tree canopy  <b>Example:</b> N/A  <b>Valid Values:</b> 0 to 100  <b>Format:</b> number  <b>Cell Size:</b> 30 meters</p>
<p>PARIS DISTRICT  NLCD2016  IMPERVIOUS</p>	<p><b>Definition:</b> the cell value of this raster entity is a number that represents urban impervious surfaces as a percentage of developed surface (MRLC, 2019)  <b>Purpose:</b> cell value of this entity shows the percent of tree canopy duration and frequency  <b>Example:</b> N/A  <b>Valid Values:</b> 0 to 100  <b>Format:</b> number  <b>Cell Size:</b> 30 meters</p>
<p>PARIS DISTRICT  NLCD2016 LAND  COVER</p>	<p><b>Definition:</b> the cell values of this raster entity is a word and a number that define the land cover class with a 16-class legend based on a modified Anderson Level II classification system (MRLC, 2019)  <b>Purpose:</b> cell values of this entity classify land cover of Paris district area  <b>Example:</b> 23; Developed, Medium Intensity</p>

Entity	Attribute (Cell Value) Description
	<p><b>Valid Word Values:</b> Open Water; Developed, Open Space; Developed, Low Intensity; Developed, Medium Intensity; Developed High Intensity; Barren Land (Rock/Sand/Clay); Deciduous Forest; Evergreen Forest; Mixed Forest; Shrub/Scrub; Grassland/Herbaceous; Pasture/Hay; Cultivated Crops; Woody Wetlands; Emergent Herbaceous Wetlands</p> <p><b>Valid Number Values:</b> 11, 21, 22, 23, 24, 31, 41, 42, 43, 52, 71, 81, 82, 90, 95</p> <p><b>Format:</b> string, number</p> <p><b>Cell Size:</b> 30 meters</p>
<p>PARIS DISTRICT SLOPE SUSCEPTIBILITY MAP</p>	<p><b>Definition:</b> the cell value of this raster entity is a number that represents the minimum duration of rainfall required to trigger slope instability,</p> <p><b>Purpose:</b> cell value of this entity shows the susceptibility to failure,</p> <p><b>Example:</b> N/A</p> <p><b>Valid Values:</b> N/A</p> <p><b>Format:</b> number</p> <p><b>Cell Size:</b> 3 meters</p>

## CHAPTER 4 SLOPE REPAIR AND MAINTENANCE MANAGEMENT GEODATABASE AND METADATA

### 4.1. INTRODUCTION

Based on the prototype logical data model (Section 3.3), ESRI ArcGIS Desktop (ArcMap and ArcGIS Pro) was used to create the physical data model. The naming of the data entities and attributes of the physical data model is based on the most recent TxDOT data architecture document. To accurately relate all the entities spatially, all the created entities were projected into the North American Datum of 1983 (NAD 83) as TxDOT's coordination system standard. Then, entities were integrated and organized in a geodatabase. Metadata for each entity was created using the ESRI ArcCatalog platform based on the Content Standard for Digital Geospatial Metadata (CSDGM) (FGDC, 1998).

### 4.2. SLOPE REPAIR AND MAINTENANCE MANAGEMENT GEODATABASE

Slope repair and maintenance management system geodatabase was created in File Geodatabase format using ESRI ArcGIS Pro. All created entities were prepared to comply with TxDOT Data Architecture and TxDOT coordination system standard based on TxDOT Survey Manual (TxDOT, 2016). The geodatabase is created based on the logical data model and consists of 207 entities represented in Table 4.1. Descriptions of entities are provided in Table 3.2.

**Table 4.1** List of Entities in Slope Repair Management Geodatabase

Category	Logical Entity	Physical Entity (Entities in Geodatabase)	Physical Entity Format	Number of entities
Vector Data: <i>General Feature</i>	PARIS DISTRICT BOUNDARY POLYGON	PARIS_DIST_BOUNDARY_POLY	Feature	1
Vector Data: <i>General Feature</i>	PARIS DISTRICT CONNECTIVITY CORRIDOR LINE	PARIS_DIST_CONNECTIVITY_CORRIDOR_LN	Feature	1
Vector Data: <i>General Feature</i>	PARIS DISTRICT PAST SLOPE FAILURE POINT	PARIS_DIST_PAST_SLOPE_FAILURE_PNT	Feature	1
Vector Data: <i>General Feature</i>	PARIS DISTRICT STABILIZED SLOPE POLYGON	PARIS_DIST_STABILIZED_SLOPE_POLY	Feature	1

Category	Logical Entity	Physical Entity (Entities in Geodatabase)	Physical Entity Format	Number of entities
Vector Data: <i>Precipitation</i>	PARIS DISTRICT PRECIPITATION ANNUAL AVERAGE POLYGON	PARIS_DIST_PRECIPITATION _ANNUAL_AVERAGE_POLY	Feature	1
Vector Data: <i>Slope Geometry Lidar</i>	PARIS DISTRICT SLOPE VECTOR3M POLYGON	PARIS_DIST_CORRIDORS_ SLOPE_VECTOR3M_POLY	Feature	1
Vector Data: <i>Slope Geometry NED</i>	PARIS DISTRICT SLOPE VECTOR10M POLYGON	PARIS_DIST_CORRIDORS_ SLOPE_VECTOR10M_POLY	Feature	1
Vector Data: <i>Soil Property</i>	PARIS DISTRICT SOIL PROPERTY POLYGON	PARIS_DIST_SOIL_PROPERTY _POLY	Feature	1
Vector Data: <i>Soil Property</i>	PARIS DISTRICT CORRIDOR SOIL PROPERTY POLYGON	PARIS_DIST_CORRIDOR_SOIL_ PROPERTY_POLY	Feature	1
Raster Data	PARIS DISTRICT SLOPE GRID3M	PARIS_DIST_SLOPE_GRID3M	Raster	1
Raster Data	PARIS DISTRICT CORRIDOR SLOPE GRID3M	PARIS_DIST_CORRIDOR_SLOPE_GRID3M	Raster	1
Raster Data	PARIS DISTRICT SLOPE GRID10M	PARIS_DIST_SLOPE_GRID10M	Raster	1
Raster Data	PARIS DISTRICT CORRIDOR SLOPE GRID10M	PARIS_DIST_CORRIDOR_SLOPE_GRID10M	Raster	1
Raster Data	PARIS DISTRICT NLCD2011 CANOPY	PARIS_DIST_NLCD2011 _CANOPY	Raster	1
Raster Data	PARIS DISTRICT NLCD2016 IMPERVIOUS	PARIS_DIST_NLCD2016 _IMPERVIOUS	Raster	1
Raster Data	PARIS DISTRICT NLCD2016 LAND COVER	PARIS_DISTRICT_NLCD2016 _LAND_COVER	Raster	1
Raster Data	PARIS DISTRICT PRECIPITATION YEARYYYY MINUTEMM	PARIS_DIST_PRECIPITATION _YEARYYYY_MINUTEMM	Raster	50

Category	Logical Entity	Physical Entity (Entities in Geodatabase)	Physical Entity Format	Number of entities
Raster Data	PARIS DISTRICT PRECIPITATION YEARYYYY HOURHH	PARIS_DIST_PRECIPITATION_YEARYYYY_HOURHH	Raster	60
Raster Data	PARIS DISTRICT PRECIPITATION YEARYYYY DURATION DAYDD	PARIS_DIST_PRECIPITATION_YEARYYYY_DURATION_DAYDD	Raster	80
Raster Data	PARIS DISTRICT SLOPE SUSCEPTIBILITY MAP	PARIS_DIST_SLOPE_SUSCEPTIBILITY_MAP	Raster	1

GIS vector entities have attribute tables, while the attribute of a GIS raster entity was the cell value of that entity. Therefore, only the attribute names of vector entities are defined. Table 3.2 provides a complete description of the logical model's feature entities attributes, and Table 4.2 relates the attributes of geodatabase entities to the corresponding attributes in the logical data model.

**Table 4.2** Attributes of feature entities in slope repair and maintenance management geodatabase

Physical Entity (Entities in Geodatabase)	Physical Attributes (Attributes in Geodatabase)	Corresponding Logical Attribute
PARIS_DIST_BOUNDARY_POLY	DIST_NM	DISTRICT NAME
PARIS_DIST_CONNECTIVITY_CORRIDOR_LN	RTE_NM	ROUTE NAME
PAST_SLOPE_FAILURE_PNT	FAILURE_TYPE	FAILURE TYPE
PAST_SLOPE_FAILURE_PNT	FAILURE_DEPTH	FAILURE DEPTH
PAST_SLOPE_FAILURE_PNT	FAILURE_OCCURRENCE	FAILURE OCCURRENCE
PAST_SLOPE_FAILURE_PNT	FAILURE_YEAR	FAILURE YEAR
PAST_SLOPE_FAILURE_PNT	FAILURE_EDITOR	FAILURE EDITOR
PARIS_DIST_STABILIZED_SLOPE_POLY	STABILIZED_SLOPE_DESCRIPTION	STABILIZED SLOPE DESCRIPTION
PARIS_DIST_STABILIZED_SLOPE_POLY	STABILIZED_SLOPE_YEAR	STABILIZED SLOPE YEAR
PARIS_DIST_STABILIZED_SLOPE_POLY	STABILIZED_SLOPE_EDITOR	STABILIZED SLOPE EDITOR
PARIS_DIST_PRECIPITATION_ANNUAL_AVERAGE_POLY	ANNUAL_AVERAGE	ANNUAL AVERAGE
PARIS_DIST_CORRIDORS_	SLOPE_ANGL	SLOPE ANGLE

Physical Entity (Entities in Geodatabase)	Physical Attributes (Attributes in Geodatabase)	Corresponding Logical Attribute
SLOPE_VECTOR3M_POLY		
PARIS_DIST_CORRIDORS_SLOPE_VECTOR10M_POLY	SLOPE_ANGL	SLOPE ANGLE
PARIS_DIST_SOIL_PROPERTY_POLY	BULK_DENSITY_DDFT	BULK DENSITY DDFT
PARIS_DIST_SOIL_PROPERTY_POLY	SATURATED_HYDRAULIC_CONDUCTIVITY_DDFT	SATURATED HYDRAULIC CONDUCTIVITY DDFT
PARIS_DIST_SOIL_PROPERTY_POLY	LIQUID_LIMIT_DDFT	LIQUID LIMIT DDFT
PARIS_DIST_SOIL_PROPERTY_POLY	PERCENT_CLAY_DDFT	PERCENT CLAY DDFT
PARIS_DIST_SOIL_PROPERTY_POLY	PLASTICITY_INDEX_DDFT	PLASTICITY INDEX DDFT
PARIS_DIST_SOIL_PROPERTY_POLY	WATER_CONTENT_DDFT	WATER CONTENT DDFT
PARIS_DIST_SOIL_PROPERTY_POLY	SOIL_TYPE	SOIL TYPE
PARIS_DIST_CORRIDOR_SOIL_PROPERTY_POLY	BULK_DENSITY_DDFT	BULK DENSITY DDFT
PARIS_DIST_CORRIDOR_SOIL_PROPERTY_POLY	SATURATED_HYDRAULIC_CONDUCTIVITY_DDFT	SATURATED HYDRAULIC CONDUCTIVITY DDFT
PARIS_DIST_CORRIDOR_SOIL_PROPERTY_POLY	LIQUID_LIMIT_DDFT	LIQUID LIMIT DDFT
PARIS_DIST_CORRIDOR_SOIL_PROPERTY_POLY	PERCENT_CLAY_DDFT	PERCENT CLAY DDFT
PARIS_DIST_CORRIDOR_SOIL_PROPERTY_POLY	PLASTICITY_INDEX_DDFT	PLASTICITY INDEX DDFT
PARIS_DIST_CORRIDOR_SOIL_PROPERTY_POLY	WATER_CONTENT_DDFT	WATER CONTENT DDFT
PARIS_DIST_CORRIDOR_SOIL_PROPERTY_POLY	SOIL_TYPE	SOIL TYPE

### 4.3. METADATA DEVELOPMENT

Metadata for each entity included in the geodatabase was developed using ESRI ArcCatalog, which includes a Content Standard for Digital Geospatial Metadata (CSDGM) compliant editor for creating and updating metadata for spatial entities. The level of metadata completeness for the data entities depends on the amount of information that was available in the source from which data were extracted. To provide sufficient information on entity and data sources, researchers updated most of the metadata tags, such as *Summary*, *Description*, *Credits*, *Citations*, *Lineage*, and *Field* of the entities using the information available in the data sources from which the entity was



extracted. Metadata of entities can also be exported outside the geodatabase in the form of an Extensible Markup Language (XML) file. The slope repair maintenance and management system geodatabase can be viewed using ESRI ArcGIS Desktop applications (ArcMap, ArcGIS Pro, ArcCatalog, etc.). The metadata can be viewed through ESRI ArcCatalog. Figure 4.1 shows metadata for an example entity visualized in ArcCatalog.

The screenshot shows the ArcCatalog interface with the metadata for a feature class. The left pane shows a tree view with the feature class selected. The right pane displays the metadata details.

Name	Metadata	Geography	Table
PARIS_DIST_PRECIPITATION_ANNUA	<p><b>PARIS_DIST_PRECIPITATION_ANNUAL_AVERAGE_POLY</b></p> <p><b>Type</b> File Geodatabase Feature Class</p> <p><b>Tags</b> Precipitation, Texas, TxDOT, Paris District, USDA, NRCS, National Geospatial Center of Excellence, Slope Repair and Maintenance Management System, SRMMS</p> <p><b>Summary</b>            PARIS_DIST_PRECIPITATION_ANNUAL_AVERAGE_POLY is derived from 1981-2010 Annual Average Precipitation by State (USDA/NRCS), and covers only the TxDOT Paris District area. PARIS_DIST_PRECIPITATION_ANNUAL_AVERAGE_POLY is created to be used in TxDOT slope repair and maintenance management system. Vector dataset provides derived average annual precipitation according to a model using point precipitation and elevation data for the 30-year period of 1981-2010. The original dataset is created by USDA/NRCS - National Geospatial Center of Excellence.</p> <p><b>Description</b>            PARIS_DIST_PRECIPITATION_ANNUAL_AVERAGE_POLY is a raster layer that provides derived annual average precipitation in inches according to a model using point precipitation and elevation data for the 30-year period of 1981-2010 (USDA/NRCS, 2011). PARIS_DIST_PRECIPITATION_ANNUAL_AVERAGE_POLY is derived from 1981-2010 Annual Average Precipitation by State (USDA/NRCS), and covers only the TxDOT Paris District area. 1981-2010 Annual Average Precipitation by State is created by USDA/NRCS - National Geospatial Center of Excellence.</p> <p><b>Credits</b>            The U.S. Department of Agriculture, Service Center Agencies</p> <p><b>Use limitations</b></p> <ul style="list-style-type: none"> <li>• Copyright 2019. Texas Department of Transportation.</li> </ul>		

**Figure 4.1** Metadata visualization in ArcCatalog

## CHAPTER 5 MAP-BASED ARCGIS INTERFACE FOR UPDATING AND VISUALIZING DATA

### 5.1. INTRODUCTION

This chapter explains the map-based interface for visualizing and updating the spatial data entities collected for assessing the stability of the slope.

### 5.2. MAP-BASED INTERFACE

The researchers developed a map-based interface called Slope Repair and Maintenance Management System (SRMMS) to facilitate the visualization of the collected spatial data and to update slope failure records. Users will be able to add, delete, and update the slope failure feature along the corridors of the TxDOT Paris district. The developed prototype map-based interface displays the information, such as soil type, soil bulk specific density, hydraulic conductivity, and annual average precipitation, at slope failures to facilitate effective decision-making during slope repairs. The map-based interface is developed using ArcGIS online platform. The spatial data entities are published in ArcGIS online and added to a web map, which is used in the map-based interface. The map-based interface runs in a web browser and can be accessed from desktop and smartphones, which use windows, macOS, Android, iOS, and Linux operating systems. Figure 5.1 shows the schematics of information flow in the developed interface.

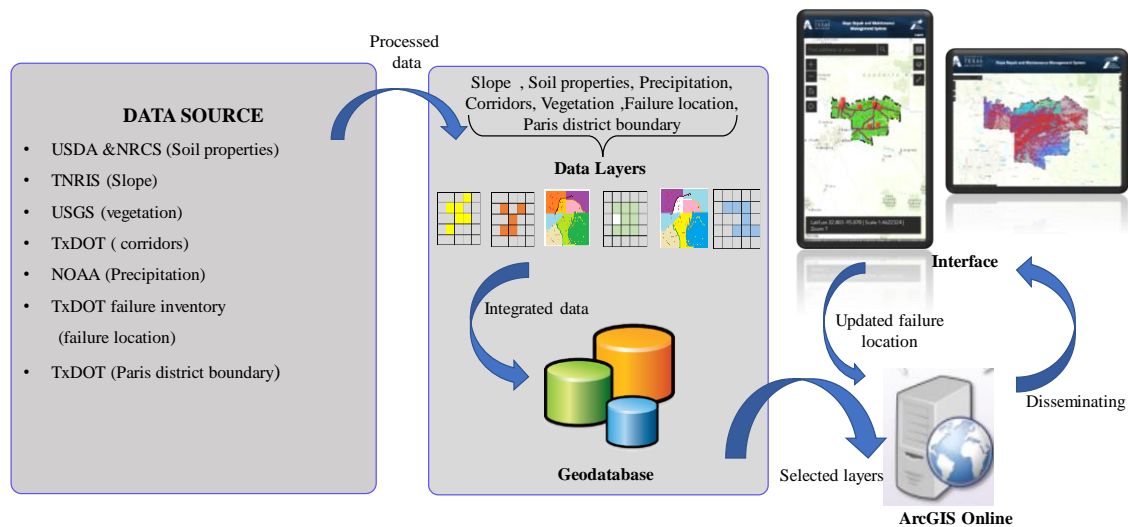


**Figure 5.1** Slope Repair and Maintenance Management System (SRMMS)



Figure 5.2 SRMSS interface showing different widgets

SRMMS includes an editor widget to add or edit a slope failure feature, as shown in Figure 5.2. To add or edit a slope failure feature, the entity that contains slope failure features should be displayed in the map-based interface. The user can display the entities in the map-based interface using the entity widget located on the top right of the map-based interface, as shown in Figure 5.2. Users can choose to display or overlay several entities on the map-based interface. Users can click on an individual slope failure feature to visualize the attributes (e.g., soil type, soil physical properties, annual average precipitation, etc.) of the slope failure feature, as shown in Figure 5.3. The legends for entities displayed in the map-based interface can be viewed by clicking on the legend widget located below the entity widget. Descriptions of the widgets in the map-based interface are shown in Table 5.1.

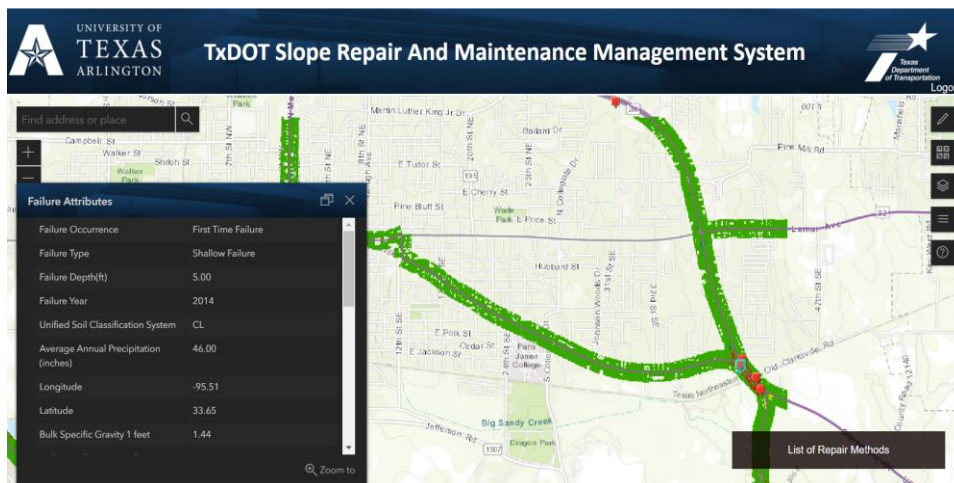


Figure 5.3 SRMSS interface displaying failure attributes

**Table 5.1** Description of Widgets in the map-based interface

<b>Widget Name</b>	<b>Description</b>
Search	This widget helps to find a specific location in the map-based interface.
Zoom In	This widget helps to zoom in the map view in the map-based interface.
Zoom Out	This widget helps to zoom out of the current map view in the map-based interface.
Home	This widget brings the map view to the initial view extent.
Locator	This widget helps to find the location of the user.
Basemap	This widget allows the user to select the basemap to be displayed in the map view of the map-based interface.
Entity	This widget displays the list of spatial data entities. Users can choose to display or remove the entities from the map in the map-based interface.
Editor	This widget allows the user to add or edit a slope failure feature in the map-based interface.
Legend	This widget displays the legends of the spatial data entities which are displayed in the map-based interface.
User Manual	This widget allows the user to access the user manual for the map-based interface.

### 5.3. ENTITIES IN MAP-BASED INTERFACE

The list of logical entities displayed in the map-based interface are mentioned below:

- 1) PAST SLOPE FAILURE
- 2) PARIS DISTRICT BOUNDARY
- 3) PARIS DISTRICT SOIL PROPERTY
- 4) PARIS DISTRICT STABILIZED SLOPE
- 5) PARIS DISTRICT CONNECTIVITY CORRIDOR
- 6) PARIS DISTRICT PRECIPITATION ANNUAL AVERAGE
- 7) PARIS DISTRICT CORRIDOR SLOPE VECTOR3M
- 8) PARIS DISTRICT SLOPE GRID3M
- 9) PARIS DISTRICT NLCD2016 LAND COVER

### 5.4. USE CASES

A use case is a set of possible sequences of interactions between a user and a system. The use case clearly indicates what action the system takes in response to what action is taken by the user. A use case diagram is a graphical table of contents for individual use-cases and defines a system

boundary. Figure 5.4 represents the use case diagram for Slope Repair and Maintenance Management System (SRMMS).

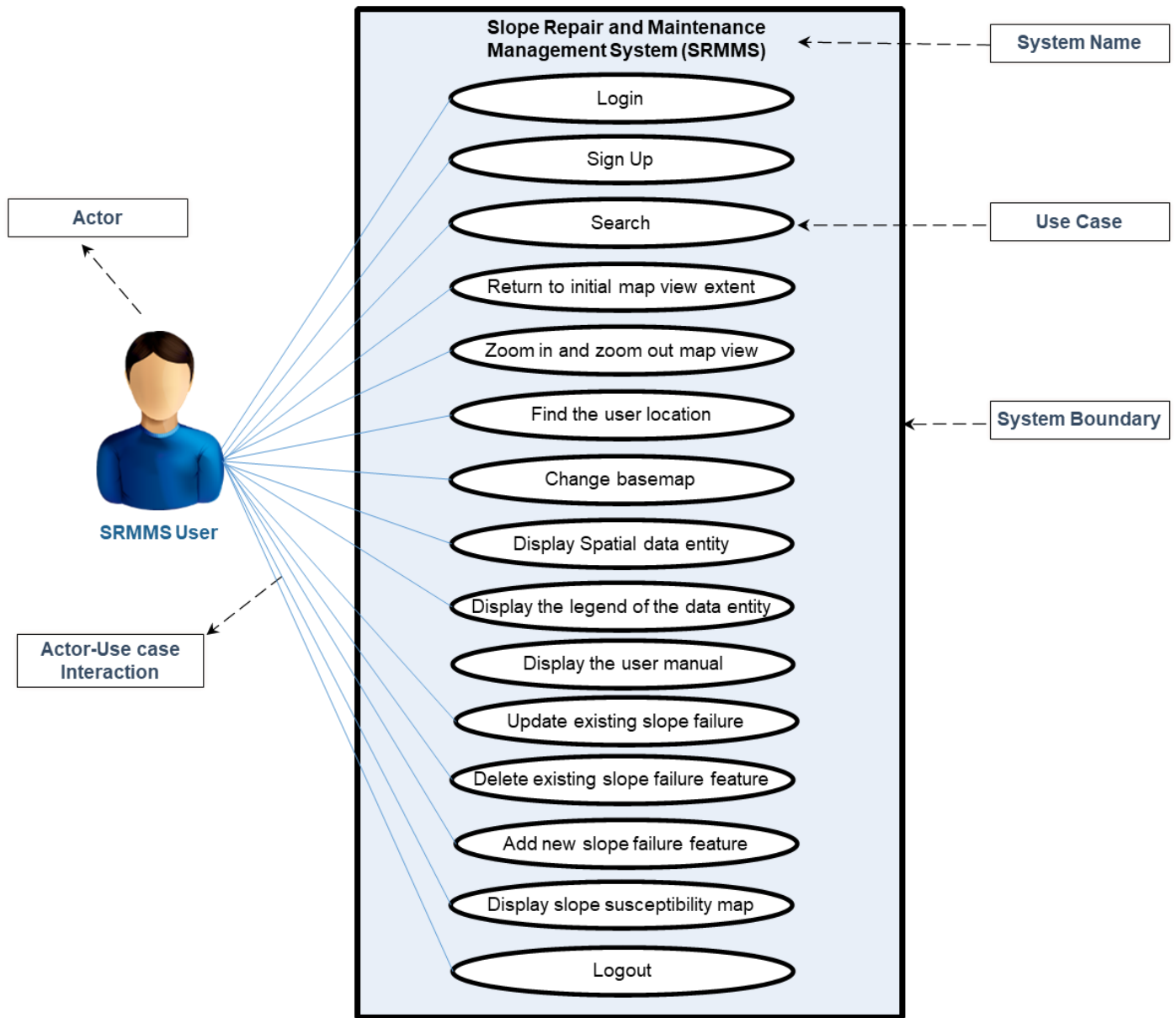


Figure 5.4 Use Case Diagram

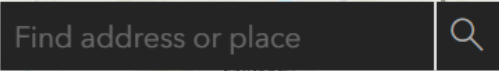
**Table 5.2 UC1: Login**

Actor: User	System: SRMMS
	0. The browser displays a web page.
1. The user enters the web address in the address bar and press enter. URL: <a href="https://axb9294.uta.cloud/SRMMS/login.php">https://axb9294.uta.cloud/SRMMS/login.php</a>	2. The system displays the login page which prompts the user to login using username and password.
3. The user enters the username and password, then clicks the login button.	4. The system displays <ul style="list-style-type: none"> <li>a. The map-based interface if username and password are entered correctly.</li> <li>b. The message requesting to recheck inputs if the user name or password is incorrect.</li> </ul>
5. The user sees the map-based interface or login error is displayed.	


**Table 5.3 UC2: Sign Up**

Actor: User	System: SRMMS
	0. The browser displays a web page.
1. The user enters the web address in the address bar and press enter.	2. The system displays the login page which prompts the user to login using username and password along with the option to sign up for a new account.
3. The user clicks on the Sign Up button.	4. The system prompts the user to sign up page.
5. The user fills the information (First Name, Last Name, Email address, Password) requested in the sign-up page and clicks the Sign Up button to complete the process.	6. The system sends an email to the user email address for activation of the account.
7. The user opens the email and clicks the activation link to activate the account.	8. The system registers the user and displays the confirmation of registration.


**Table 5.4 UC3: Search**

Actor: User	System: SRMMS
	0. The system displays the map-based interface.
1. The user enters the location on the search bar. 	2. The system displays the searched location.

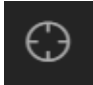
**Table 5.5** UC4: Return to initial map view extent

Actor: User	System: SRMMS
	0. The system displays the map-based interface.
1. The user clicks the home button. 	2. The system returns to the initial map view extent.

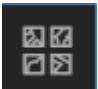
**Table 5.6** UC5: Zoom in and zoom out of the map view

Actor: User	System: SRMMS
	0. The system displays the map-based interface.
1. The user clicks the zoom in or zoom out button. 	2. The system zooms in or zooms out in the map view of the map-based interface.


**Table 5.7** UC6: Find the user location

Actor: User	System: SRMMS
	0. The system displays the map-based interface.
1. The user clicks the locator widget. 	2. The system displays the location of the user in the map-based interface.

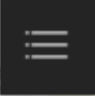
**Table 5.8** UC7: Change basemap

Actor: User	System: SRMMS
	0. The system displays the map-based interface.
1. The user clicks the basemap widget. 	2. The system displays the available basemaps from which the user can make the selection.
3. The user clicks on the desired basemap.	4. The system changes the existing basemap to the basemap selected by the user.
5. The user clicks on the basemap widget.	6. The system closes the expanded basemap widget.

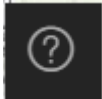
**Table 5.9** UC8: Display spatial data entity

Actor: User	System: SRMMS
	0. The system displays the map-based interface.
1. The user clicks the entity widget. 	2. The system expands the entity widget and displays the list of spatial data entities.
3. The user clicks on the entity to turn it on and off.	4. The system displays or removes the entity from the map view.
5. The user clicks on the entity widget to close the list of entities.	6. The system closes the expanded entity widget.

**Table 5.10** UC9: Display the legend of the data entity


Actor: User	System: SRMMS
	0. The system displays the map-based interface.
1. The user clicks the legend widget. 	2. The system displays the legend of the entities displayed in the map-based interface.

**Table 5.11** UC10: Display the user manual


Actor: User	System: SRMMS
	0. The system displays the map-based interface.
1. The user clicks the legend widget. 	2. The system expands the widget and provides the user an option “click here” to open the user manual.
3. The user clicks on “click here” to open the user manual.	4. The system opens the user manual.




**Table 5.12** UC11: Update existing slope failure feature

<b>Actor: User</b>	<b>System: SRMMS</b>
	0. The system displays the map-based interface.
1. The user clicks the editor widget. 	2. The system displays the editor tab with two options: a. Edit feature b. Add Feature
3. The user clicks on the edit feature.	4. The system prompts the user to select the slope failure feature to edit.
5. The user zooms and clicks on the desired slope failure feature that needs to be updated.	6. The system displays the attributes of the failure.
7. The user a. Updates the following information and clicks on the update button. o Failure Occurrence ✓ First-time failure or, ✓ Recurring Failure o Failure Type ✓ Shallow failure or, ✓ Deep Failure o Failure Depth (ft) o Failure Year (YYYY) b. Click on the back button without performing edits.	8. The system a. Updates the failure location and prompts the user to select another failure feature to update. b. Prompts the user to select another slope failure feature to update.
9. The user a. Clicks on the back button and returns to step 2. b. Clicks on the back button and returns to step 2.	10. The system displays the editor tab as in step 2.
11. The user clicks on the editor widget.	12. The system closes the expanded editor widget.


**Table 5.13** UC12: Delete a slope failure feature

<b>Actor: User</b>	<b>System: SRMMS</b>
	0. The system displays the map-based interface.
1. The user clicks the editor widget. 	2. The system displays the editor tab with two options: a. Edit feature b. Add Feature
3. The user clicks on the edit feature.	4. The system prompts the user to select the slope failure feature to edit.
5. The user zooms and clicks on the desired slope failure feature that needs to be deleted.	6. The system displays the attributes of the slope failure feature.
7. The user a. Clicks the delete button to remove the slope failure feature. b. Clicks on the back button without performing edits.	8. The system a. Asks the user for confirmation to delete the slope failure feature. b. Prompts the user to select another slope failure feature.
9. The user a. Clicks confirm to remove the selected failure site. b. Clicks on the back button to return to step 2.	10. The system a. Prompts the user to select another slope failure feature. b. Display the editor tab as in step 2.
11. The user a. The user clicks on the back button to return to step 2 and clicks the editor widget. b. The user clicks on the editor widget.	12. The closes the expanded editor widget.

**Table 5.14** UC13: Add new slope failure feature

<b>Actor: User</b>	<b>System: SRMMS</b>
	0. The system displays the map-based interface.
1. The user clicks the editor widget. 	2. The system displays the editor tab with two features: a. Edit feature b. Add Feature
3. The user clicks on add feature.	4. The system prompts the user to select a recurring failure or first-time failure.
5. The user clicks on one of the following options: a. First Time Failure b. Recurring Failure	6. The system prompts the user to add a feature.
7. The user zooms and clicks on the desired failure location and add a slope failure feature.	8. The system displays the tab to update the attributes of the failure.
9. The user a. Fills the following information and clicks the add button. ○ Failure Occurrence ✓ First-time failure or, ✓ Recurring Failure ○ Failure Type ✓ Shallow failure or, ✓ Deep Failure ○ Failure Depth (ft) ○ Failure Year (YYYY) b. Clicks on the back button.	10. The system a. Adds the slope failure feature and ask the user to add a new failure. b. Informs the user that the failure location will not be added to the system.
11. The user a. Clicks on the back button to return to step 2. b. Clicks on discard to remove the added slope failure feature and clicks back.	12. The system displays the editor tab as in step 2.
13. The user clicks on the editor widget.	14. The system closes the expanded editor widget.

**Table 5.15** UC14: Display slope susceptibility map

<b>Actor: User</b>	<b>System: SRMMS</b>
	0. The system displays the map-based interface.
1. The user clicks the entity widget. 	2. The system expands the entity widget and displays the list of spatial data entities.
3. The user clicks on the slope susceptibility map from the list of entities.	4. The system accordingly displays and slope susceptibility map in the map-based interface.
5. The user clicks on the entity widget to close the displayed entity tab.	6. The system closes the expanded entity widget.

**Table 5.16** UC15: Logout

<b>Actor: User</b>	<b>System: SRMMS</b>
	0. The system displays the map-based interface.
1. The user clicks the logout out button on the application.	2. The system exits the application.

## CHAPTER 6 SLOPE FAILURE PREDICTIVE MODELING

### 6.1. INTRODUCTION

This chapter explains the development of the slope failure predictive model for identifying the critical slope segments in the TxDOT Paris district. First, a literature review on slope failure susceptibility analysis methods is performed. Second, the causative factors for the slope instabilities are identified. Finally, the slope failure susceptibility model developed for identifying the critical slope segments is outlined.

### 6.2. LITERATURE REVIEW

#### 6.2.1. Slope Susceptibility Analysis Methods

Slope susceptibility analysis methods are broadly classified into qualitative and quantitative methods (Zimmerman et al., 1986; Guzzetti et al., 1999; Huabin et al., 2005; Carrara et al., 1999; Clerici et al., 2002; Ramanathan et al., 2014; Mohseni et al., 2018). Quantitative methods can be categorized into statistical models and physical geotechnical models. Qualitative methods include techniques such as geomorphological mapping, landslide inventory mapping, and heuristic or index-based approach.

#### Quantitative Analysis

- *Statistical Models*

This approach uses statistical techniques, such as bivariate analysis and multivariate analysis, to establish the relationship between the causative factors and failure at the site (Carrara, 1983; Baeza et al., 2001; Baeza et al., 2003; Shahabi et al., 2013). Both bivariate and multivariate approaches depend on the quality and quantity of the collected data. These data-driven techniques need adequate information on past slope failures; inadequate and underrepresented data may give unreasonable results (Nandi et al., 2010).

- *Physical geotechnical models*

Physics-based models use geotechnical methods to establish the relationship among a set of physical parameters (e.g., engineering soil properties, slope angles, and rainfall) to determine slope stability (Iverson, 2000; Bhattarai et al., 2004; D'Odorico et al., 2005, Berti et al., 2010; Mohseni et al., 2018; Zhang et al., 2018; Hidalgo et al., 2018). The infinite slope stability theory coupled with the hydrological model is a commonly used approach for the assessment of slopes instability due to rainfall (Iverson, 2000; D'Odorico et al., 2005).

## **Qualitative Method**

- *Geomorphological Mapping*

Geomorphological mapping is a widely accepted technique to develop a map of an area depicting the landform and surface as well as subsurface material, generally by an interpretation of data collected in the field, aerial photographic interpretation, sub-surface investigation and monitoring (Whitworth et al., 2011; Lee, 2001; Zimmerman et al., 1986; Seeley and West, 1990). Geomorphological maps can act as a preliminary tool for land management and geological risk management (Smith et al., 2011).

- *Landslide inventory mapping*

Landslide inventory mapping is a technique to develop a landslide hazard map of a region by recording landslides location, date of occurrence, and geographical extent of each landslide in an area (Guzzetti et al., 1999; Guzzetti, 2012). Landslide inventory map is an important tool for hazard and risk assessment of slopes.

- *Heuristic or Index-based method*

The heuristic analysis is based on experts' opinions and past slope failure experience to assess the stability of slopes (Neeley et al., 1990; Singh et al., 2008; Ramanathan et al., 2012). Factors, such as slope angles, soil properties, precipitation, vegetation, and groundwater table, that influence

slope stability are identified based on the past slope failures. These factors are then weighted to assess the stability of slopes.

### **6.2.2. Causative Factor for Slope Instability**

A list of major causative factors is determined from the literature that would be relevant for assessing the stability of slopes in the TxDOT Paris district (Bhattarai et al., 2004; Chau et al., 2004; Ramanathan et al., 2012; Mohseni et al., 2018). These causative factors are listed below:

#### **Slope Angle**

A slope angle is one of the most widely selected factors for slope stability analysis. Slope failure can take place gradually or suddenly when the shear strength of the soil cannot resist the gravimetric forces, which increases with the increase in slope angle, moving the soil mass down the slope (Hossain et al., 2017). Steeper slopes are more susceptible to failure compared to shallow slopes (Nelson, 2013). However, the slope angle alone should not be used to determine the stability of slopes. Other factors, such as soil properties, vegetation, and drainage system, which influence the stability of slopes, may cause the relatively shallow slope to be prone to failure, while a relatively steep slope to be stable (Mohseni et al., 2018).

#### **Soil Type and Properties**

The stability of slopes is highly dependent on the geotechnical properties (shear strength, permeability) of the soil. Clayey soils are susceptible to shallow slope failure during intense and prolonged rainfall events (Khan et al., 2017). The soil with higher friction angle and cohesion are less prone to failure (Stark et al., 2005; Nelson, 2013). Physical geotechnical models take into consideration the soil type and properties for analyzing the stability of slopes. The determination of rainfall intensity and duration that causes the failure of slopes depends on the hydraulic properties (e.g., saturated conductivity, water holding capacity) of soil (Iverson, 2000; D'Odorico et al., 2005).

## **Precipitation**

The shallow slope failures are typically followed by rainfalls (Hossain, 2013). Empirical equations have been formulated to obtain minimum intensity duration relation that can initiate shallow landslide and debris flow (Caine, 1980; Innes, 1983; Crosta et al., 2001; Guzzetti et al., 2008). Highway slopes with clayey soils are prone to desiccation due to the wetting and drying weather cycle, which allows greater moisture infiltration into the embankment from precipitation (Jafari et al., 2018). This causes an increase in the moisture content of the soil and a reduction in the shear strength.

## **Vegetation**

Vegetation enhances slope stability modifying the soil water regime, which results in a change in pore water pressure and soil suction, and through root reinforcement (Coppin et al., 1990; Chok et al., 2004). Trees increase the stability of slopes hydrologically by increasing the matric suction of soil that leads to an increase in the shear strength (Ali et al., 2012). The root density within the soil mass and tensile strength of the roots mechanically increase the soil strength (Greenwood et al., 2004). Plant rooting systems in many biotechnical methods provide better reinforcement and drainage characteristics than the earthwork associated with mechanical methods such as slope repair, retaining walls, and sheet piles (Shahandashti et al., 2019). One of the studies in Maryland revealed that 56% of the total number of slope failures occurred in the area with medium to low grass density (Ramanathan et al., 2014). Vegetation also aids in the stability of slopes by reducing the infiltration and providing erosion protection for the top layer of the soil (Zuazo et al., 2009).

## **Drainage System**

Water drainage systems are essential to the durability and performance of embankment slopes. Many slope failures are caused due to the absence of a surface and subsurface drainage system (Shahandashti et al., 2019). The surface drainage system must be used to reduce infiltration and subsurface drainage system must be used to control groundwater. Effective water drainage decreases driving forces for slope instability and increases soil shear strength (Lohnes et al. 2001).



### 6.3. DEVELOPMENT OF SLOPE FAILURE PREDICTIVE MODEL

A slope failure predictive model was developed using the existing body of modeling approaches and hydrological concepts within the realm of geotechnical engineering. Infinite slope instability theory, in combination with the transient rainfall response model (Iverson, 2000), was used to determine the duration of rainfall that triggers slope instability. The developed slope failure predictive model was used to assess the condition of highway slopes in the TxDOT Paris district. The critical segments of highway embankments were identified and classified based on rainfall duration that triggers the slope instability. The next section provides the detailed stepwise description of the slope failure predictive model used to predict and classify the critical segments of embankments in clayey soils.

#### 6.3.1. Steps for Determining Highway Slopes Susceptibility

##### **Step 1:** *Determining Fully softened Frictional angle*

Shear strength of embankments constructed in clayey soils is reduced to fully softened strength due to the effect of weathering, infiltration, wetting, swelling and stress relief (Skempton 1970; Wright et al. 2007; Castellanos et al., 2015). Back analyses of failed embankments have shown that fully softened shear strength is mobilized in the first-time failures for compacted embankments constructed of highly plastic clays (Kayyal and Wright 1991; Wright et al. 2007) and for cuts in stiff clays (Skempton 1970, 1977). The softening of the soil occurs in soils with a liquid limit above 40 and a plastic index above 20 (Castellanos et al., 2015). Stark et al. (2013) and Gamez and Stark (2014) determined a fully softened frictional angle as a function of liquid limit (LL), clay-size fraction (CF), and effective normal stress. The effective normal stress at different soil depths can be determined using the unit weight of soil. The data on soil liquid limit, clay-size fraction, and unit weight was obtained from the geodatabase created in Task 1 of the project. These data were used to determine the fully softened shear strength at the desired depth for slope stability analysis. The correlation function to obtain a fully softened frictional angle with the liquid limit for different clay fractions and effective stresses is shown in Figure 6.1 (Gamez and Stark 2014). The shallow failures occur at low effective normal stresses (i.e., less than 50 kPa). The correlation equation (Equation 1) for determining the fully softened frictional angle for effective normal

stresses of 12 kPa and 50 kPa was obtained from Stark et al. (1997, 2013) and Gamez and Stark (2014). The fully softened frictional angle due to effective normal stress between 12 kPa and 50 kPa was linearly interpolated.

$$CF \leq 20; 30 \leq LL < 80$$

$$\phi_{12kPa}(LL) = 35 \cdot 33 - 5 \cdot 85 \times 10^{-2}(LL) + 9.71 \times 10^{-5}(LL)^2 \quad (1a)$$

$$\phi_{50kPa}(LL) = 34 \cdot 85 - 0.0709(LL) + 2.35 \times 10^{-4}(LL)^2 \quad (1b)$$

$$25 \leq CF \leq 45; 30 \leq LL < 130$$

$$\phi_{12kPa}(LL) = 38 \cdot 1 - 1.19 \times 10^{-1}(LL) + 2.48 \times 10^{-4}(LL)^2 \quad (1c)$$

$$\phi_{50kPa}(LL) = 36 \cdot 18 - 0.1143(LL) + 2.354 \times 10^{-4}(LL)^2 \quad (1d)$$

$$CF \geq 50; 30 \leq LL < 300$$

$$\phi_{12kPa}(LL) = 36.45 - 9.18 \times 10^{-2}(LL) - 1.09 \times 10^{-4}(LL)^2 + 1.1 \times 10^{-7}(LL)^3 \quad (1e)$$

$$\phi_{50kPa}(LL) = 33.37 - 0.11(LL) + 2.34 \times 10^{-4}(LL)^2 - 2.96 \times 10^{-7}(LL)^3 \quad (1f)$$

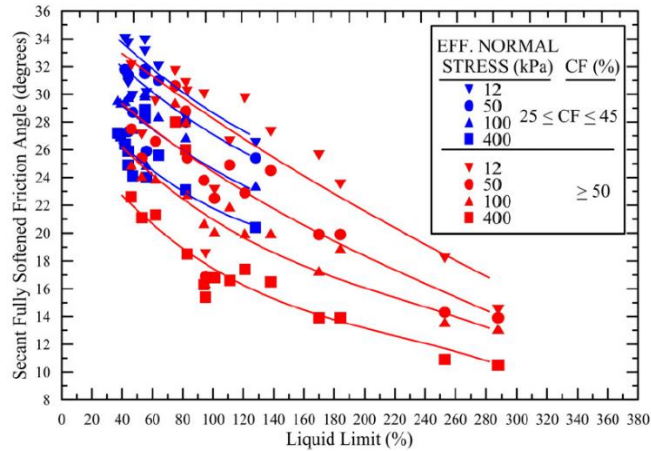


**Figure 6.1** Drained fully softened frictional angle correlation between for CFs 25-45% and CF  $\geq$  50% (Gamez and Stark, 2014)

### Step 2: Determining unstable slopes

Infinite slope stability theory was used to determine the factor of safety (FOS) for slopes. Infinite slope failure is the movement of the soil mass approximately parallel to the slope face (Das, 2010). Failure of a slope occurs when the downslope component of gravitational force on soil mass exceeds the resisting force due to column friction. Equation (2) was used to determine the FOS of a slope at depth  $z$  (Figure 6.2) from the upper slope surface.

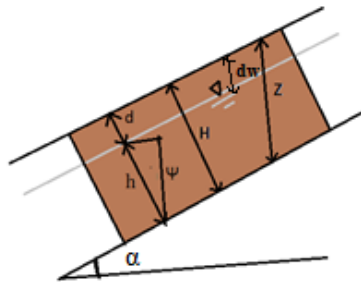


**Figure 6.2** Slope failure parallel to surface showing the model parameters

$$\text{FOS} = F_f + F_w + F_c \quad (2a)$$

$$F_f = \frac{\tan\phi}{\tan\alpha} \quad (2b)$$

$$F_c = \frac{c}{\gamma_s z \sin\alpha \cdot \cos\alpha} \quad (2c)$$

$$F_w = - \frac{\Psi(\gamma_w)\tan\phi}{\gamma_s z \sin\alpha \cos\alpha} \quad (2d)$$

Where  $c$  is the cohesion of soil,  $z$  is the depth of failure,  $\gamma_s$  is the unit weight of soil,  $\gamma_w$  is the unit weight of water,  $\phi$  is a fully softened internal angle of friction,  $\alpha$  is the slope angle, and  $\Psi$  is the soil water pressure at depth  $z$ .

The maximum plausible failure depth must be specified in the analysis of slopes using the infinite slope stability theory. Without the specification, no bound exists for slope failure thickness (Iverson, 2000). Mohseni et al. (2018) assumed a failure depth of 6 feet for developing slope failure susceptibility maps of two counties in Minnesota. Shallow slope failures in clayey embankments occur within the upper 3 to 10 feet of the slope (Castellanos et al., 2015; Khan et al., 2017). Moisture variation in soil due to rainfall infiltration also varies within upper 10 ft of slope surface (Hossain, 2013; Castellanos et al., 2015). The geodatabase developed in Task 1 of this project provided the information on soil properties for the depth up to 7 feet from the surface. The value of FOS was calculated for the depths of 3, 4, 5, 6, and 7 feet using the fully softened frictional angle obtained for each depth. The cohesion was assigned a value of zero for clayey soils with high swelling and shrinkage potential following the recommending of Stark et al. (2005). The FOS for a slope at varying depths is calculated assuming the entire soil column is filled with water (i.e.,  $\Psi = z \cos^2 \alpha$ ). The analysis result showed that 7 feet depth caused more slopes to fail. So, a uniformly constant thickness of 7 feet was considered for developing slope failure susceptibility maps. The slopes with  $FOS > 1$  were considered unconditionally stable. Slopes having  $FOS < 1$  were considered unstable and were further analyzed to determine the duration of rainfall that triggers the slope instability.

### **Step 3:** *Obtaining dimensionless critical soil water pressure that initiates failure*

For the slopes with the factor of safety (FOS) smaller than 1, the ratio of soil water pressure ( $\Psi$ ) to the depth of failure ( $z$ ),  $\Psi^*_{crit}$ , which would initiate the failure (i.e., assuming  $FOS = 1$ ), was obtained.  $\Psi^*_{crit}$ , also termed as dimensionless critical soil water pressure, was determined using Equation (3) (D'Odorico et al., 2005):

$$\psi^*_{crit} = \frac{\Psi}{z} = \frac{\gamma_s}{\gamma_w} \left(1 - \frac{\tan \alpha}{\tan \phi}\right) \cos^2 \alpha + \frac{c}{\gamma_w z \tan \phi} \quad (3)$$

**Step 4:** Obtaining the duration of rainfall that causes dimensionless critical soil water pressure

Change in soil water pressure in response to vertical rainfall infiltration for a shallow depth and wet soils (i.e., the hydraulic conductivity,  $K_z$ , is equivalent to saturated hydraulic conductivity,  $K_{sat}$ ) was obtained using Equation (4) (Iverson, 2000).

$$\frac{\partial \psi}{\partial t} = D_0 \cos^2 \alpha \frac{\partial^2 \psi}{\partial z^2} \quad (4)$$

Where  $\psi$  is the soil water pressure and  $D_0 = k_{sat} / C_0$ .  $C_0$  is the minimum value of  $C(\Psi)$ .

$C(\psi) = d\theta / d\psi$  is the change in volumetric water content per unit change in pressure head.  $C_0$  depends on soil type (Table 6.1).

**Table 6.1** Ratio of Volumetric water content versus pressure head at saturation (Mohseni et al., 2018)

USCS Soil Class	Description	$C_0(1/m)$
CH	Clay of high plasticity, fat clay	0.01
CL	Clay of low plasticity, lean clay	0.01
CL-ML	Silty clay	0.01
GM	Silty gravel	0.001
MH	Silt of high plasticity	0.01
SC-CL	Clayey sand with many fines	0.12
SW	Well-graded sand fine to coarse sand	0.02

The time-varying dimensionless soil water pressure,  $\Psi^*(t^*)$ , due to rainfall rate,  $I_z$ , was obtained by solving Equation (4) with suitable initial and boundary conditions (Iverson, 2000) driving Equation (5):

$$\Psi^*(t^*) = \frac{\Psi(t^*)}{z} = \left(1 - \frac{d_w}{z}\right) \cos^2 \alpha + \frac{I_z [R(t^*)]}{k_z} \quad 0 \leq t^* \leq T^* \quad (5a)$$

$$\Psi^*(t^*) = \frac{\Psi(t^*)}{z} = \left(1 - \frac{d_w}{z}\right) \cos^2 \alpha + \frac{I_z[R(t^*) - R(t^* - T^*)]}{k_z} \quad t^* \geq T^* \quad (5b)$$

$\Psi(t^*)$  is the pore water pressure at time  $t^*$  and  $d_w$  is the depth of the initial groundwater table (Figure 6.2).

$T^*$  is nondimensional rainfall duration, and  $t^*$  is nondimensional time given by:

$$t^* = \frac{4D_0 \cos^2 \alpha}{z^2} t \quad T^* = \frac{4D_0 \cos^2 \alpha}{z^2} T \quad (6)$$

In Equation (6),  $T$  is the rainfall duration, and  $t$  is the time at which soil water pressure should be calculated.

$R(t^*)$  is a response function given by:

$$R(t^*) = \sqrt{\frac{t^*}{\pi}} \exp\left(-\frac{1}{t^*}\right) - \text{erfc}\left(\sqrt{\frac{1}{t^*}}\right) \quad (7)$$

Where  $\text{erfc}$  is the complementary error function.

In the study of slope stability, it is essential to determine the time,  $t_p^*$ , at which the peak value of pressure head occurs for the duration of rainfall,  $T^*$ . The peak time,  $t_p^*$ , was determined by solving the condition  $d\psi^*(t^*)/d(t^*) = 0$  for Equation (5):

$$\frac{I_z}{k_z} \frac{dR(t^*)}{dt^*} = \frac{I_z}{k_z} r(t^*) = 0 \quad 0 \leq t^* \leq T^* \quad (8a)$$

$$\frac{I_z}{k_z} \frac{dR(t^*)}{dt^*} = \frac{I_z}{k_z} (r(t^*) - r(t^* - T^*)) = 0 \quad t^* \geq T^* \quad (8b)$$

where,

$$r(t^*) = \frac{dR(t^*)}{d(t^*)} = \frac{1}{2\sqrt{\pi t^*}} \exp\left(-\frac{1}{t^*}\right) \quad (8c)$$

Equation (8) can be solved, providing the estimate of  $t_p^*$  for different rainfall duration,  $T^*$ . Figure 6.3 shows the plot of  $t_p^*$  for the rainfall duration of  $T^*$ . For the duration of rainfall  $T^* \leq 1$ , the time to peak is almost constant,  $t_p^* \sim 2$ , and linearly increases with  $T^*$  when  $T^* > 1$ . For longer rainfall durations, peak soil water pressure occurs at the end of rainfall duration and  $t_p^* \sim T^*$ .

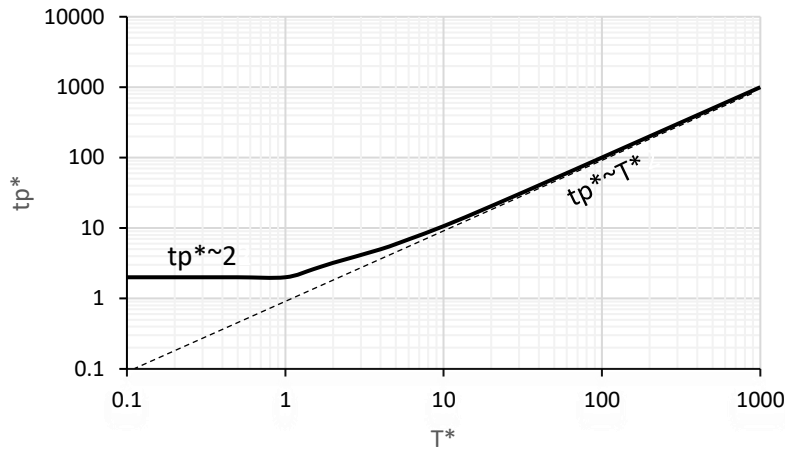


**Figure 6.3** Graph of peak response duration,  $tp^*$ , for a wide range of normalized rainfall duration  $T^*$  (Iverson, 2000)

With the increasing return period, the rainfall intensity increases for any specified duration of rainfall. Therefore, the steady-state rainfall rate  $I_z$  (the ratio of rainfall intensity (depth) to the duration of rainfall) also increases with the increasing return period. Ideally, the soil water pressure should also increase with increasing return period; but, this occurs only if  $I_z/k_z < 1$  (i.e., rainfall rate is less than infiltration rate) in Equation (5). If the rainfall rate is greater than the infiltration rate ( $I_z/k_z > 1$ ), the maximum value of  $I_z/k_z$  is limited to 1. The surplus rainfall runs off as Horton overland flow, and soil water pressure becomes independent of the rainfall return period. This is supported by a stability analysis of clayey embankments in Texas, where FOS was found to be independent on the rainfall return period but decreased with the increasing duration of rainfall (Hossain et al., 2012). In clayey soils, the conductivity is usually lower compared to the rainfall rate. Hence, it is more convenient and practical to categorize the slope stability based on the rainfall duration rather than the return period.

The data from intensity distribution frequency (IDF) obtained from the National Oceanic and Atmospheric Administration (NOAA) was used to estimate the duration of a rainfall triggering slope failure. The rainfall intensities (depths) for different durations were converted to a steady-state rainfall rate ( $I_z$ ) for use in Equation (5). The peak pressure heads corresponding to different rainfall durations, intensities, and return periods were determined for the slopes as shown in Figure 6.4. The critical rainfall that triggers a slope failure is of duration  $T^*_+$  (Figure 6.4), which develops

a dimensionless peak soil water pressure  $\Psi_p^*(t^*)$  equivalent to dimensionless critical soil water for the failure ( $\Psi^*_{crit}$ ) calculated in Step 3.

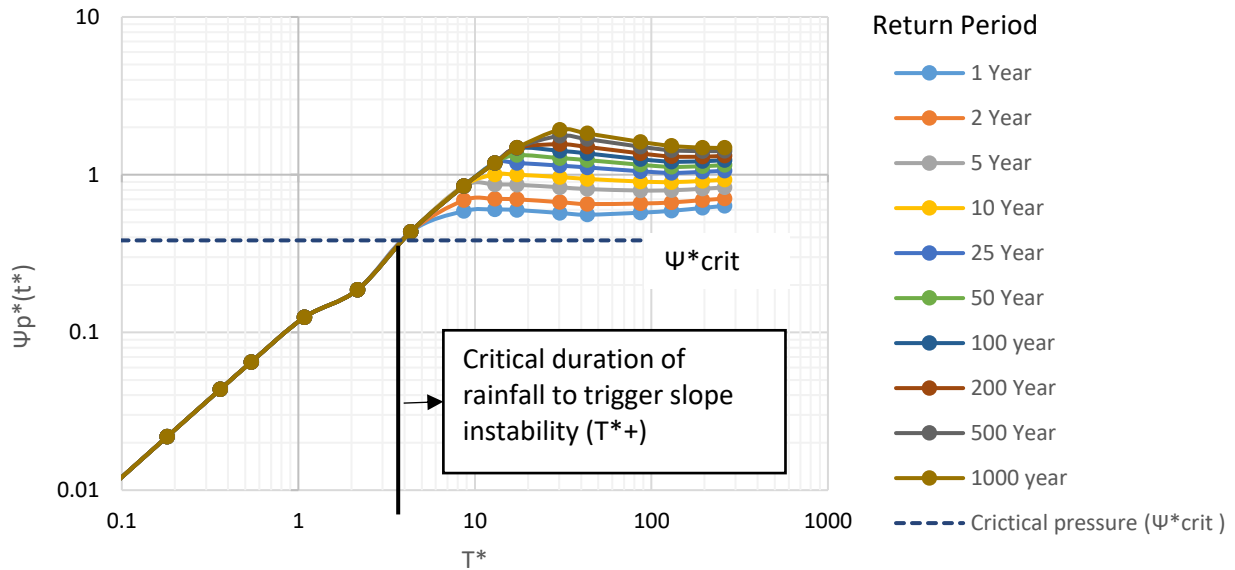


**Figure 6.4** Graphs of pressure head  $\Psi_p^*(t^*)$  versus normalized rainfall duration  $T^*$  for different return periods

### 6.3.2. Failure Susceptibility Indicator Scheme

Based on the duration of rainfall that triggers slope instability, we developed slope failure susceptibility maps. A slope failure susceptibility map represents slopes in four categories:

**Highly Critical:** slopes that are susceptible to failure due to the rainfall duration of fewer than 3 days.

**Critical:** slopes that are susceptible to failure due to the rainfall duration between 3-10 days.

**Moderately Critical:** slopes that are susceptible to failure due to the rainfall duration between 10-45 days.

**Non-Critical:** slopes that are susceptible to failure due to the rainfall duration of more than 45 days.

The selection of the breakpoint in the categorization of the slopes is subjective and can be altered based on the past rainfall durations that induced slope failures in the embankments.



#### 6.4. SLOPE FAILURE SUSCEPTIBILITY MAPS

Slope failure susceptibility maps were developed by performing the slope failure susceptibility analysis in two different grid sizes; 3 m grid size uses the slope angles derived from the LiDAR dataset, and 10 m grid size uses the slope angles derived using National Elevation Data (NED). Figure 6.5 shows the corridors where LiDAR data is available. Figure 6.6 and Figure 6.7 show the slope failure susceptibility maps developed for a 1000m stretch of a highway corridor with a grid size of 3 m and 10 m, respectively. These maps show a stretch of road near US 75 and Randall Lake Rd intersection in Grayson county. It is observed that the slope failure susceptibility map developed using the slope angles derived from NED predicts longer durations of rainfall for slope instability. This is because the slope angles obtained using NED are less steep in comparison to slope angles obtained from the LiDAR dataset. The LiDAR-derived slopes are more accurate and available in higher resolution compared to NED. Therefore, the LiDAR-derived slope angles with the granularity of 3 m were used to develop the slope failure susceptibility maps. The slope failure susceptibility maps of highway embankments were created for corridors shown in Figure 6.5. Ten past slopes failures were located in the corridors shown in Figure 6.5. Nine slope failures lie in highly critical regions, which require rainfall duration of fewer than 3 days to trigger slope instability, and one slope failure lies in the critical region, which requires less than 7 days rainfall to trigger slope instability.

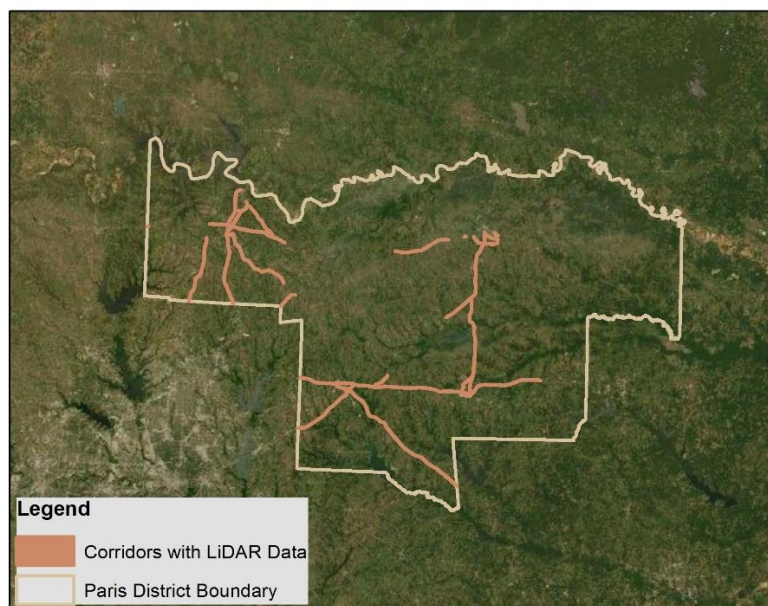


**Figure 6.5** Corridors with the availability of LiDAR data

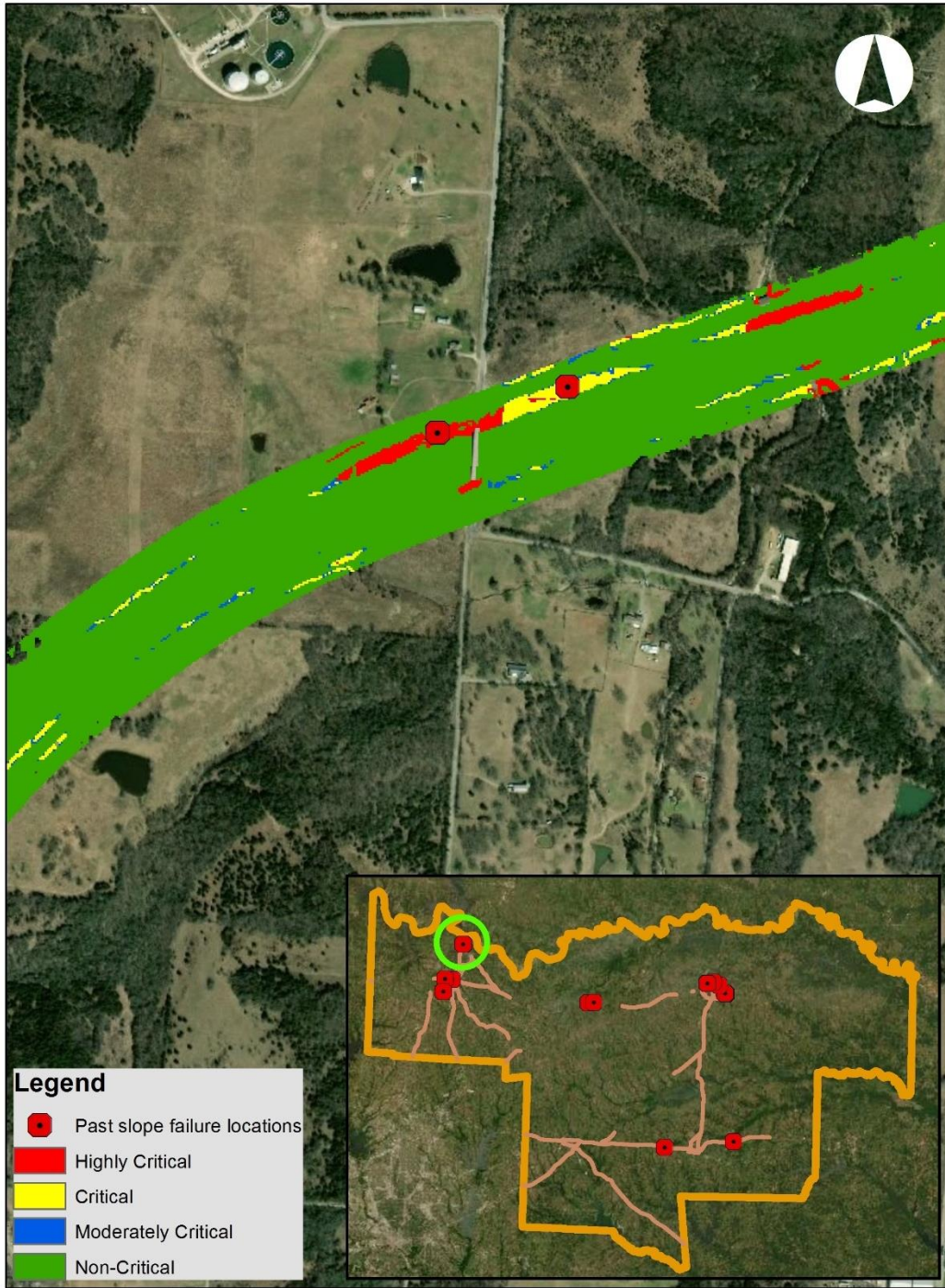


**Figure 6.6** Slope failure susceptibility map of Grayson county at US 75 and Randall Lake Rd intersection using LiDAR-derived slope angles

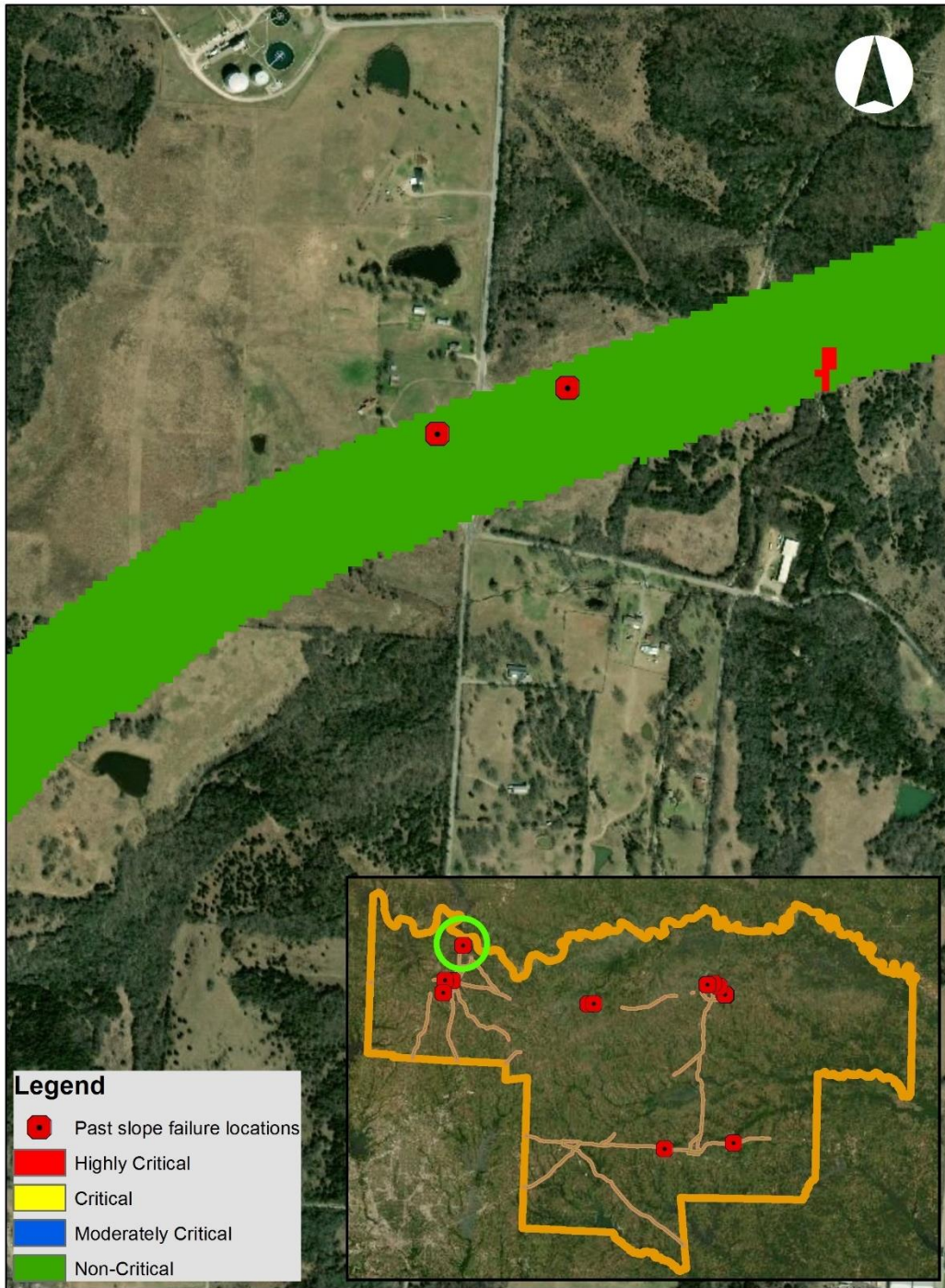
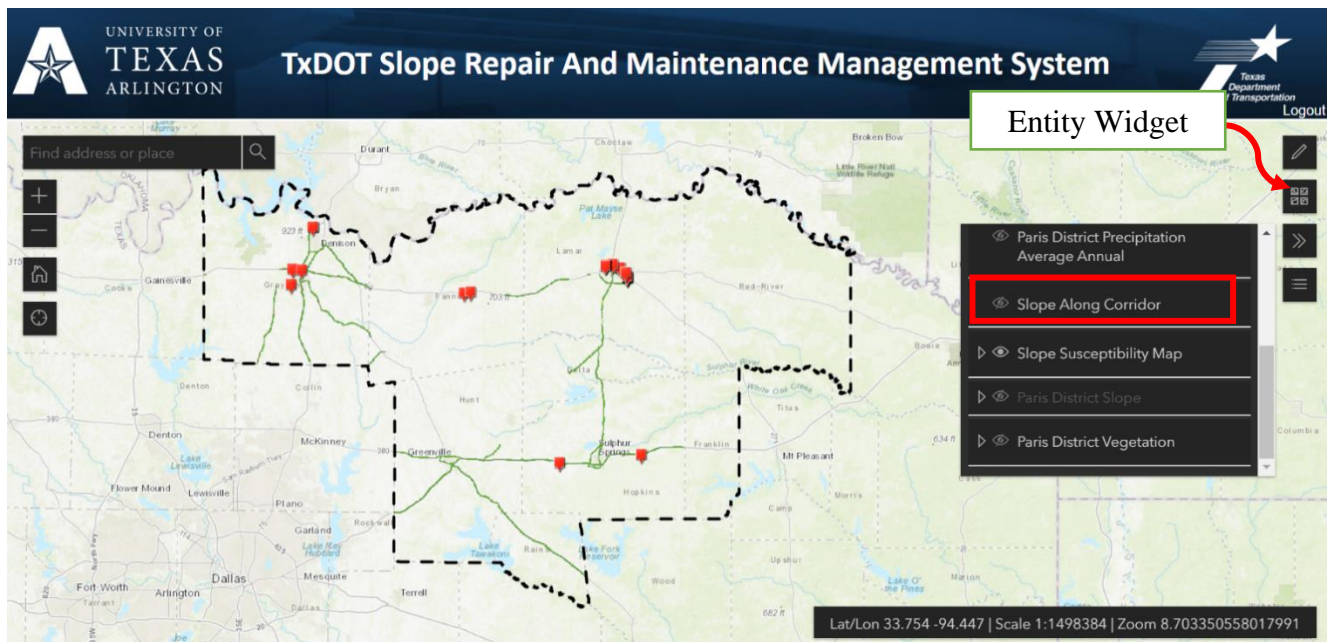


**Figure 6.7** Slope failure susceptibility map of Grayson county at US 75 and Randall Lake Rd intersection using NED derived slope angles

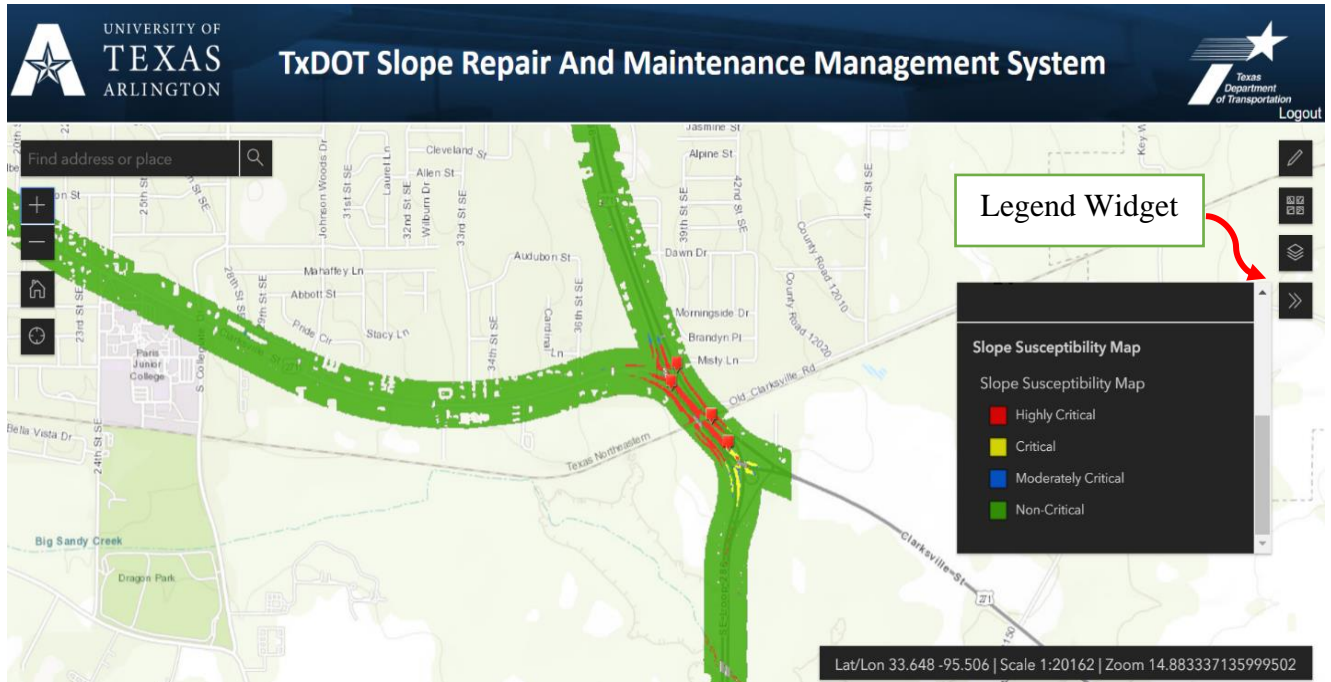
## 6.5. MAP-BASED INTERFACE TO VISUALIZE CRITICAL SLOPE

Users can access the map-based application using the web address: ["https://axb9294.uta.cloud/SRMMS/login.php"](https://axb9294.uta.cloud/SRMMS/login.php). The slope failure susceptibility maps were included in the entity widget and can be visualized in the map-based interface, as shown in Figure 6.8. Entity widget also contains past slope failures, Paris district connectivity corridors, Paris district boundary, Paris district soil properties, average annual precipitation, slope angles along corridors, and Paris district vegetation. The legend widget as shown in Figure 6.9 displays the slope susceptibility level when a slope failure susceptibility map is displayed in the map-based interface. Legends for entities (e.g., past slope failures, Paris district soil properties, average annual precipitation), which are displayed on the map, are also be shown in the legend widget. The map should be zoomed to an appropriate level to visualize the slope failure susceptibility at a specific site.

have



**Figure 6.8** Map-Interface displaying the slope failure susceptibility map of the TxDOT Paris district

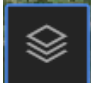


**Figure 6.9** Map-based interface displaying slope susceptibility levels for embankments along the TxDOT Paris district highway corridors


### 6.5.1. Steps for Visualizing a Slope Failure Susceptibility Map

Table 6.2 and Table 6.3 show the steps to display the slope failure susceptibility map and the legends in the map-based interface, respectively.

**Table 6.2** Display slope failure susceptibility map

Actor: User	System: SRMMS
0. Login to the system using the web address: “ <a href="https://axb9294.uta.cloud/SRMMS/login.php">https://axb9294.uta.cloud/SRMMS/login.php</a> ”	1. The system will display the map-based interface.
2. The user clicks the entity widget. 	3. The system expands the entity widget and displays the list of spatial data entities.
4. The user clicks on the slope susceptibility map from the list of entities.	5. The system displays and slope failure susceptibility map in the map-based interface.
6. The user zooms the desired location to visualize the slope failure susceptibility along the corridors.	7. The system zooms the slope failure susceptibility map.
8. The user clicks on the entity widget to close the displayed entity tab.	9. The system closes the expanded entity widget.

**Table 6.3** Display the legend for slope failure susceptibility map

<b>Actor: User</b>	<b>System: SRMMS</b>
	0. The system displays the map-based interface.
1. The user clicks the legend widget. 	2. The system displays the legend of the entities displayed in the map-based interface.

## **CHAPTER 7 CALIBRATING SLOPE FAILURE PREDICTIVE MODEL**

### **7.1. INTRODUCTION**

A physically-based slope failure predictive model was developed and used to assess slope failure susceptibility along the highway corridors. The slope failure predictive model considered slope geometry, soil properties, and rainfall data to identify slope segments susceptible to rainfall-induced failures. The physically-based slope failure predictive model did not take into account the effect of land cover on slope stability. The following sections discuss the impact of land cover on the slope stability and the approach for calibrating slope failure susceptibility maps.

### **7.2. THE EFFECT OF LAND COVER ON SLOPE FAILURE PREDICTIVE MODELING**

Slope failure susceptibility maps categorize the slopes in four different groups: highly critical, critical, moderately critical, and non-critical. These four categories were established based on rainfall duration that can cause the soil water pressure to be sufficiently high to trigger slope instabilities. The slope failure predictive model considers the effect of slope geometry, soil type and properties, and rainfall for assessing slope failure susceptibility level of slopes but does not incorporate the effects of land cover on the susceptibility level. However, retaining structures stabilize the steep slopes, and fully established grass can prevent surface erosion, while barren and sparsely vegetated areas exhibit faster erosion (Bhatt, 2013; Collin et al. 2008; Greenwood et al., 2004). Data sources, such as the US Department of Agriculture (USDA) and Texas Natural Resources Information System (TNRIS) databases that were used to derive soil properties and slope geometry data, did not contain sufficient land cover information. For example, USDA soil data sets do not take into account any surface structures, and TNRIS LiDAR datasets do not differentiate between the grass and the bare ground. Therefore, land coverage information could not fully be derived from LiDAR and USDA soil datasets.

#### **7.2.1. Land Cover Categories**

Studying the background of slope stability analysis showed that researchers had used different categories of land cover depending on the landcover types and the project needs. For example, Yalcin et al. (2011) categorized a landslide study area into deciduous, pasture, agriculture,

coniferous, hazelnut, tea, rocky, and settlement. Land cover classes in Bhatt's landslide study were forest, cultivation, and water (Bhatt, 2013). Greenwood et al. (2004) considered the impact of vegetation on the slope stability in two general forms: trees and grasses.

An approach was developed and implemented for determining the land cover types and categorizing land covers of slopes in this study. First, the slope susceptibility map was developed, which represented slopes in four categories: highly critical, critical, moderately critical, and non-critical. Then, the land covers of all highly critical slopes (more than 550 locations) were inspected using Google Earth street view images. These images were used to determine the land cover in all highly critical slopes. Based on the images obtained from the google earth, some of the highly critical slopes were mechanically stabilized (Figure 7.1), while others were vegetated with trees and grasses with varying vegetation density (Figure 7.2). Ten highly critical slope locations were randomly selected for comparing and validating the Google Earth images with the real-time land cover of slopes. This validation process is discussed in subsection 7.3.2.

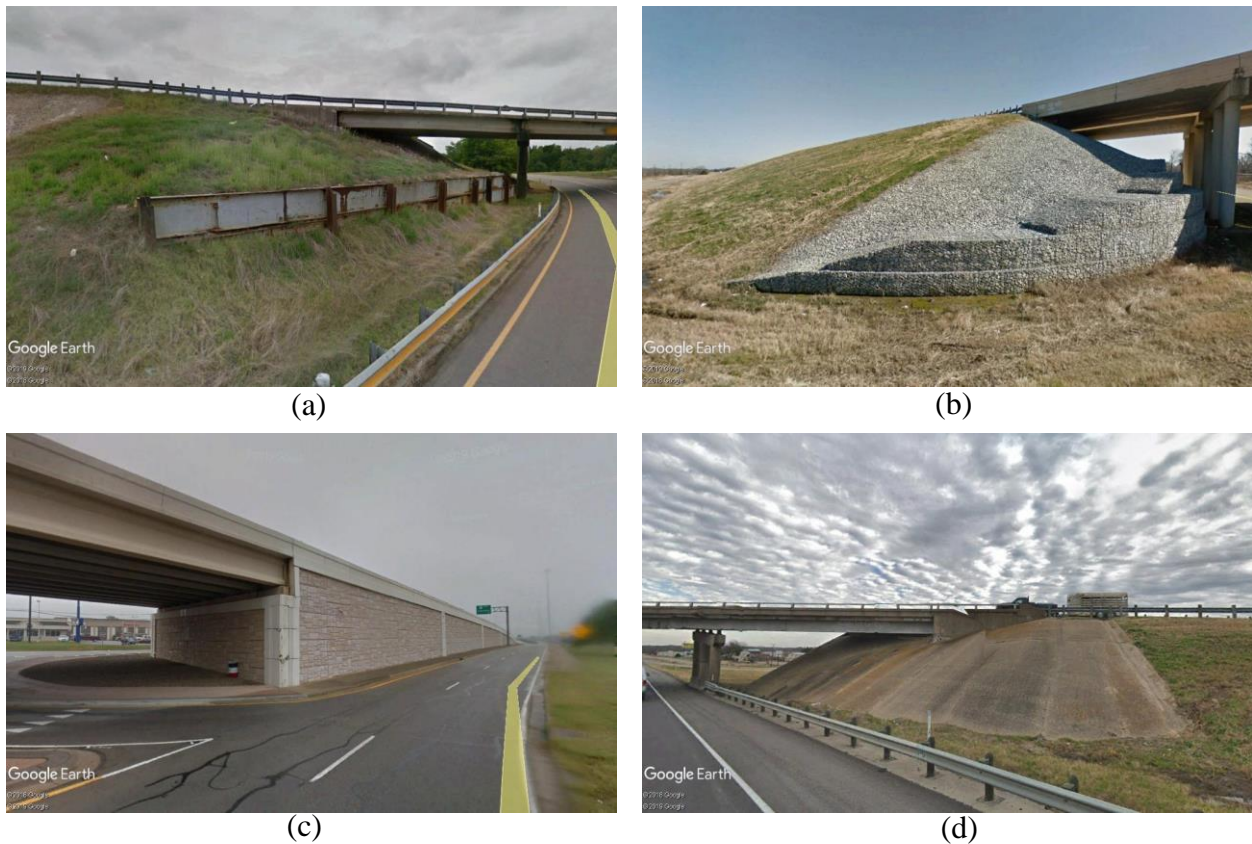


**Figure 7.1** Mechanically stabilized slopes (a) Intersection of SE Loop 286 and old Clarksville Rd., Lamar Co. (b) Intersection of State Highway 24 and FM 499, Hunt Co. (c) Intersection of NE Loop 286 and Pine mill Rd., Lamar Co. (d) Intersection of IH-30 and State Highway 24, Hunt Co.



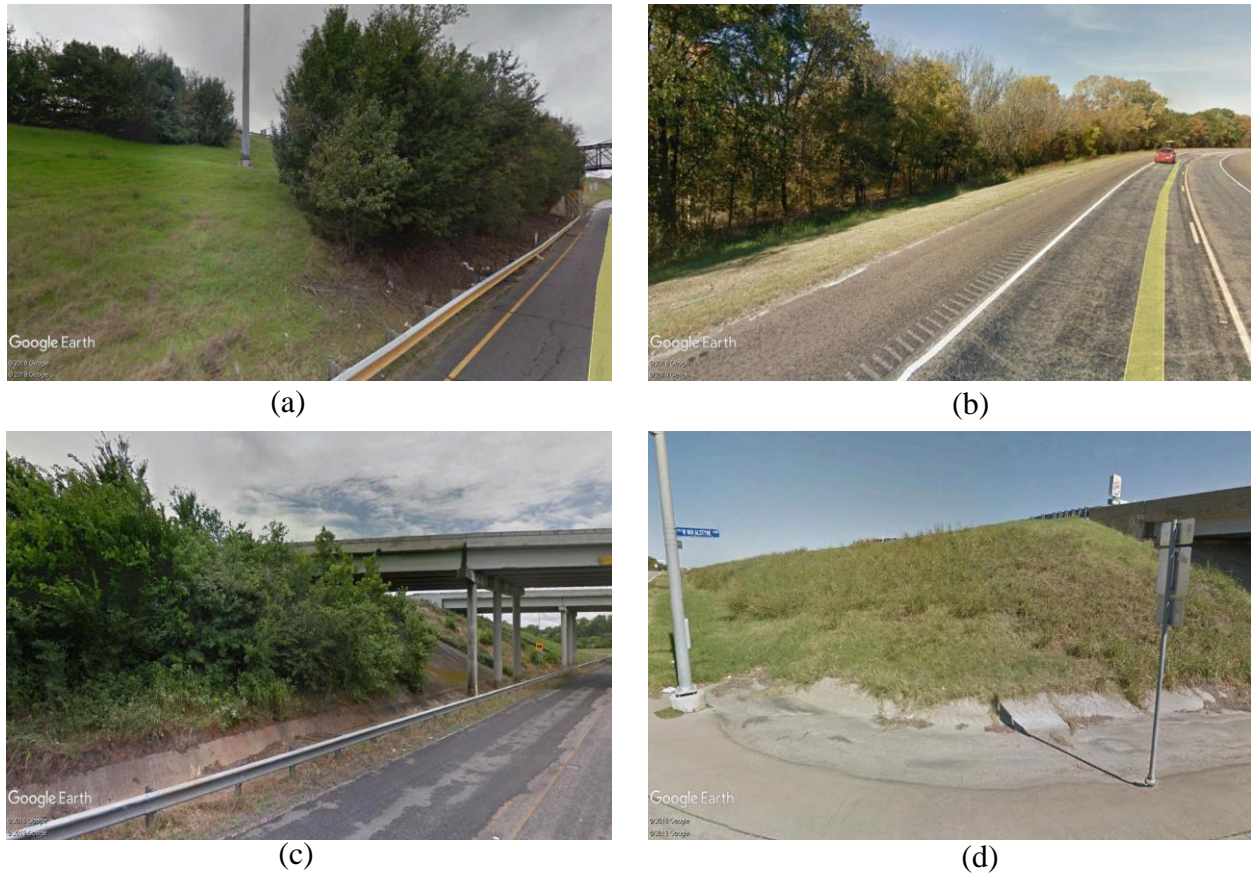


**Figure 7.2** Vegetated slopes (a) Along US 271, near the intersection of SE Loop 286 and Old Clarksville road, Lamar Co. (b) Intersection of State Highway 11 and Golden Rd intersection, Grayson Co. (c) Intersection of Tx-503 SPUR-E and Theresa Dr. Grayson Co. (d) Intersection of US 75 and FM 121, Grayson Co.

The investigation of the land cover types of highly critical slopes in the TxDOT Paris district showed that two main categories of land cover should be defined for adjusting the result from the slope failure predictive model. The two categories of land cover are related to mechanically stabilized slopes and vegetated slopes. The impacts of these two land cover types on slope stability are discussed in the following sub-sections.

### ***Mechanically Stabilized Slopes***

Failure of slope occurs when the downslope force component due to the gravitational force exceeds the resisting force due to column friction. Mechanical slope repair methods, including but not limited to, retaining walls, launched soil nails, recycle plastic pins, geosynthetics, and gabions provide a high level of resistance to lateral earth pressures and bear the gravitational stress (Tuttle

et al., 1992; Onyelowe Ken and Okafor, 2006). Therefore, in the mechanically stabilized slopes, the slope susceptibility level shown in the slope failure susceptibility maps does not depict the actual slope condition, which means the slope areas that are mechanically stabilized are no longer susceptible and must be displayed as non-critical in the slope failure susceptibility map.

### ***Vegetated Slopes (Trees and Grasses)***

Several parameters reflect the impact of vegetation on stability analysis including, enhanced cohesion, the mass of vegetation, evapotranspiration and infiltration, and tensile root strength (Greenwood et al., 2004; Yalcin et al., 2011; Coppin and Richard, 1990; Chok et al., 2004). The summary of each parameter's influence is as follows:

*Enhanced cohesion:* Fine roots of the vegetation maintain the integrity of the surface layer and hence enhance the cohesion of the surface layer and prevent erosion (Yalcin et al., 2011).

*The mass of vegetation:* Only large trees (diameter at breast height (dbh) > 0.3m) influence slope stability through their weight (Greenwood et al., 2004). However, such influence is not always helpful, depending on the location of the tree. If a large tree (dbh=0.8m) is located at the toe of a slope, it can add 10% to the factor of safety, but the same tree reduces the factor of safety by 10% if it is located at the top (Coppin and Richard, 1990; Perry et al., 2003).

*Evapotranspiration & infiltration:* Evapotranspiration (soil moisture removal by roots) will enhance soil strength (Ali et al., 2012). However, during wet periods or short heavy rainfalls, the enhanced soil strength will almost be lost entirely (Overton and Meadows, 2013). Furthermore, vegetation may also increase the soil infiltration, which can result in greater accumulation of water in the soil during rainfall (Yalcin et al., 2011).

*Tensile root strength:* The tensile root strength increases the soil stability by reinforcing the soil (Greenwood et al., 2004; Abdullah et al., 2011; Shahandashti et al., 2019). Several parameters need to be considered in determining the root reinforcement values including, the diameter of the root, type of species, embedment and adhesion with the soil, and the root distribution, which are suggested to be assessed through the in situ experiments (Yalcin et al., 2011; Coppin and Richard, 1990). The influence zone of a tree is limited to its root distribution zone. Although the zones of root influence need to be measured for individual species, the main zone of influence is suggested to be 4d below the ground in which d is the diameter at breast height (Greenwood et al., 2004). In

two cases studied by Greenwood et al. (2004), the tensile root strength is shown to add up to 10% to the factor of safety at 1m depth and 0% at a depth of 1.5m.

Greenwood's research showed that vegetation prevents surface erosion by maintaining the integrity of the surface layer in the root distribution zone, but according to the methodology of this research, the factor of safety was calculated for the depths of 1-7 feet that are lower than the root distribution zone and are not impacted by the roots. Therefore, the vegetation has a limited influence on the stability of soil layers that are analyzed using this research methodology. Nevertheless, as the vegetation are effective in preventing surface erosion, planting vegetation in barren slopes or slopes with sparse vegetation is one of the major recommendations for reducing the slope failure susceptibility of highway embankments and cut slopes.

### **7.3. CALIBRATING SLOPE FAILURE PREDICTIVE MODEL USING LAND COVER DATA**

As discussed in subsection 7.2.1, land covers of the slopes were categorized into mechanically stabilized slopes and vegetated slopes. Mechanically stabilized slopes decrease the slope failure susceptibility of the slope soil, either by altering the physical composition of the soil or by placing a barrier in or on the soil. Although vegetation prevents surface erosion by holding the soil in position and preventing it from being blown or washed away, it does not necessarily add to the safety factor. Therefore, the slope failure predictive model was calibrated to consider the effect of mechanical stabilization on slope stability. For applying the impact of land cover on slope susceptibility, first, the land cover data were collected using Google Earth street view images; then, the susceptibility level of highly critical slopes that are mechanically stabilized were changed to non-critical in the slope failure susceptibility map.

#### **7.3.1. Collecting Land Cover Data**

A polygon feature layer was developed to represent the mechanically stabilized slopes along the corridors where slope failure susceptibility analysis was performed. First, highly critical slopes were detected using the slope failure susceptibility maps. Using Google Earth Pro, images of highly critical slopes were collected. The images of the highly critical slopes were inspected to identify the land cover at the failure site. Then, for the slopes that are mechanically stabilized, a

polygon shapefile that indicates the locations and extent of mechanically stabilized slopes is created (see Figure 7.3). The polygon feature layer to represent the mechanically stabilized slopes was only developed for the regions where slopes were highly susceptible to failures. This polygon feature layer is included in the geodatabase.

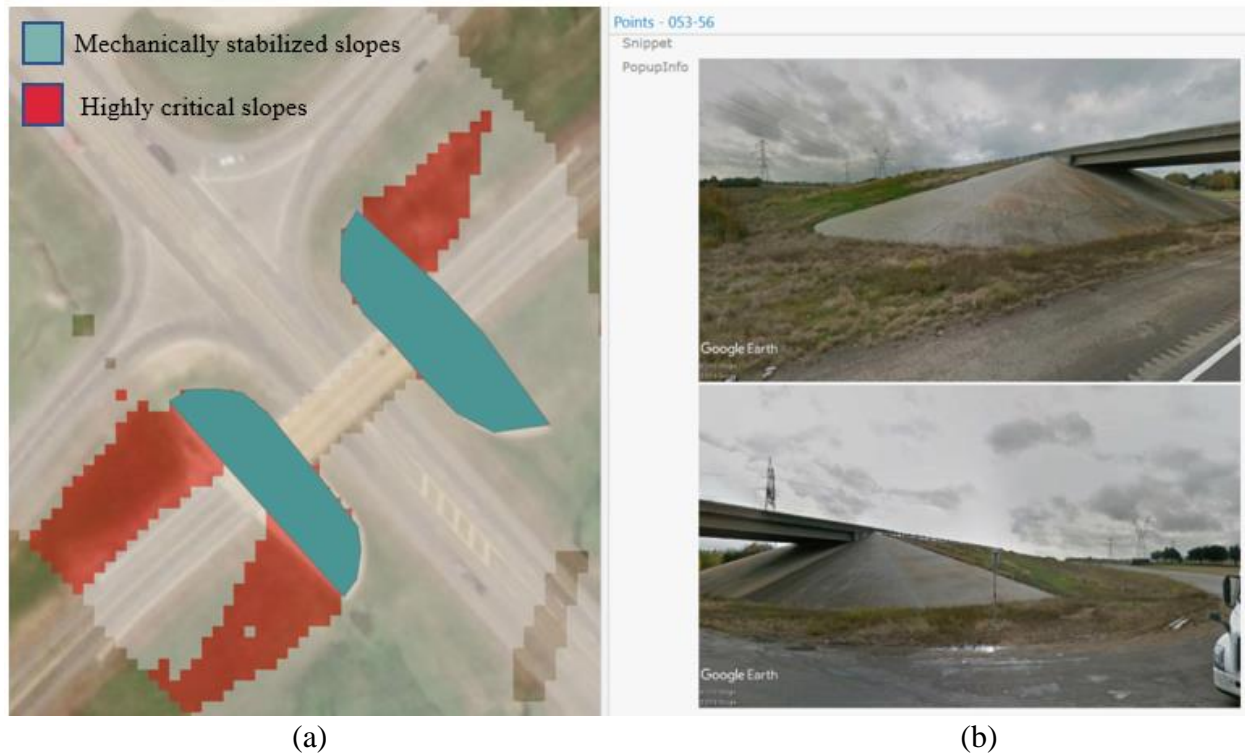


**Figure 7.3** Mechanically stabilized slopes at the intersection of SW Loop 286 and Farm Road 137 in Lamar Co. (a) Polygon shapefiles showing mechanically stabilized slope segments (b) images of mechanically stabilized slopes obtained from google earth.

### 7.3.2. Validating Land Cover Data

Data collected from Google Earth street view images should be validated to find possible discrepancies in the condition of land covers of slopes. Ten highly critical slope locations were randomly selected for visual inspection, and real-time photos were taken by the research team to compare them with the Google Earth street view images. The validation results indicated that there were no discrepancies in the slope conditions shown in Google Earth street view images. Figure 7.4 shows the comparison of land cover obtained at a site using the image obtained from google earth and site investigation.

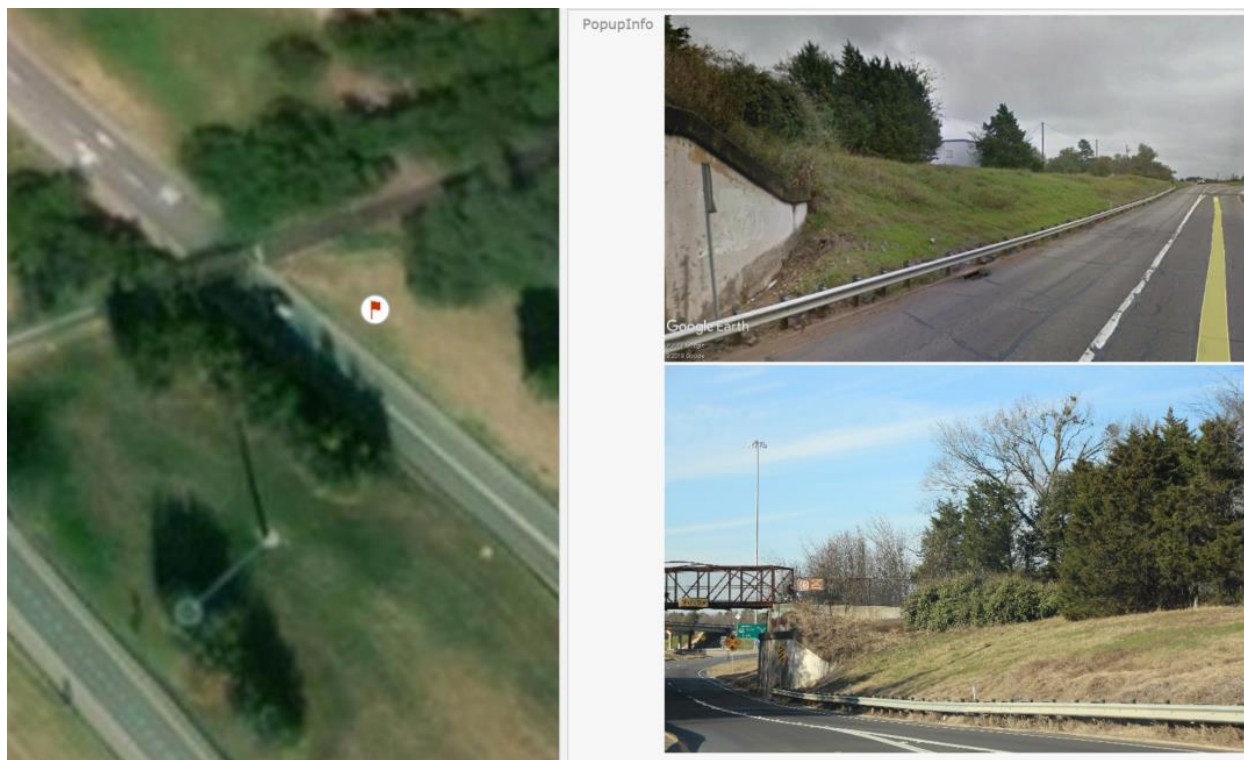


**Figure 7.4** Validation of land cover (left image: validation point at the intersection of SE Loop 286 and old Clarksville Rd., Lamar Co.; top-right image: Google Earth image associated with the shown validation point; bottom-right image: Photo taken at the site for validating the Google Earth image)

### 7.3.3. Calibrating Susceptibility Maps

The slope failure susceptibility maps were calibrated to represent mechanically stabilized slopes as non-critical slopes. To represent mechanically stabilized slopes as non-critical, the feature layer representing the mechanically stabilized slopes were converted to a raster file, and raster overlay

analysis was performed with the existing slope failure susceptibility maps. All the mechanically stabilized slopes were represented as non-critical slopes after the raster overlay analysis. Also, sharp drops in the elevation of some structures (e.g., bridges, drains) were interpreted as critical slope segments by the slope failure susceptibility model. This effect was also removed during the calibration of slope failure susceptibility maps. Figure 7.5 shows the calibration of the slope failure susceptibility map at the intersection of NE Loop 286 and Pine mill Rd in Lamar County.

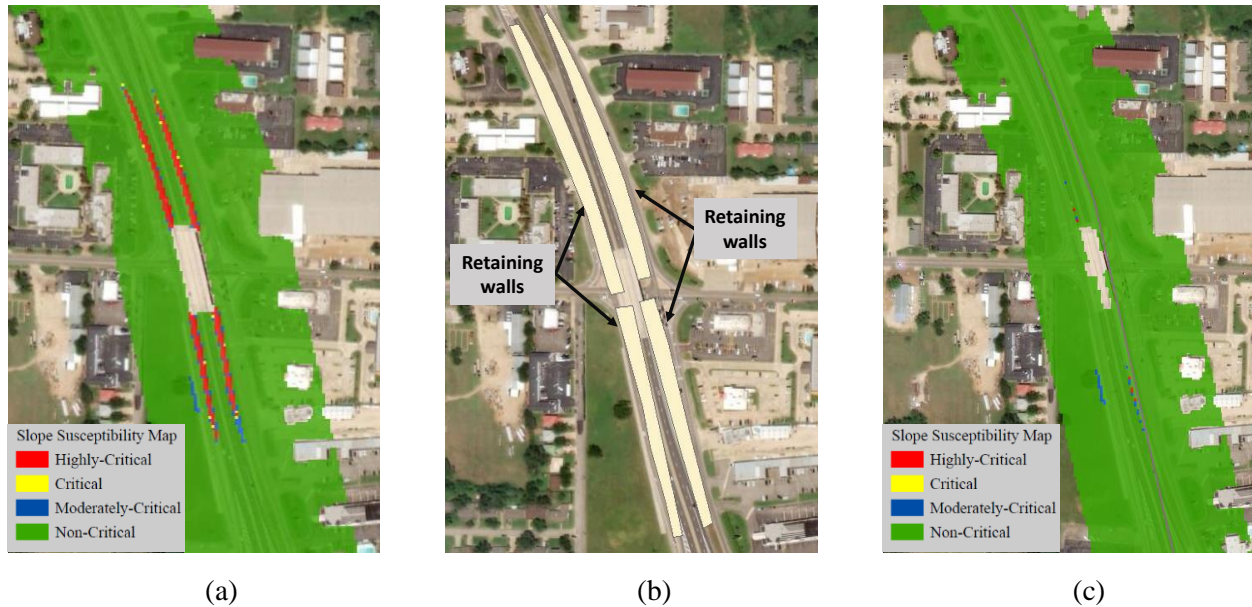


**Figure 7.5** Calibration of slope failure susceptibility map (Intersection of NE Loop 286 and Pine mill Rd., Lamar Co); (a) Slope susceptibility map developed using the physically-based model; (b) Stable slope identified from Google Earth; (c) Slopes classified as non-critical in calibrated susceptibility map

---

## **CHAPTER 8 RECOMMEND REPAIR METHODS TO PREVENT RECURRING SLOPE FAILURES**

### **8.1. INTRODUCTION**

A multi-criteria decision support system was developed to provide a ranked list of slope repair methods to facilitate the selection of repair methods. This system does not force engineers to select a specific method; it only provides a ranked list of slope repair methods. Recommended implementation practices were also proposed to avoid recurring slope failures. The decision support system and recommended implementation practices were integrated with the map-based slope repair and maintenance management system.

### **8.2. MULTI-CRITERIA DECISION SUPPORT SYSTEM FOR GENERATING A RANKED LIST OF REPAIR AND MAINTENANCE METHODS**

A multi-criteria decision support system was created to provide a ranked list of slope repair methods. The multi-criteria decision support system consists of several components. First, the results of the survey conducted in TxDOT Project 0-6957 (Shahandashti et al., 2019), titled “Synthesis on Rapid Repair Methods for Embankment Slope Failure” was used for identifying the slope repair methods and selection criteria involved in the decision-making process. Second, irrelevant slope repair methods based on soil type and failure type (shallow or deep) were eliminated using the recommendations made in TxDOT Project 0-6957 (Shahandashti et al., 2019). Third, a slope repair decision matrix was generated using the responses of experts interviewed in TxDOT Project 0-6957 (Shahandashti et al., 2019). Fourth, the relative importance of the ranking criteria (e.g., impact on traffic, the service life of repair method, and the need of special equipment) were derived from the survey results (Shahandashti et al., 2019) using the Entropy method. Finally, the Technique for Order Preference by Similarity of Ideal Solution (TOPSIS) was used to generate a ranked list of slope repair methods. Figure 8.1 shows the flowchart of the multi-criteria decision support system.

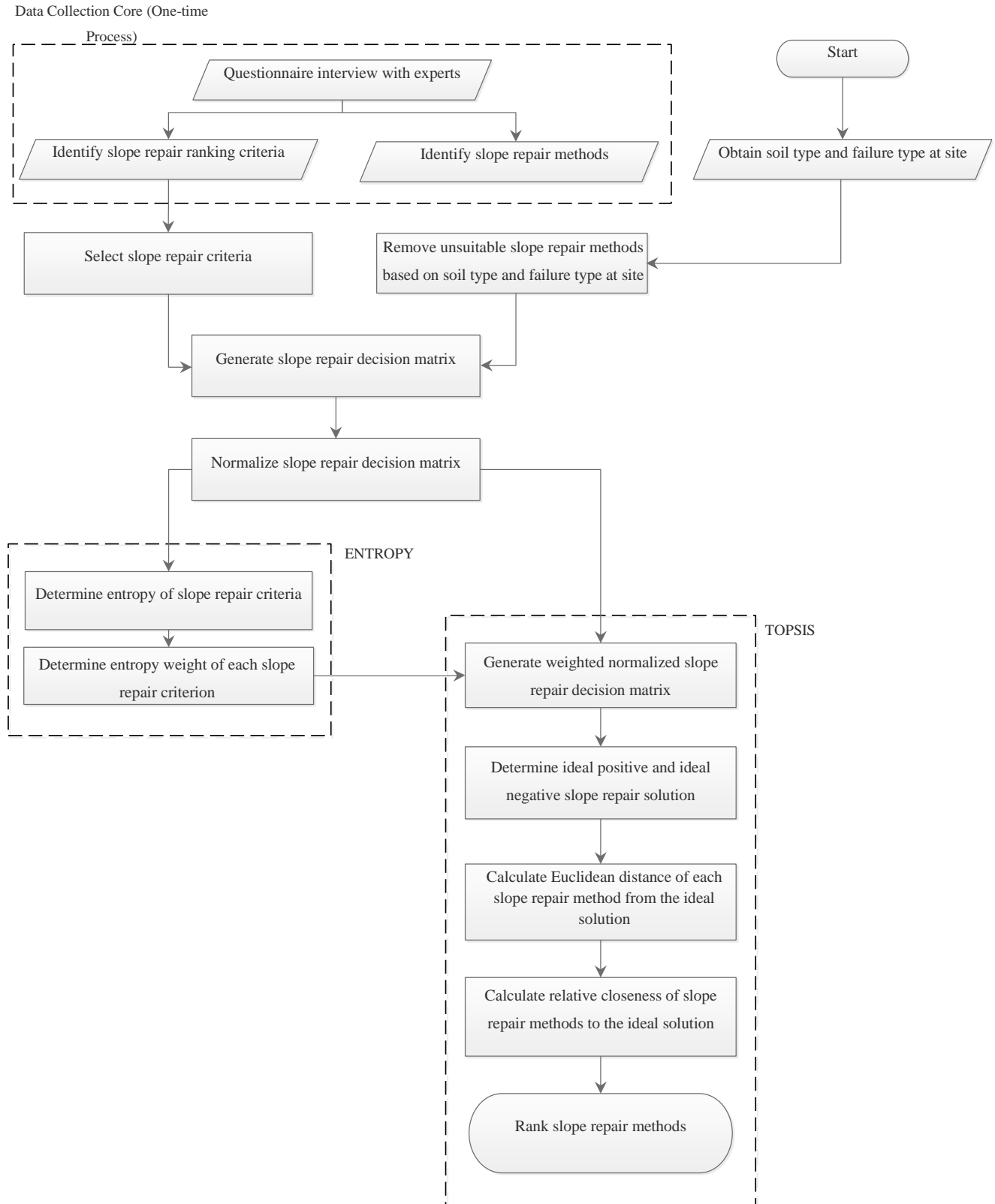


**Figure 8.1** Components of the multi-criteria decision support system to propose a ranked list of slope repair methods



### 8.2.1. Identification of Slope Repair Methods and Development of Ranking Criteria

The questionnaire survey and interviews with the experts documented in TxDOT Project 0-6957, titled “Synthesis on Rapid Repair Methods for Embankment Slope Failure” (Shahandashti et al., 2019) were used to identify a list of slope repair methods and develop ranking criteria. The experts, who responded to the survey, include engineers, maintenance supervisors, and members of the Transportation Research Board (TRB) Standing Committee on Engineering Geology who have long-term experience in dealing with slope failures and repairs in highway embankments.

#### *Slope Repair Methods*

In TxDOT Project 0-6957, subject matter experts were presented with a list of slope repair methods (Figure 8.2) and asked to identify the methods that are frequently used for slope repairs of highway embankments. The slope repair methods that were selected fewer than five times were eliminated from this implementation project since they are assumed not to be common in Texas. For example, buttressing and biotechnical methods have not been proposed as a slope repair method in this study.

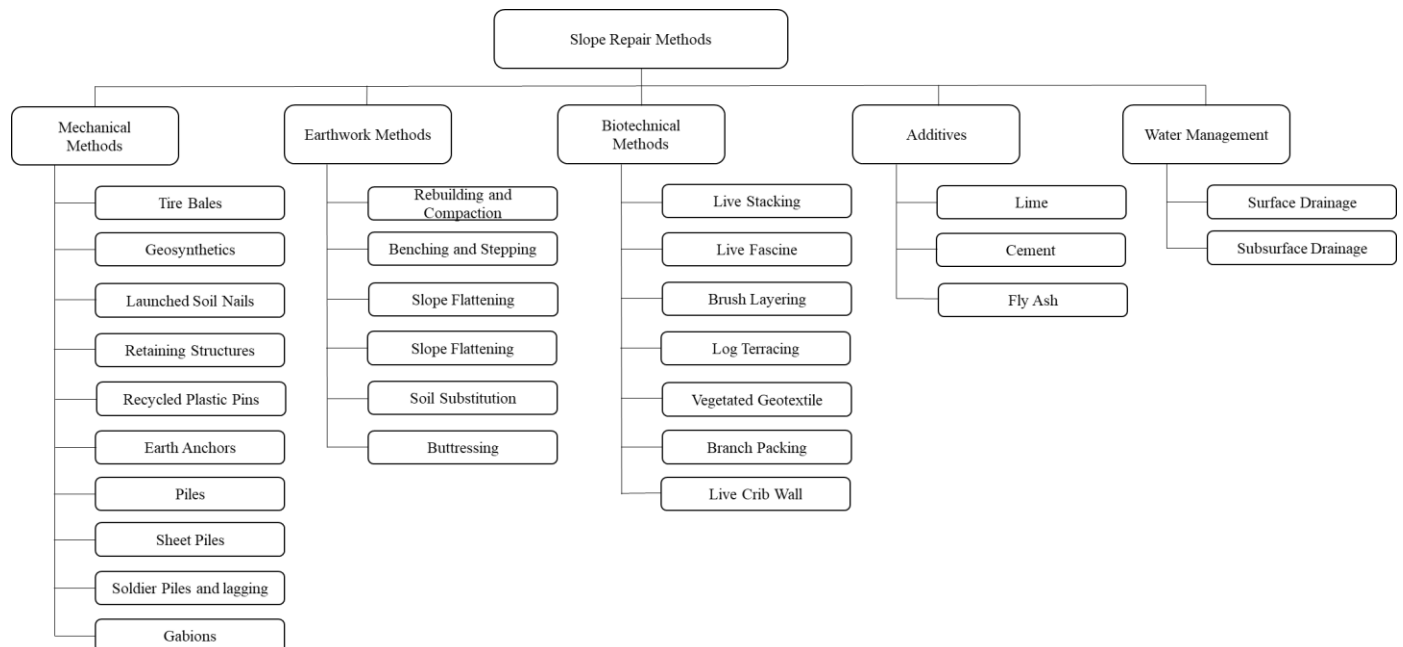


**Figure 8.2** Classification of Slope Repair Methods (Shahandashti et al., 2019)

### *Slope Repair Criteria*

Through discussions with the experts via interview and survey questionnaire, eight slope repair criteria were adopted (Shahandashti et al., 2019). The slope repair criteria considered for the evaluation of slope repair methods are long service life, low impact on traffic, rapid repair, low skilled worker requirement, engineering drawing requirement, geotechnical soil test requirement, special equipment requirement, and low cost.

#### **8.2.2. Elimination of Irrelevant Slope Repair Methods**

Applicability of a slope repair method depends on characteristics of slope failure location, such as the soil type and failure type (shallow or deep). The applicability of different slope repair methods for different soils and failure types is detailed in Shahandashti et al. (2019). The recommendations in Shahandashti et al. (2019), which are summarized in Table 8.1, were used to eliminate irrelevant methods for repairing a slope.

**Table 8.1** Applicability of slope repair method based on soil and failure type

<b>Slope Repair Method</b>	<b>Recommend failure type</b>	<b>Recommended soil type</b>	<b>Not Applicable</b>
Launched Soil Nails	Shallow to Deep Failure	Applicable most type of soil (sand, gravel, silt, clay, and soil with fewer cobbles and boulders)	Not applicable for slopes with excessive cobbles and boulders
Retaining Structures	Shallow to Deep Failure	Applicable for all type of soils	
Piles (Plate Piles)	Shallow Failure	Applicable for silty and clayey soils in the region of frequent wetting and drying	
Rebuilding and Compaction	Shallow to Deep Failure	Applicable for most type of soils	Not applicable for organic soil
Benching and Stepping	Shallow to Deep Failure	Recommended for slopes with weathered rocks Cost-effective in the repair of deep slides. Recommended for slopes steeper than 4H:1V.	Not applicable for slopes with sandy, non-cohesive, or highly erodible soil
Gabions	Shallow to Deep Failure	Applicable to silty and clayey soil Suitable for slopes with limited space	
Slope Flattening	Shallow to Deep	Applicable in small slope Applicable to most soil types	Not suitable for large slopes
Additives (Lime)	Shallow to Deep Failure	Applicable for plastic clays, silts, and dirty sands Applicable for soil with plasticity greater than or equal to 10% Applicable for shallow slope failures less than 4ft.	
Additives (Cement)	Shallow Failure	Applicable for cohesive and granular soil Applicable for soil with plasticity index less than 20% or PH lower than 5.3	
Additives (Fly Ash)	Shallow to Deep Failure	The recommended soil type is silt. Also applicable with sand and gravel.	Not applicable for soil with sulfate content greater than 10%

*Note: Adapted from Shahandashti et al. (2019),  
“Synthesis of Rapid Repair Methods for Embankment Slope Failure”*

### 8.2.3. Creation of Slope Repair Decision Matrix

The experts were asked to evaluate different repair methods based on the eight slope repair criteria. The binary scale was used to represent the decision of the experts, where “1” and “0” refer to the selection or rejection (i.e., not selection) of a method by an expert with respect to a criterion, respectively. The average values of the responses were determined; the final values are shown as a base matrix in Table 8.2. The value of 0.25 corresponding to the impact of geosynthetics on traffic represents that 25% of experts reported that the implementation of geosynthetics has minimum impact on the moving traffic.

From the base matrix, a slope repair decision matrix is generated for a site where the slope has to be restored. The slope repair decision matrix for a failure site is developed based on the desired slope repair criteria and after the elimination of irrelevant repair methods for a repair site. The size of the slope repair decision matrix is dependent on the slope repair selection criteria. For example, if 13 slope repair methods and three slope repair criteria are considered, then the size of the matrix is  $13 \times 3$ .

**Table 8.2** Base matrix for representing expert evaluations

Slope Repair Methods	Low Impact on Traffic	Long Service Life	Rapid Repair	Low Skilled worker	Engineering Drawing	Geotechnical Tests	Special Equipment	Low Cost
Geosynthetics	0.25	0.63	0.56	0.56	0.81	0.94	0.63	0.50
Launched soil nails	0.40	0.60	0.60	0.80	0.80	0.80	0.80	0.00
Retaining Structures	0.16	0.74	0.26	0.79	0.84	0.79	0.79	0.32
Earth Anchors	0.60	0.80	0.00	0.80	0.80	1.00	1.00	0.00
Piles	0.40	0.60	0.40	0.80	0.40	0.60	0.60	0.40
Sheet Piles	0.40	0.60	0.30	0.90	0.90	0.80	0.90	0.30
Gabions	0.13	0.60	0.40	0.73	0.60	0.87	0.80	0.20
Rebuilding and compaction	0.52	0.06	0.81	0.39	0.26	0.55	0.45	0.84
Benching and Stepping	0.17	0.33	0.83	0.67	0.83	1.00	0.50	0.67
Slope Flattening	0.45	0.45	0.73	0.64	0.55	0.64	0.45	0.36
Soil Substitution	0.45	0.45	0.73	0.64	0.55	0.64	0.45	0.36
Additives	0.40	0.20	0.40	0.60	0.40	0.80	0.20	0.60
Water Management Methods	0.25	0.56	0.56	0.56	0.75	0.88	0.63	0.50

### 8.2.4. Determination of Weights of Slope Repair Criteria Using The Entropy Method

In a multiple criteria decision-making system, it is crucial to determine the relative importance of each slope repair criterion to evaluate various slope repair methods based on repair method selection criteria. Their importance is usually given in terms of weights, which, after normalization, adds to 1. The entropy method is adopted to assess the weight of the slope repair criteria because there is direct access to the values of the slope repair decision matrix obtained from the survey. The entropy method works best on a predefined matrix (Shanian and Savadogo, 2006). Entropy, in information theory, is a measure of uncertainty that is formulated using probability theory where a broad distribution represents more uncertainty than a sharply peaked one (Deng et al., 2000; Li et al., 2011). The method consists of the following procedure:

#### *Normalization of slope repair decision matrix*

The slope repair decision matrix is defined by a set of slope repair criteria  $C_j$  where  $\{j = 1, 2, 3, \dots, n\}$  and slope repair methods  $M_i$  where  $\{i = 1, 2, 3, \dots, m\}$ .

$$\begin{array}{rcccc}
 & & \mathbf{C1} & \mathbf{C2} & \dots & \mathbf{Cn} \\
 \mathbf{D} = & \mathbf{M1} & d_{11} & d_{12} & \dots & d_{1n} \\
 & \mathbf{M2} & d_{21} & d_{22} & \dots & d_{2n} \\
 & \dots & \dots & \dots & \dots & \dots \\
 & \mathbf{Mm} & d_{m1} & d_{m2} & \dots & d_{mn}
 \end{array}$$

where  $D$  is the decision matrix,  $C_n$  is the number of slope repair criteria,  $M_m$  is the number of slope repair methods, and  $d_{ij}$  is the elements of the decision matrix.

To normalize the above decision matrix  $D$  for benefit criteria,

$$n_{ij} = \frac{d_{ij} - \min_i d_{ij}}{\max_i d_{ij} - \min_i d_{ij}}, \quad (i = 1, \dots, m; j = 1, \dots, n) \quad (9)$$

For cost criteria,

$$n_{ij} = \frac{\max_i d_{ij} - d_{ij}}{\max_i d_{ij} - \min_i d_{ij}}, \quad (i = 1, \dots, m; j = 1, \dots, n) \quad (10)$$

Where  $N$  is the normalized slope repair decision matrix, and  $n_{ij}$  are elements of the normalized slope repair decision matrix (Zou et al., 2006).

### ***Calculation of slope repair criteria entropy***

The entropy value for  $n$  number of slope repair criteria and  $m$  number of slope repair methods is given by the equation below:

$$E_j = -k \sum_{i=1}^m f_{ij} \ln f_{ij}, \quad i = 1, 2, \dots, m; j = 1, 2, \dots, n \quad (11)$$

$$f_{ij} = \frac{n_{ij}}{\sum_{i=1}^m n_{ij}}, \quad k = \frac{1}{\ln n}, \text{ and suppose when } f_{ij} = 0, \text{ then } \ln f_{ij} = 0$$

Where  $E_j$  is the entropy value for  $j^{\text{th}}$  slope repair criteria,  $f_{ij}$  is the normalized slope repair decision matrix element for entropy,  $k$  is the constant of entropy, and  $n_{ij}$  is the elements of the normalized slope repair decision matrix.

### ***Calculation of slope repair criteria's entropy weight***

The weights of  $n$  number of slope repair criteria are given by:

$$W_j = \frac{1 - E_j}{n - \sum_{j=1}^n E_j}, \quad \sum_{j=1}^n W_j = 1, \quad (j = 1, \dots, n) \quad (12)$$

Where  $W_j$  is the weight of the slope repair criteria, and the sum of weights of all criteria adds to 1.

Entropy contains useful information about criteria. The higher the weights of a slope repair criterion, the more critical the criterion.

### 8.2.5. Ranking of Slope Repair Methods Using Technique for Order Preference by Similarity of Ideal Solution (TOPSIS) Method

The Technique for Order Preference by Similarity of Ideal Solution (TOPSIS) is an outranking method (Hwang and Yoon, 1981). This method chooses the best alternative from a set of alternatives that have the shortest Euclidian distance from the positive ideal solution and the longest Euclidean distance from the negative ideal solution (Shanian and Savadogo, 2006; Roszkowska, 2011). The positive ideal solution is the one that has all the best values of the criteria achievable, and the negative ideal solution has all the worst values of the criteria achievable. The positive ideal solution maximizes the benefit, and the negative ideal solution maximizes the cost.

Unlike other multiple decision-making methods, such as the Analytical Hierarchical Process (Saaty, 1990), TOPSIS does not require pair-wise comparisons of criteria and alternatives. In pairwise comparisons, the addition of a slope repair criterion and a slope repair method makes the computation large. The reduction in pairwise comparison is useful in this research as we have a large number of slope repair criteria and slope repair methods. Further, TOPSIS is simple and fast with a systematic procedure (Azadeh et al., 2011). Thus, we have adopted TOPSIS to rank the repair methods. The method consists of the following procedures:

#### *Normalization of slope repair decision matrix:*

The slope repair decision matrix is normalized using the following equation:

$$r_{ij} = \frac{d_{ij}}{\sqrt{\sum_i^m d_{ij}^2}}; i = 1, 2, \dots, m \quad (13)$$

Where n is the number of slope repair criteria, m is the number of slope repair methods,  $r_{ij}$  is the element of normalized slope repair decision matrix, and  $d_{ij}$  are the elements of the slope repair decision matrix for TOPSIS.

#### *Determination of weighted normalized slope repair decision matrix*

The elements of the normalized slope repair decision matrix are multiplied by the weights obtained by the entropy method.

$$V_{ij} = r_{ij}W_j \quad (i = 1, 2, \dots, m; j = 1, 2, \dots, n) \quad (14)$$

Where  $V_{ij}$  are the elements of the weighted normalized slope repair matrix,  $r_{ij}$  are the normalized elements of the slope repair matrix and  $W_j$  is the weight of the  $j^{\text{th}}$  slope repair criterion.

### ***Determination of ideal slope repair solution***

The positive and negative ideal solution are determined respectively by using the equations below:

$$\{v_1^+, v_2^+, \dots, v_n^+\} = \{(\max_i V_{ij} | j \in K), (\min_i V_{ij} | j \in K') | j = 1, 2, \dots, n; i = 1, 2, \dots, m\} \quad (15)$$

$$\{v_1^-, v_2^-, \dots, v_n^-\} = \{(\min_i V_{ij} | j \in K), (\max_i V_{ij} | j \in K') | j = 1, 2, \dots, n; i = 1, 2, \dots, m\}$$

Where  $V_{ij}$  are the elements of weighted normalized slope repair decision matrix,  $v_n^+$  and  $v_n^-$  is the positive ideal and the negative ideal solution for  $j^{\text{th}}$  slope repair criterion, respectively, and  $K$  is for benefit criteria, and  $K'$  is for cost criteria.

### ***Measure the distance of slope repair methods from ideal solutions***

The Euclidean distance of each, slope repair method from positive ideal and negative ideal solutions are respectively given as follows:

$$S_i^+ = \left\{ \sum_{j=1}^n (v_{ij} - v_j^+)^2 \right\}^{0.5} ; i = 1, 2, \dots, m; j = 1, 2, \dots, n \quad (16)$$

$$S_i^- = \left\{ \sum_{j=1}^n (v_{ij} - v_j^-)^2 \right\}^{0.5} ; i = 1, 2, \dots, n; j = 1, 2, \dots, m$$

Where  $S_i^+$  is the positive Euclidean distance for each slope repair method and  $S_i^-$  is the negative Euclidean distance for each slope repair method,  $v_{ij}$  are the elements of the weighted normalized slope repair decision matrix, and  $v_i^+$  and  $v_i^-$  are the ideal positive and ideal negative solutions for the  $j^{\text{th}}$  slope repair criteria, respectively.



### *Calculation of relative closeness of slope repair methods*

The relative closeness of a slope repair method to an ideal solution is given by:

$$C_i = \frac{S_i^-}{S_i^+ + S_i^-}, i = 1, 2, \dots, m; 0 \leq C_j \leq 1 \quad (17)$$

Where  $C_i$  is the relative closeness of the  $i^{\text{th}}$  slope repair method to the ideal solution,  $S_i^+$  and  $S_i^-$  are the distances of each slope repair method from positive ideal and negative ideal solutions, respectively. The higher the  $C_i$  value, the better the rank of the slope repair method.

### **8.3. MAP-BASED INTERFACE FOR PROVIDING A LIST OF RANKED SLOPE REPAIR METHODS**

The decision support system was integrated into the slope repair and maintenance management system and its map-based interface. A user can access the map-based application using the web address: "<https://axb9294.uta.cloud/SRMMS/login.php>." Figure 8.3 shows steps to be followed in the map-based interface for accessing a ranked list of slope repair methods. The "List of Repair Methods" button is included in the bottom right corner of the interface. When a user clicks on the "List of Repair Methods" button, a list of slope repair criteria is displayed in a pop-up window. The user can select the criteria desired for the repair of a failed slope. The user shall also select the soil type and slope failure type at the site. The soil type can be obtained by clicking on the failure location in the map-based interface. The decision support system will generate a ranked list of slope repair methods for slope restoration. The user can further click on the desired slope repair method to view the recommended implementation practices for avoiding the recurring slope failures.

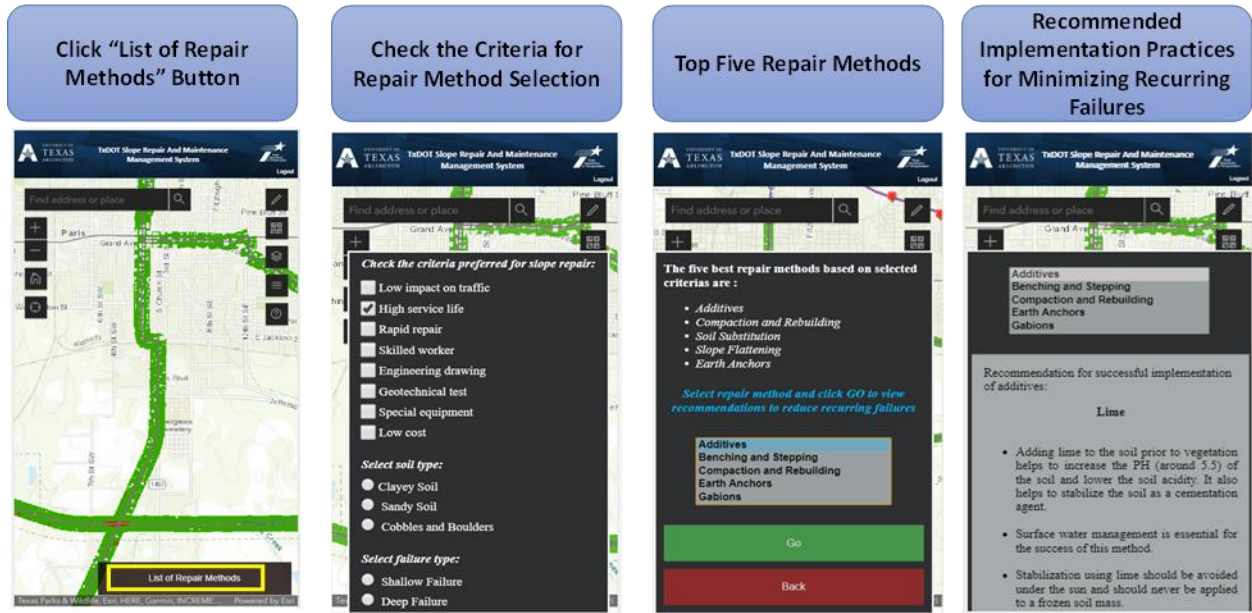


Figure 8.3 Process of accessing the list of slope repair methods and recommended implementation practices for avoiding recurring failures using the map-based interface

## CHAPTER 9 SLOPE REPAIR AND MAINTENANCE MASTER PLAN

### 9.1. MASTER PLAN VISION

The objective of the slope repair and maintenance master plan is to identify the highly critical highway slopes in the TxDOT Paris district to facilitate the proactive slope maintenance decision to minimize recurring slope failures. It is expected that achieving the objective will fulfill the following goals:

- Prolong the functional life span of cut slopes and highway embankments
- Reduce emergency stabilization
- Improve traffic safety
- Improve performance of highway bridges
- Minimize operational disruption
- Decrease life-cycle cost of geotechnical assets

Figure 9.1 shows the shallow slope failure in the TxDOT Paris District.



**Figure 9.1** Slope failure at the intersection of SE Loop 286 and Clarksville St, Paris, Texas

## 9.2. INVESTIGATED CORRIDORS

The slope repair and maintenance master plan has been developed for two highway corridors in the TxDOT Paris district. The highway corridors were determined in coordination with TxDOT representatives and district engineers. US 75 and the southern portion of Loop 286 were the two selected highway corridors in the TxDOT Paris district. The slope failure susceptibility maps were developed for these corridors using the methodology described in Chapter 6. These maps identified many critical slope segments adjacent to US 75 and Loop 286 highway corridors. Figure 9.2 shows the location of US 75 and Loop 286 highway corridors which were selected for developing the slope repair and maintenance master plan. US 75 and Loop 286 highway corridors were divided into a strip of 1.5 miles to create large-scale maps. Large-scale maps of each 1.5-mile strip are provided in Section 9.3.

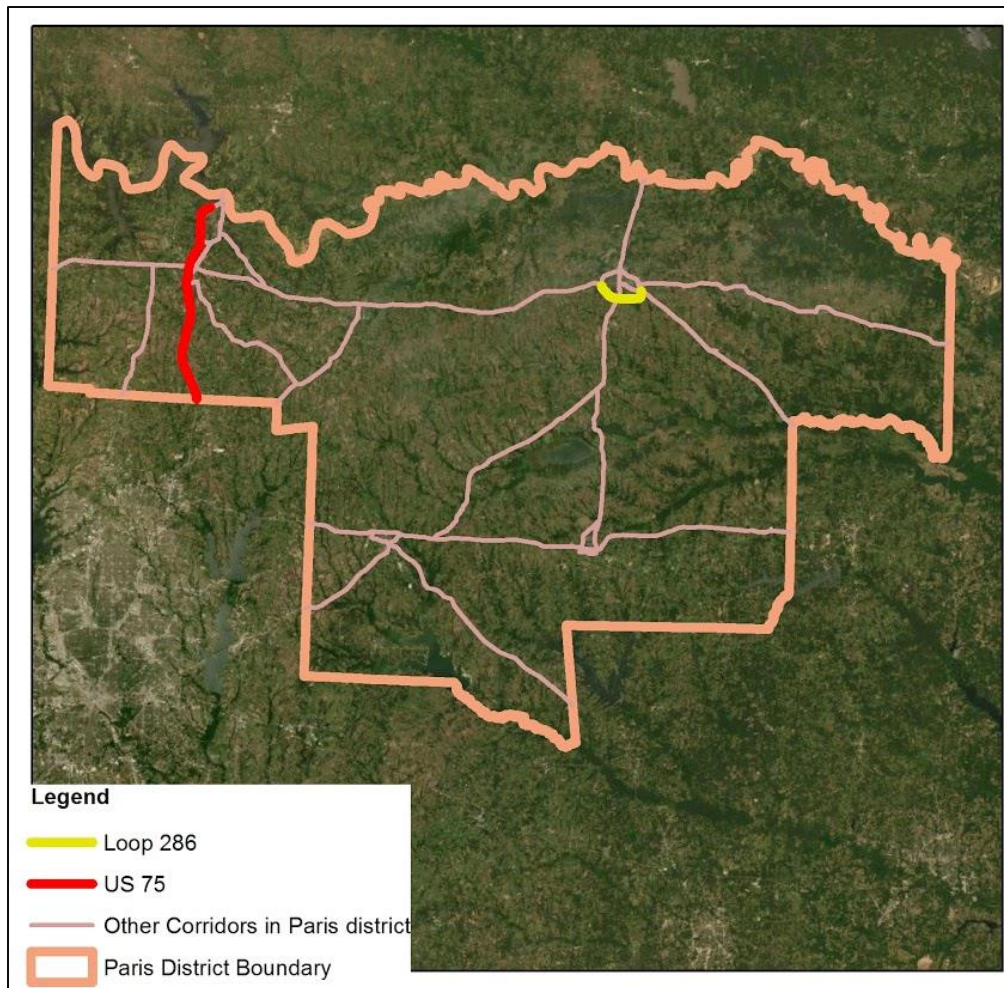


**Figure 9.2** Location of selected corridors for the development of the master plan

### 9.3. CRITICAL SEGMENTS IN THE CORRIDOR

#### 9.3.1. Maps of Critical Slope Segments

This section presents maps showing the critical slope segments along the US 75 and the southern portion of Loop 286 corridors. Both highway corridors were divided into strips of 1.5 miles (2.4 km) along the corridor length. The width of the strip was 1.15 miles (1.8 km) along the cross-section of the roadway. Each strip was assigned an index number. For US 75, the strip index number was assigned in ascending order moving from north to south. For Loop 286, the strip index number was assigned in ascending order moving from west to east. A large-scale map of each strip was developed to show the critical slope segments within the strip. The critical slope segments in a strip were assigned a unique name as “Corridorname\_County\_StripIndex\_Segment”, where “Corridorname” is the name of the corridor, “County” is the county name in the TxDOT Paris district that the corridor passes through, “StripIndex” is the strip index number of the corridor, and “Segment” is number assigned to the critical segment in the selected strip, moving from north to south for US 75 and west to east for Loop 286. For example, the failure segment “*US75\_GRA\_1\_3*” shown in Figure 9.3 represents the third slope failure segment in the first strip of US 75 in Grayson county.

The location of critical segments in each strip along a corridor has been referenced using Texas Reference Marker Number. The distance of each critical segment from the Reference Marker Number in the strip moving north to south in the case of US 75 and west to east in the case of Loop 286 is included in Table 9.1 and Table 9.2. The distances from the origin (DFO) of the US 75 and Loop 286 to each critical segment in the corridors was also determined to facilitate the tracking of critical slopes for repair and maintenance works (Table 9.3 and Table 9.4).

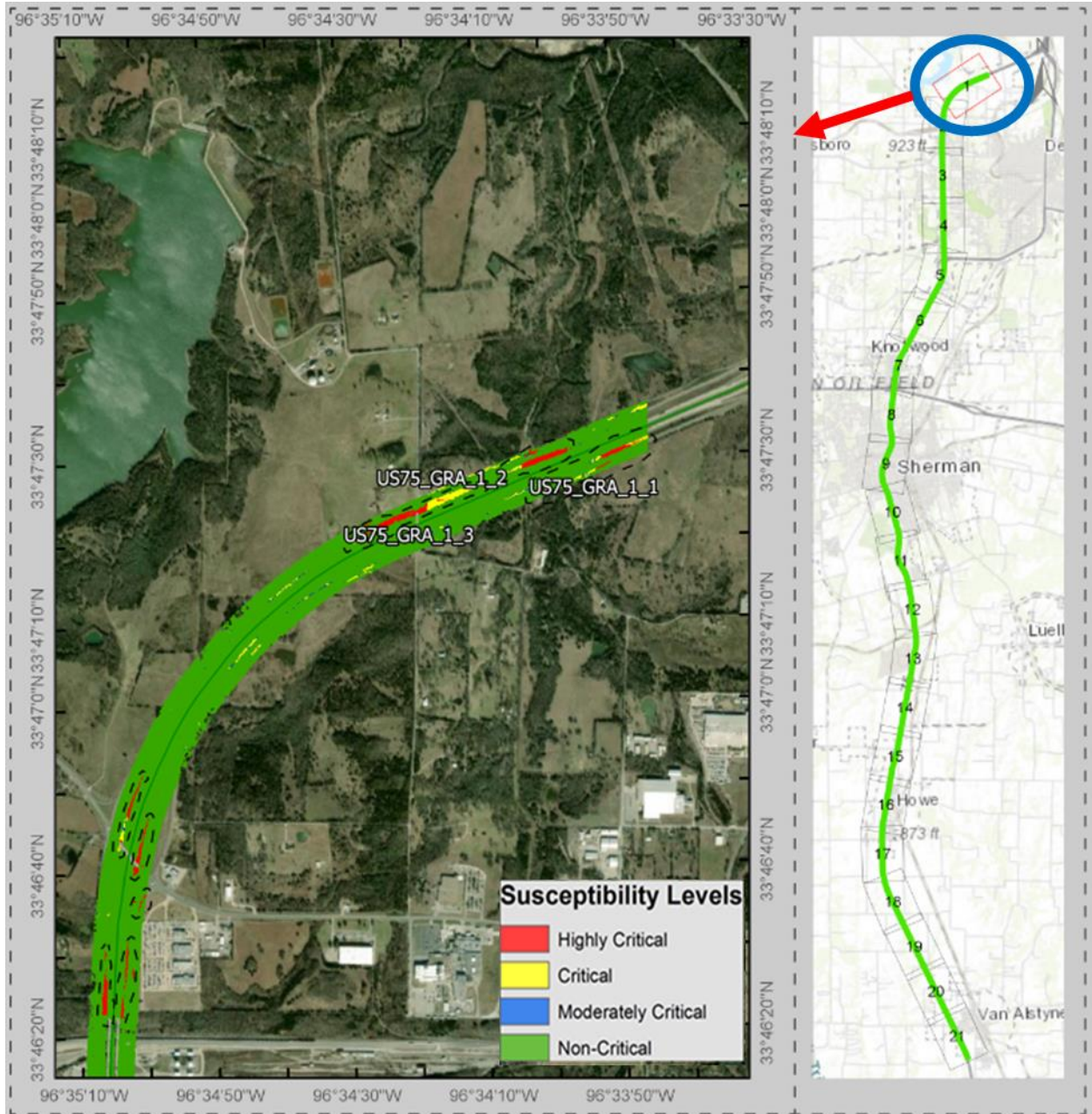
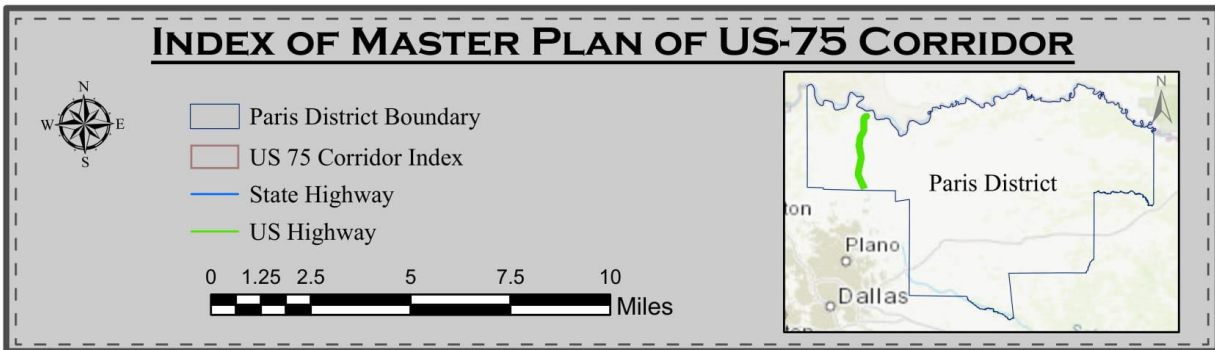
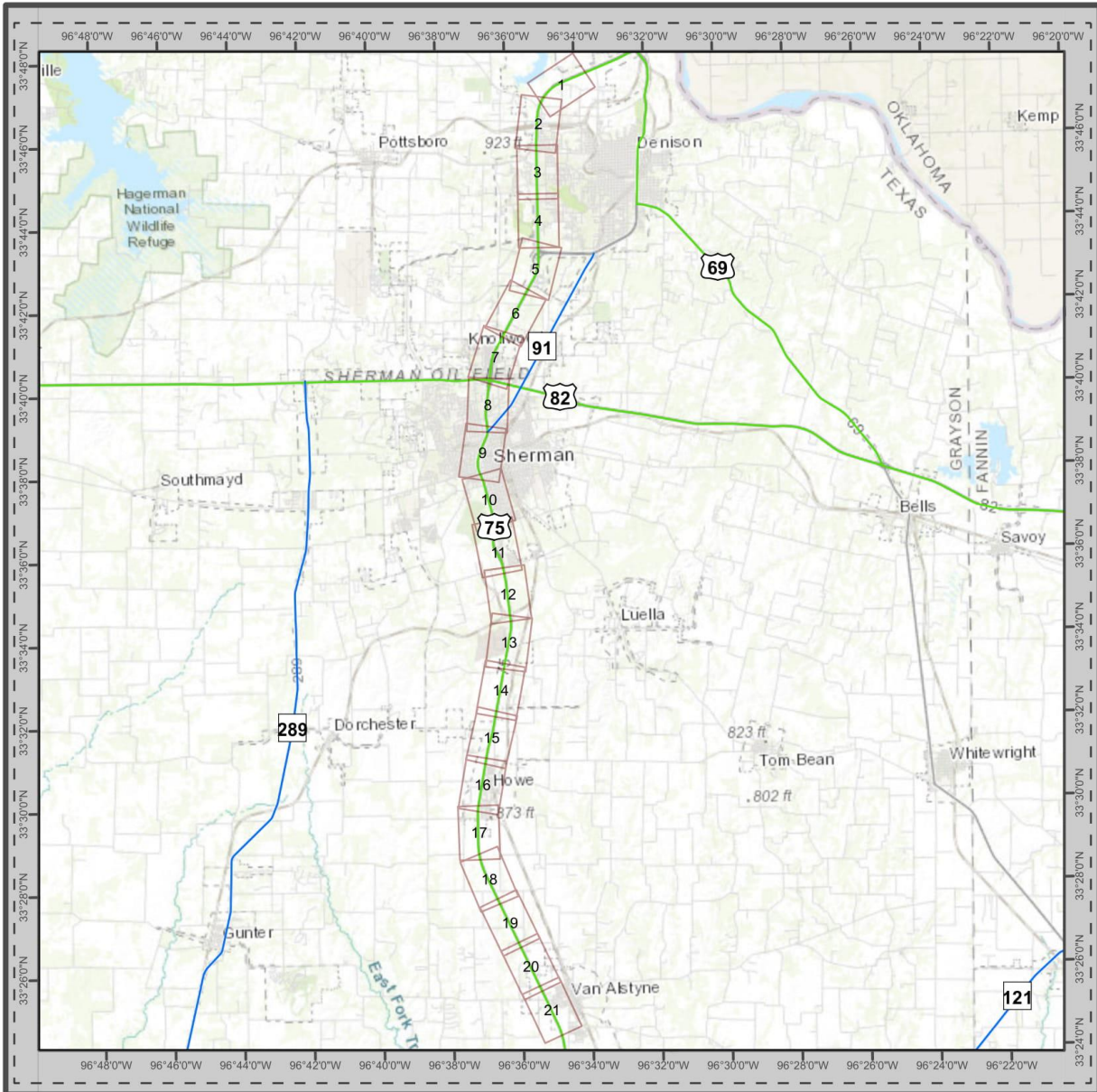
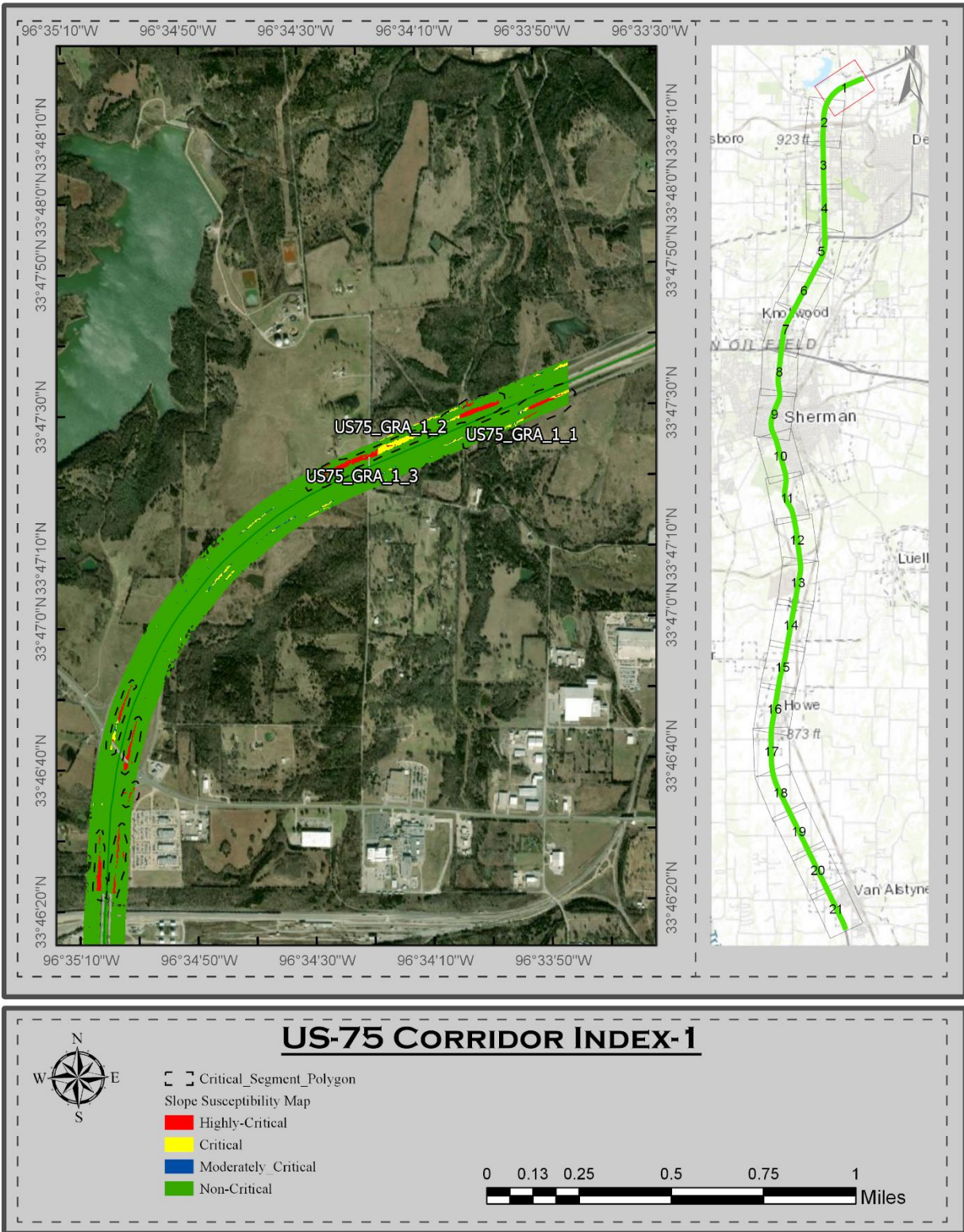


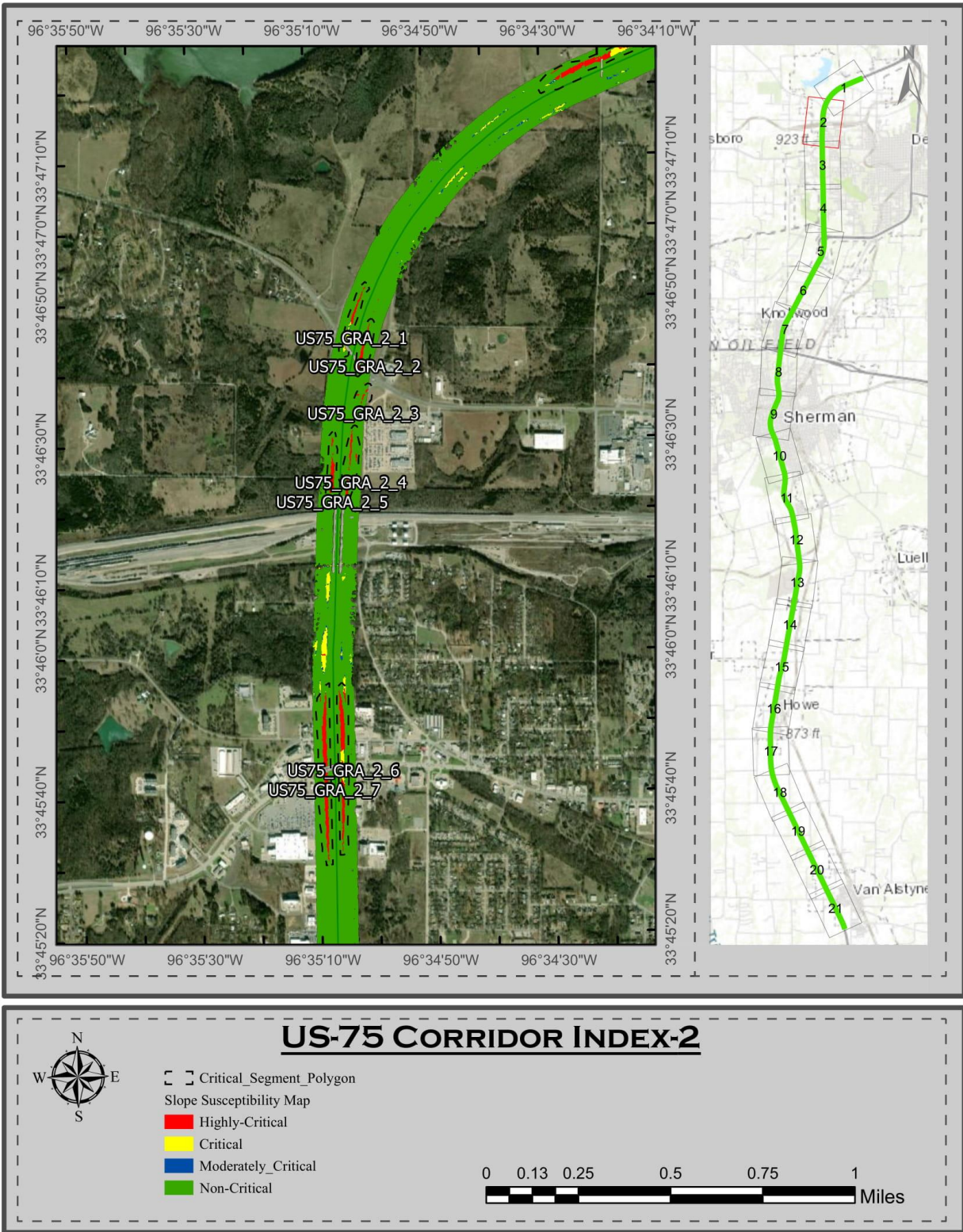
Figure 9.3 A large-scale map of the first strip of US 75 starting at intersection of US 75 and SH 91, Denison, Texas

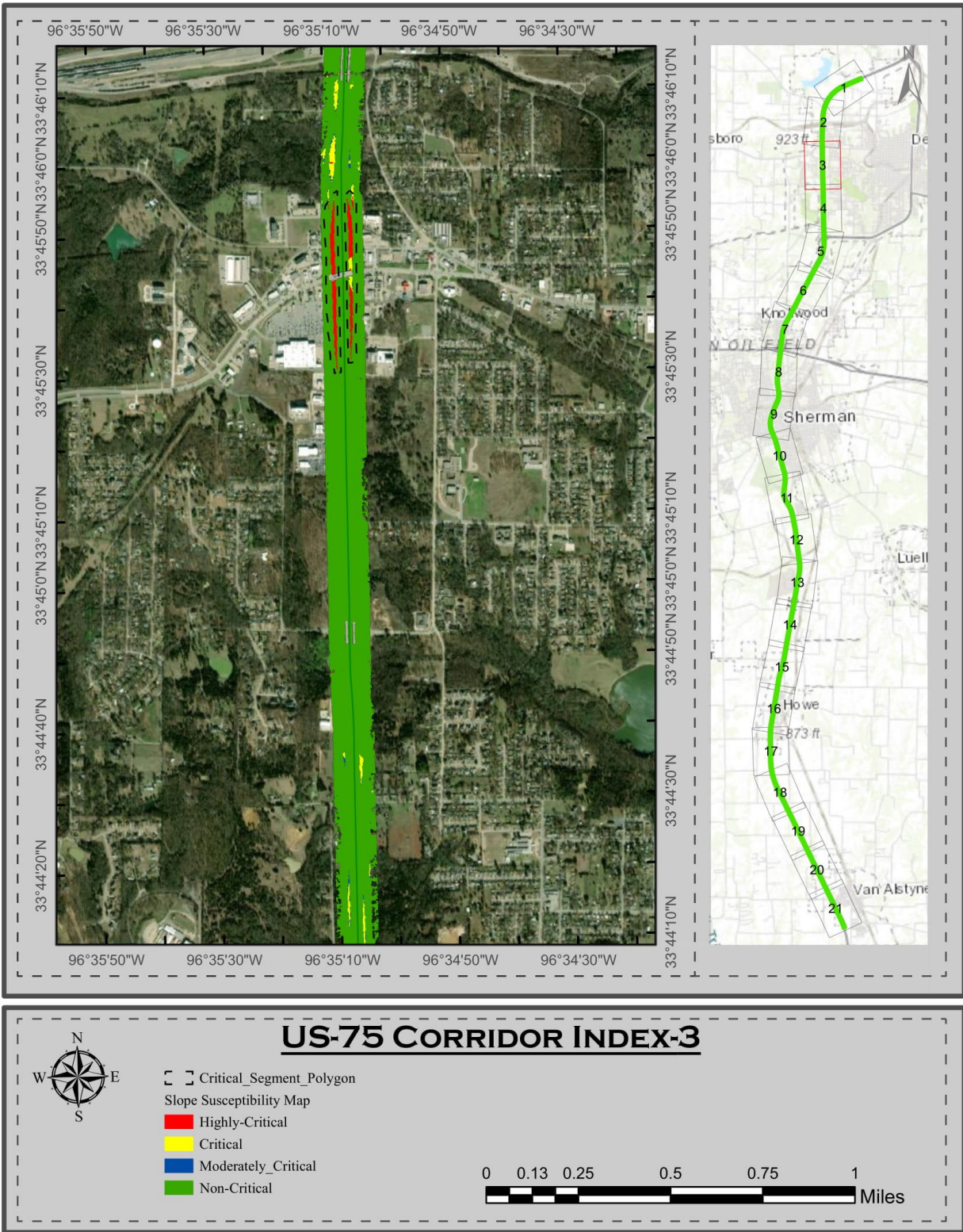
Map Book of Critical Segments for US 75

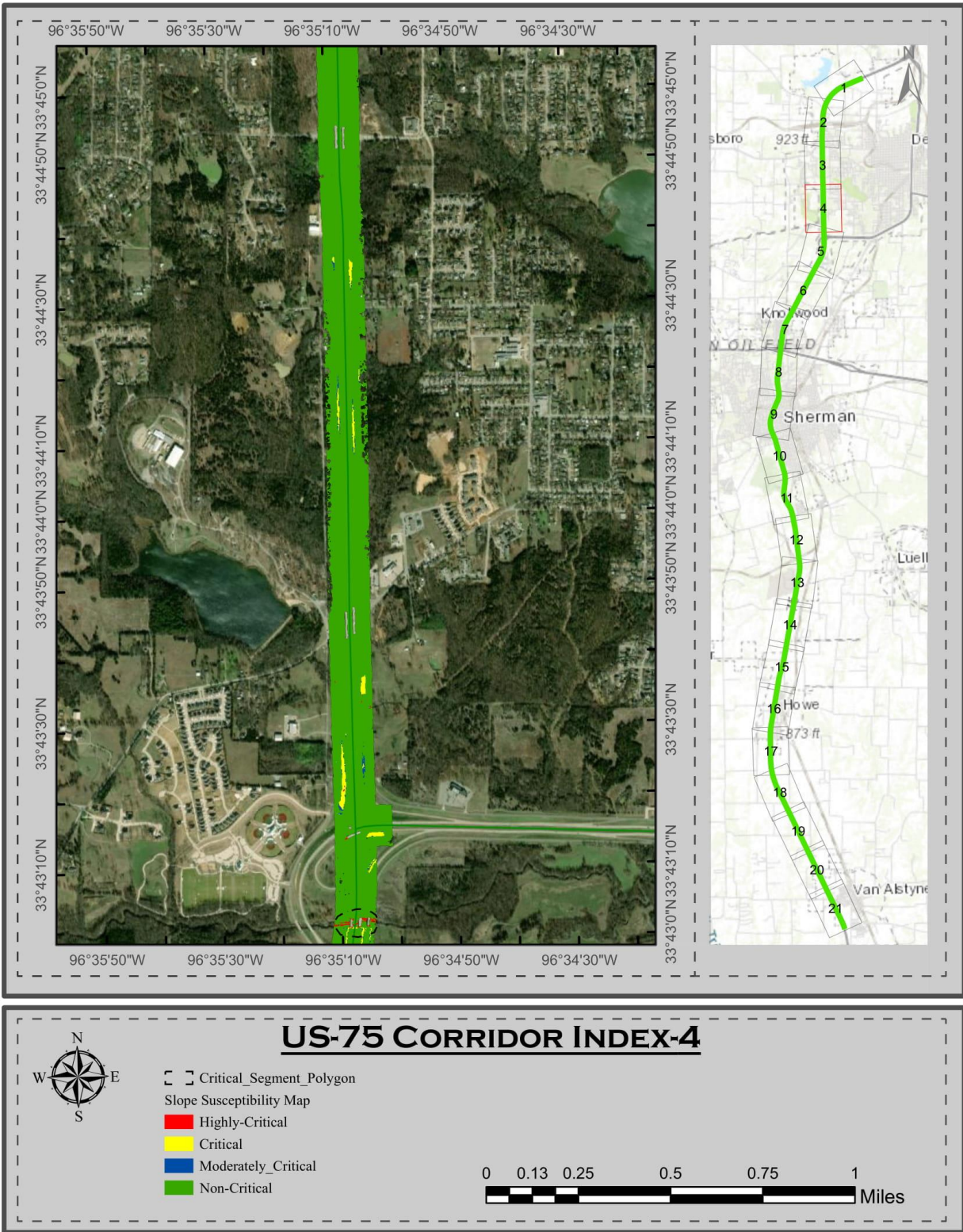


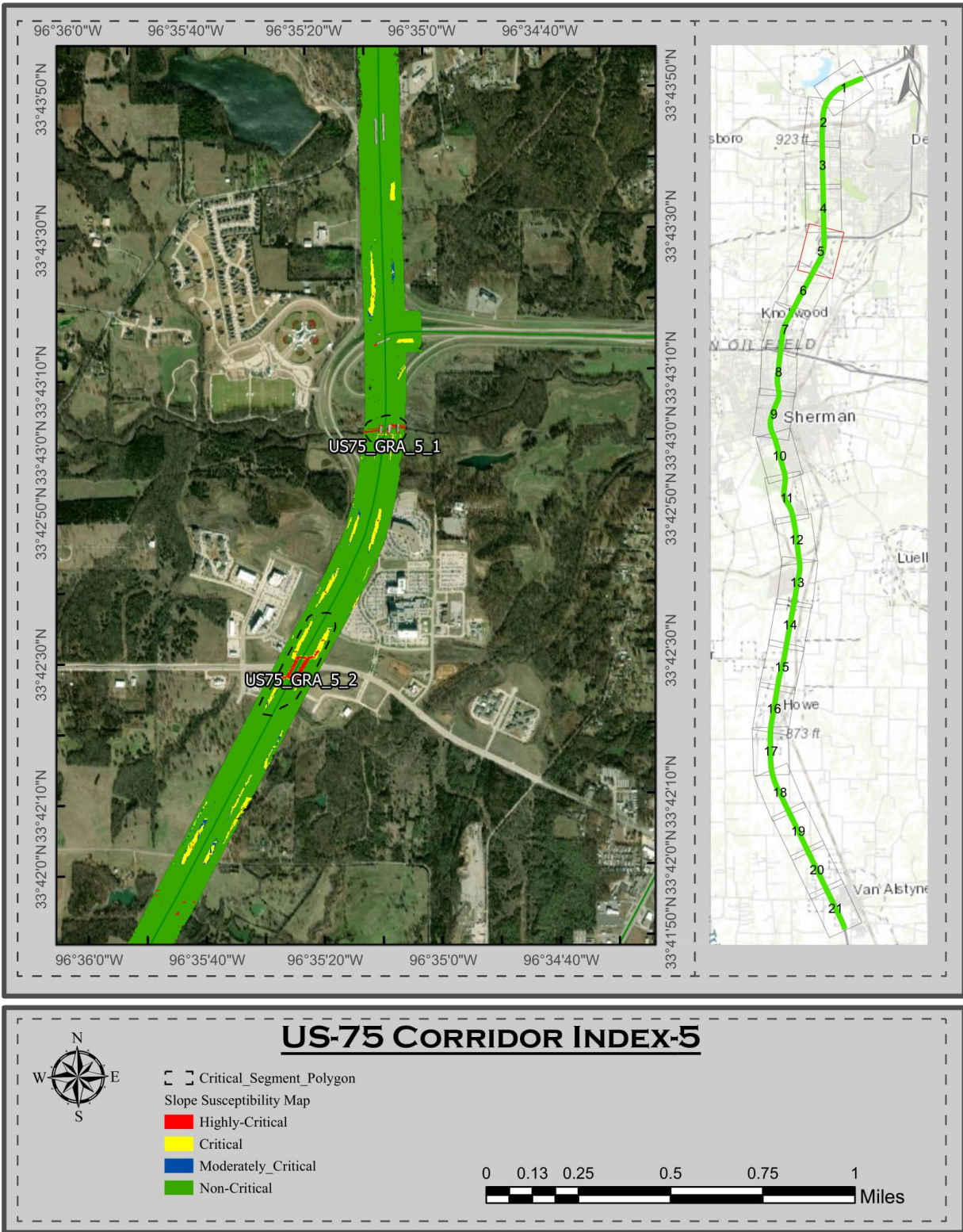


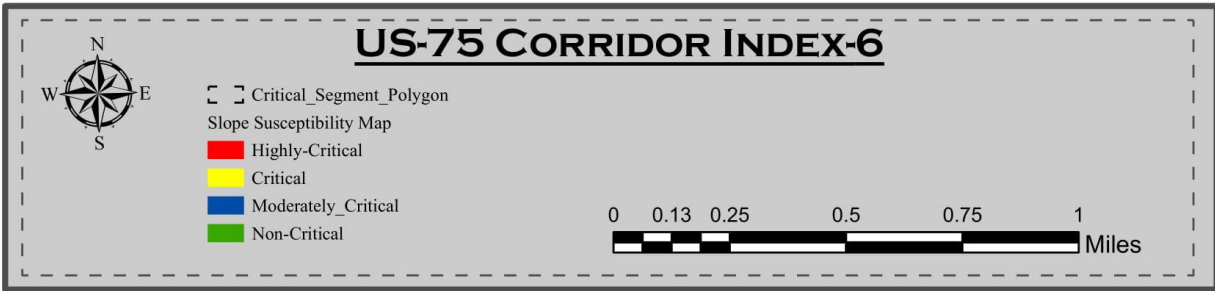


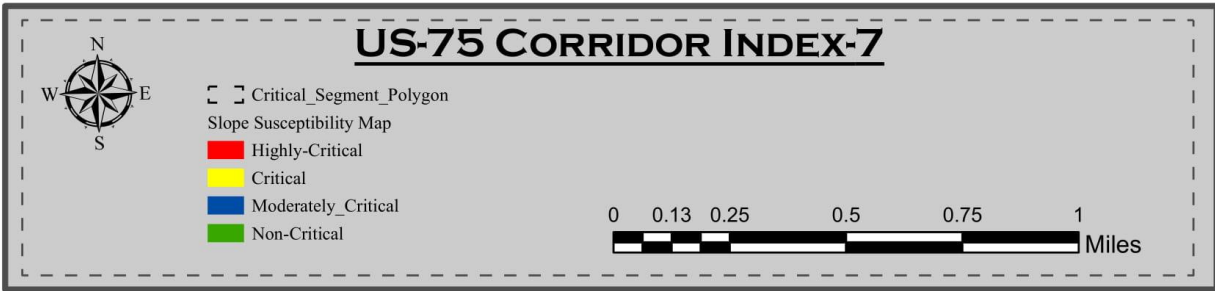
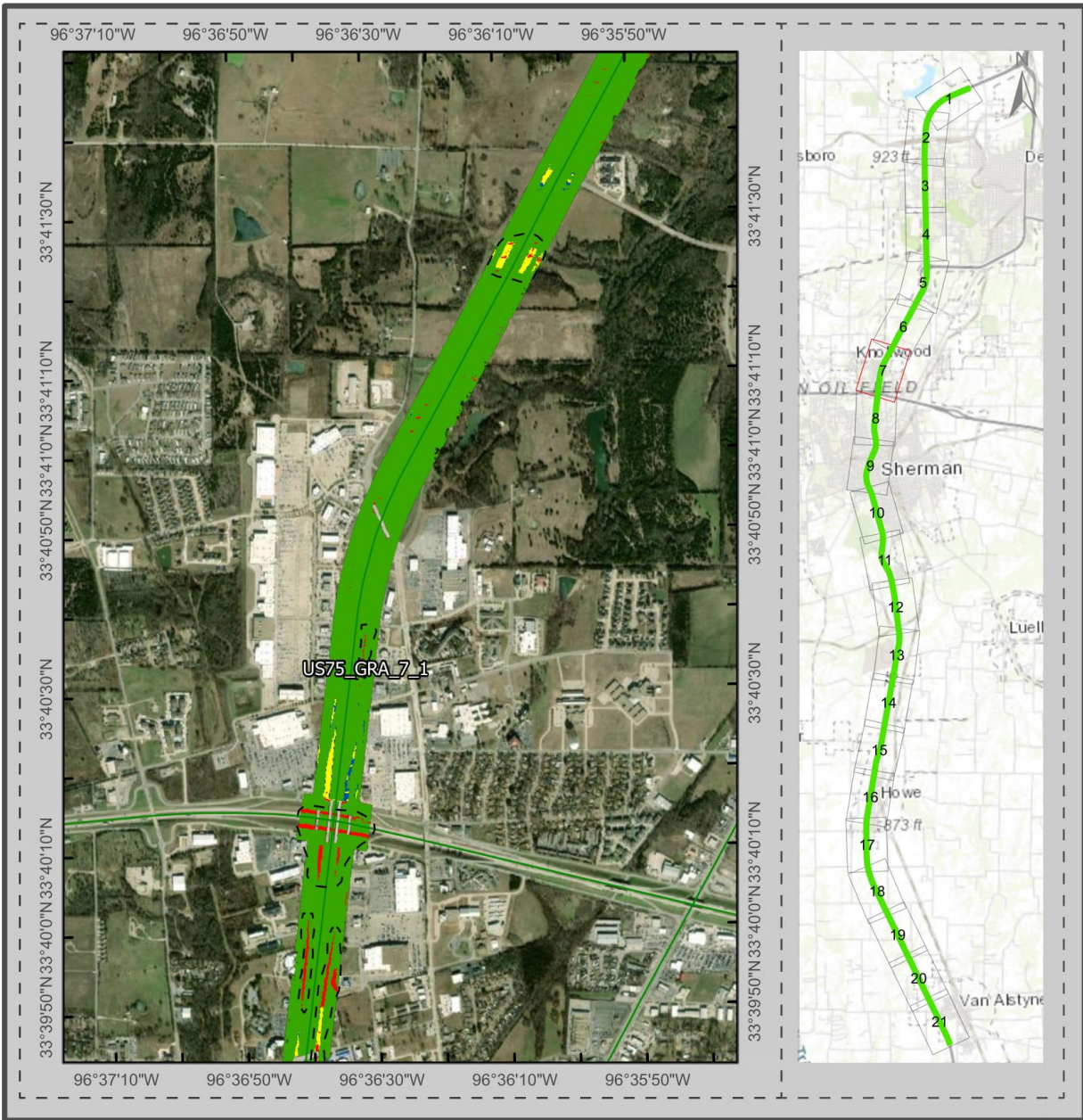


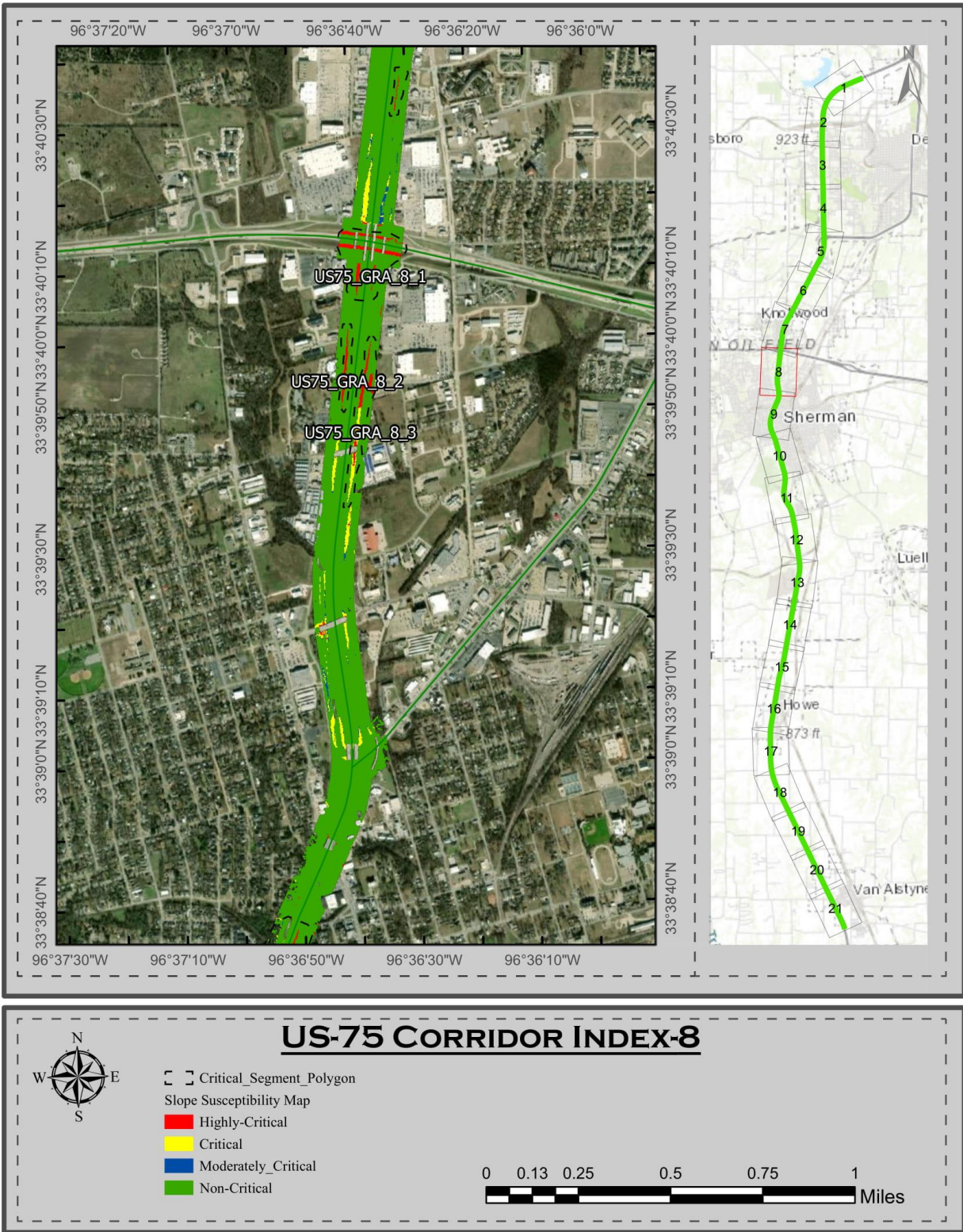


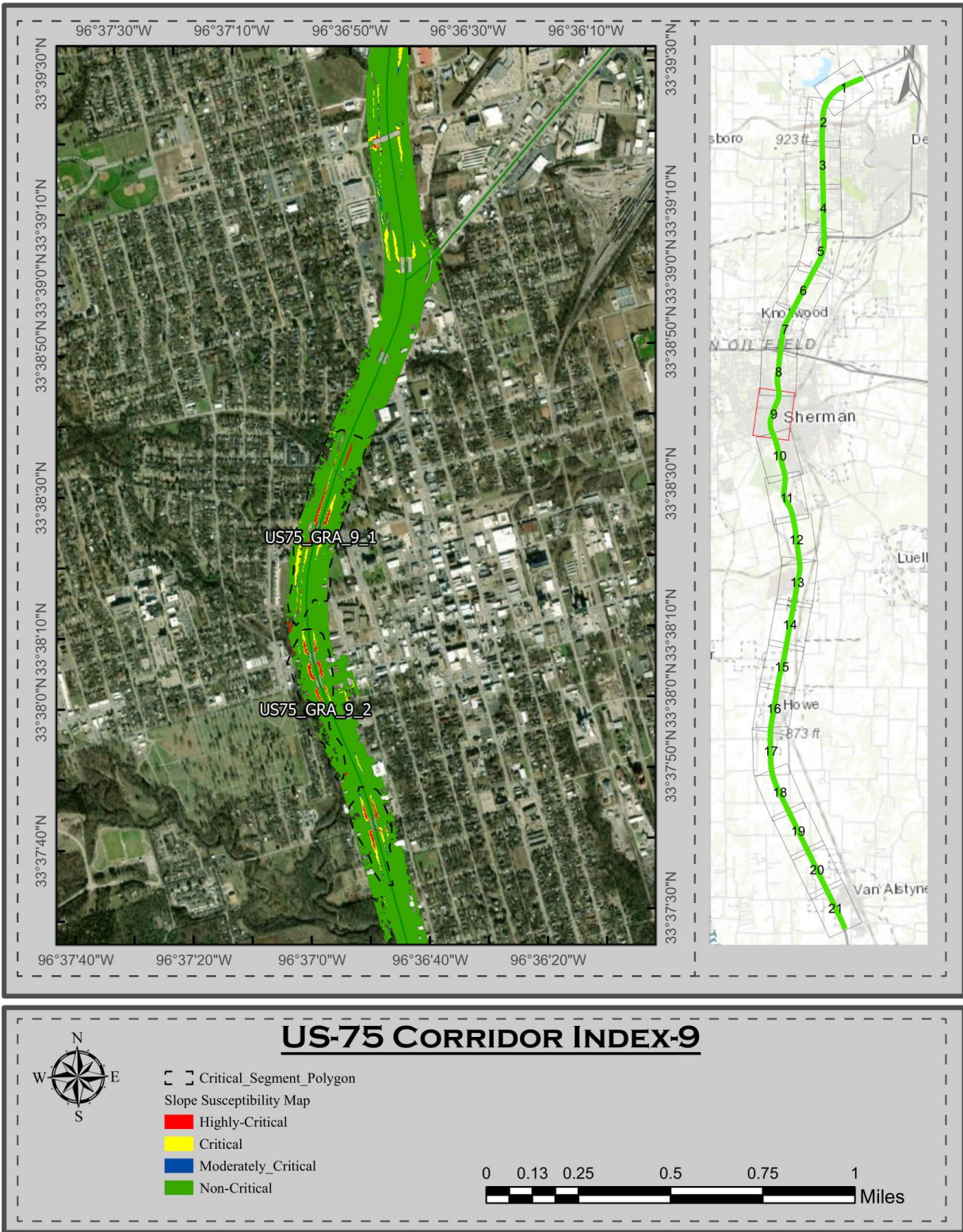




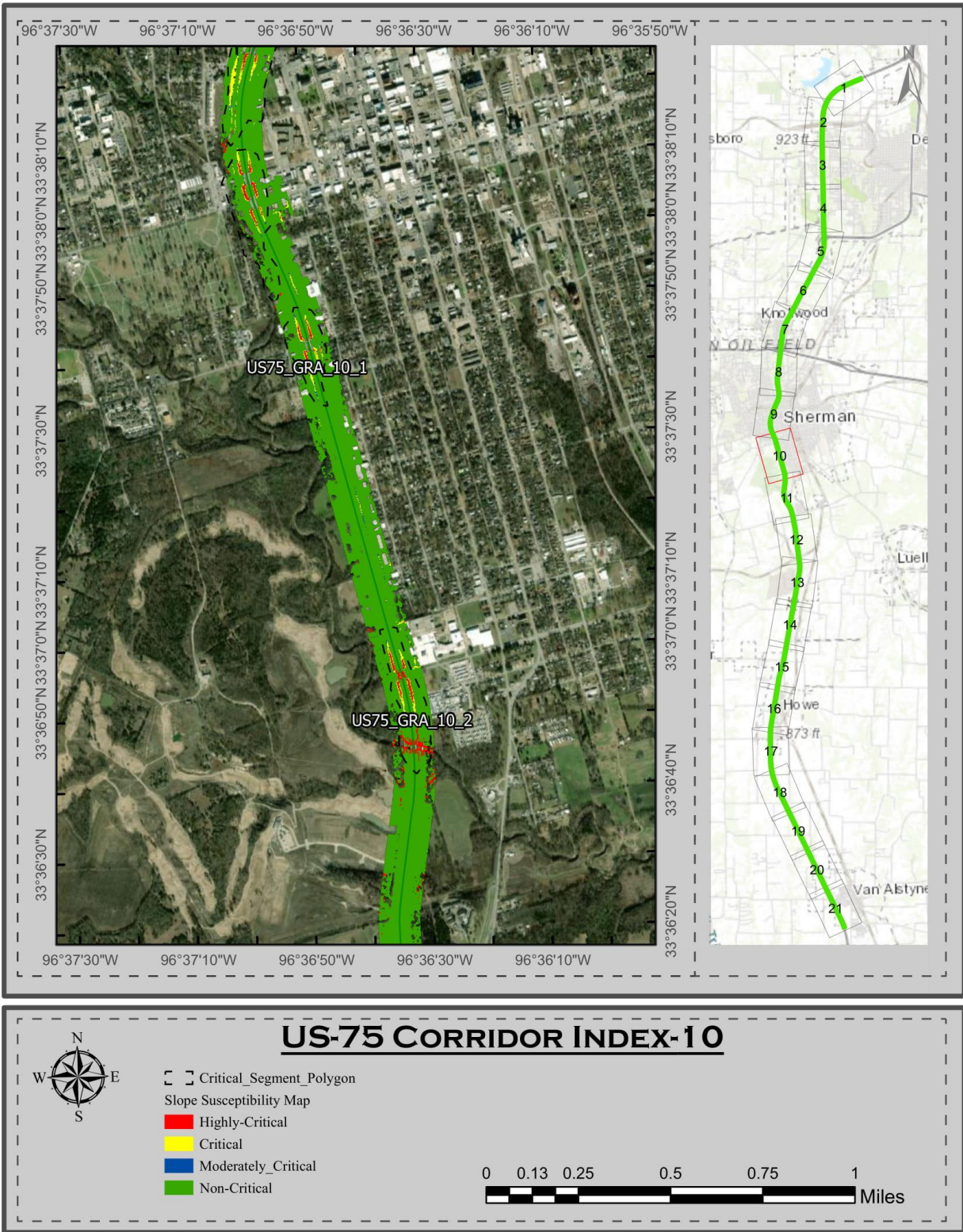


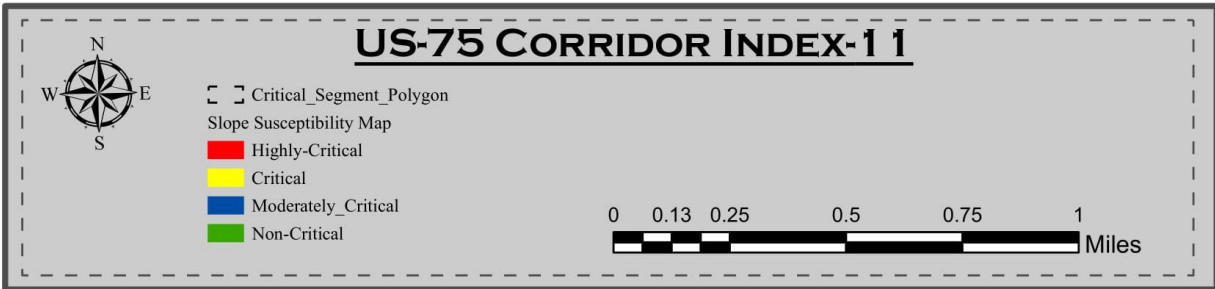


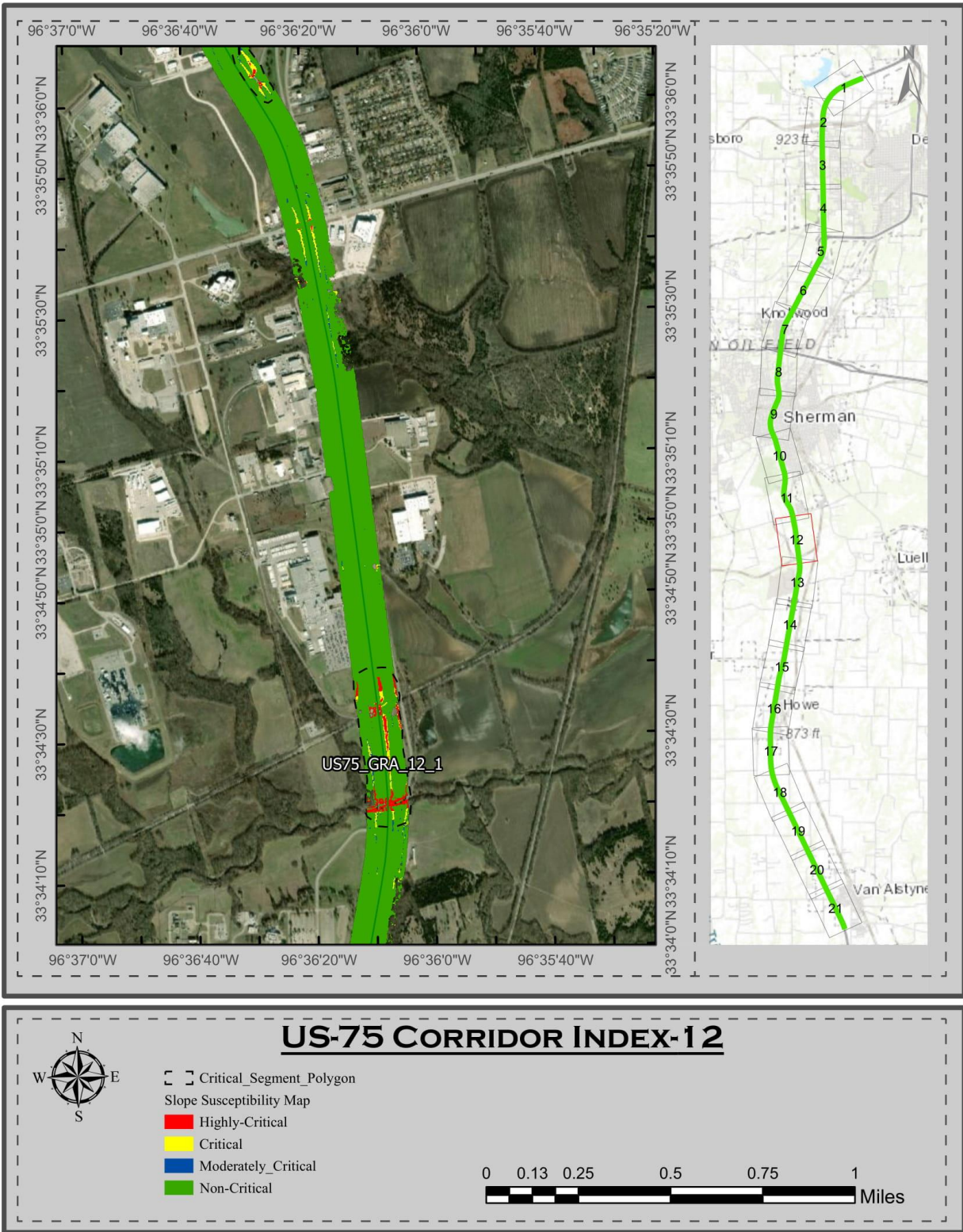


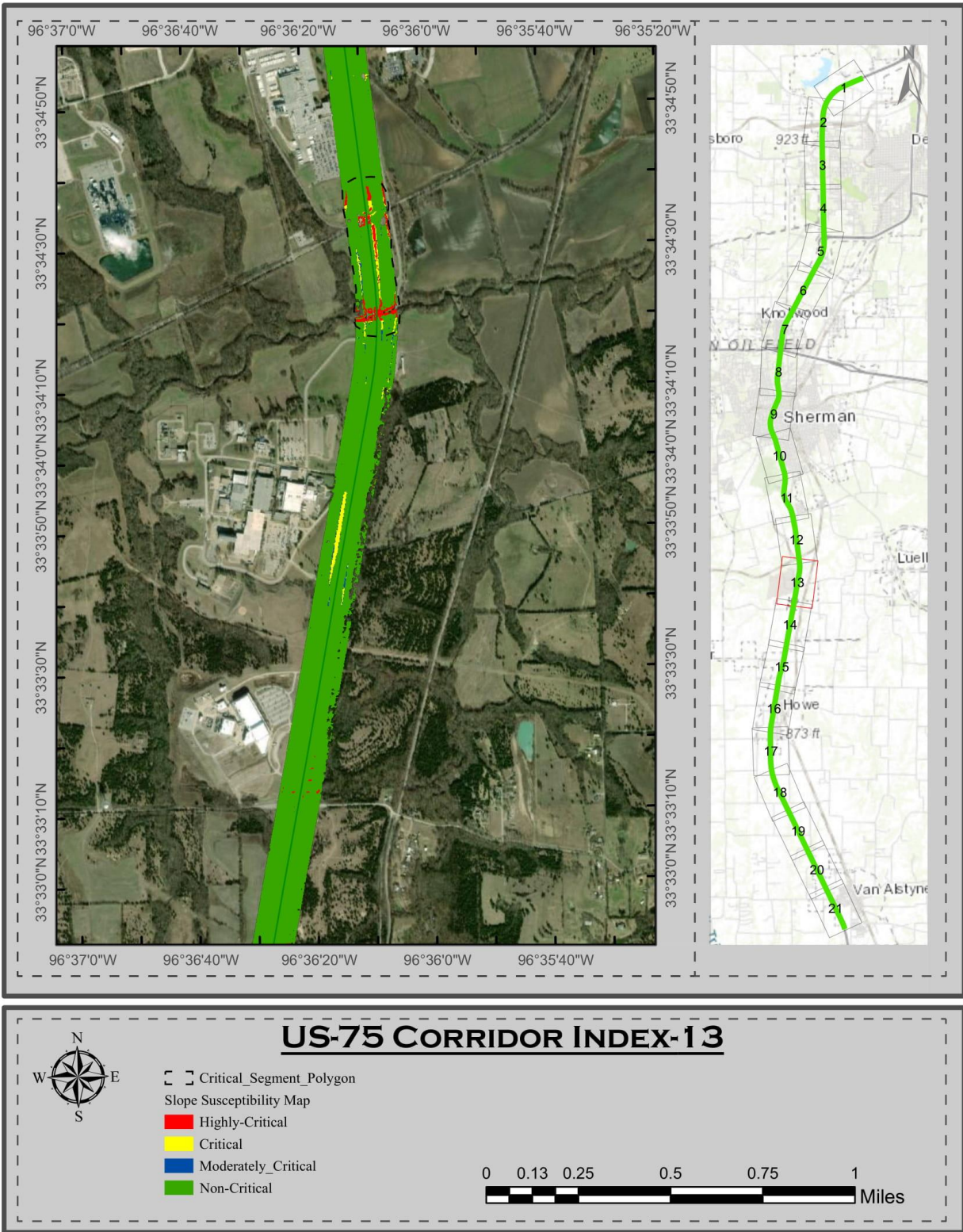


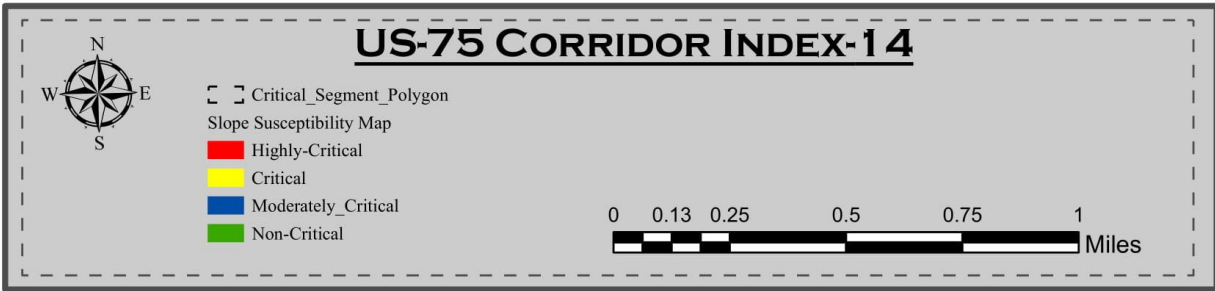
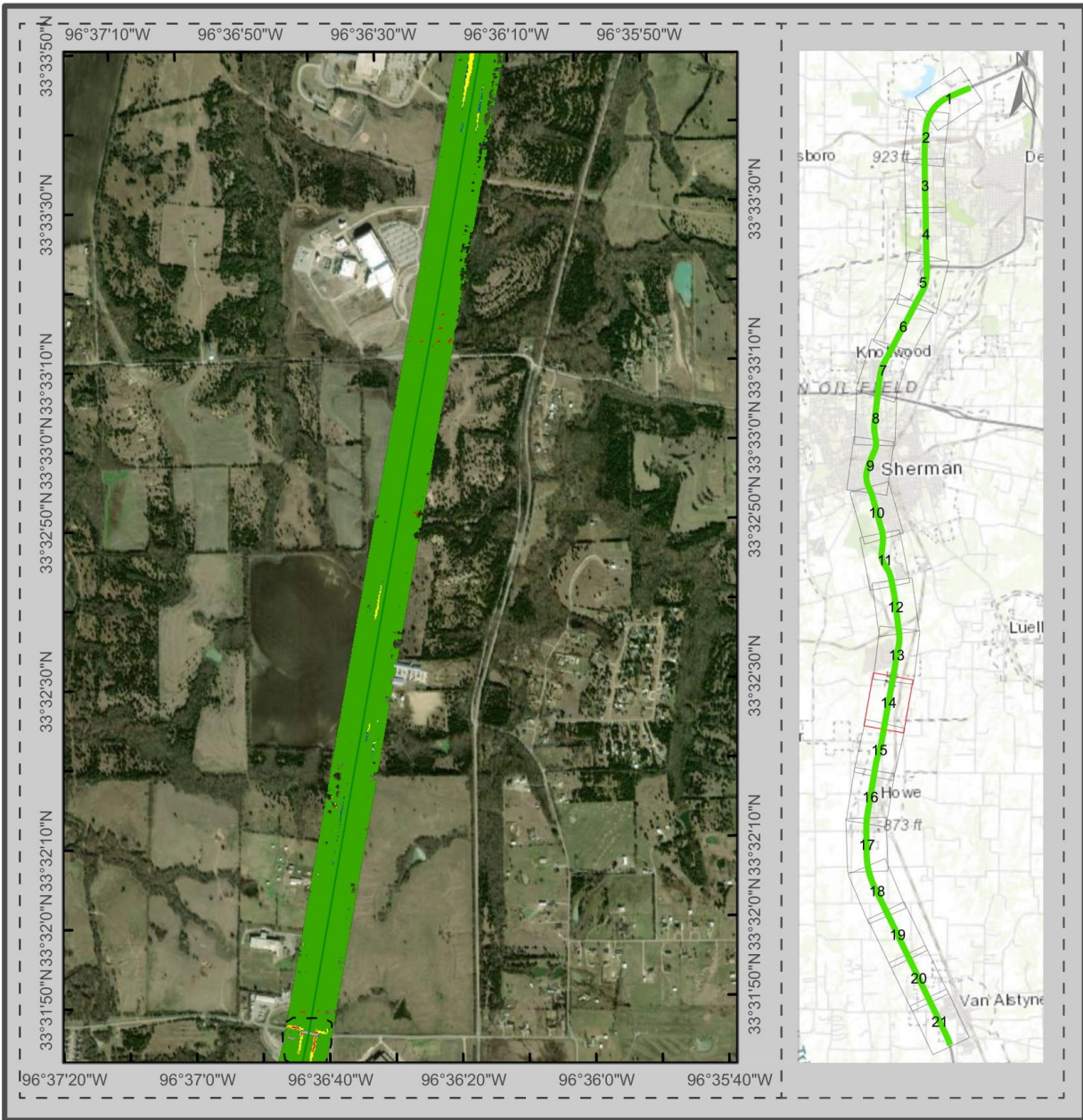


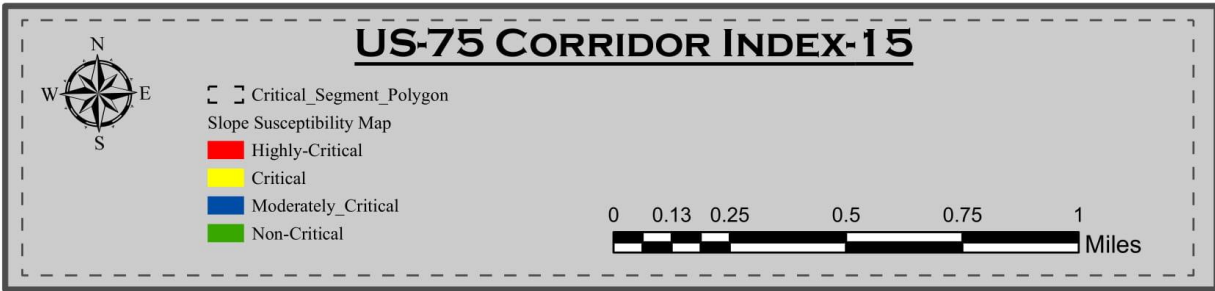


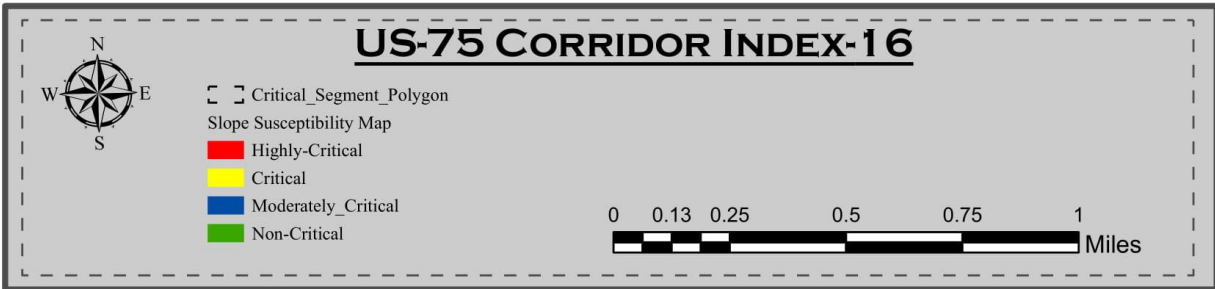
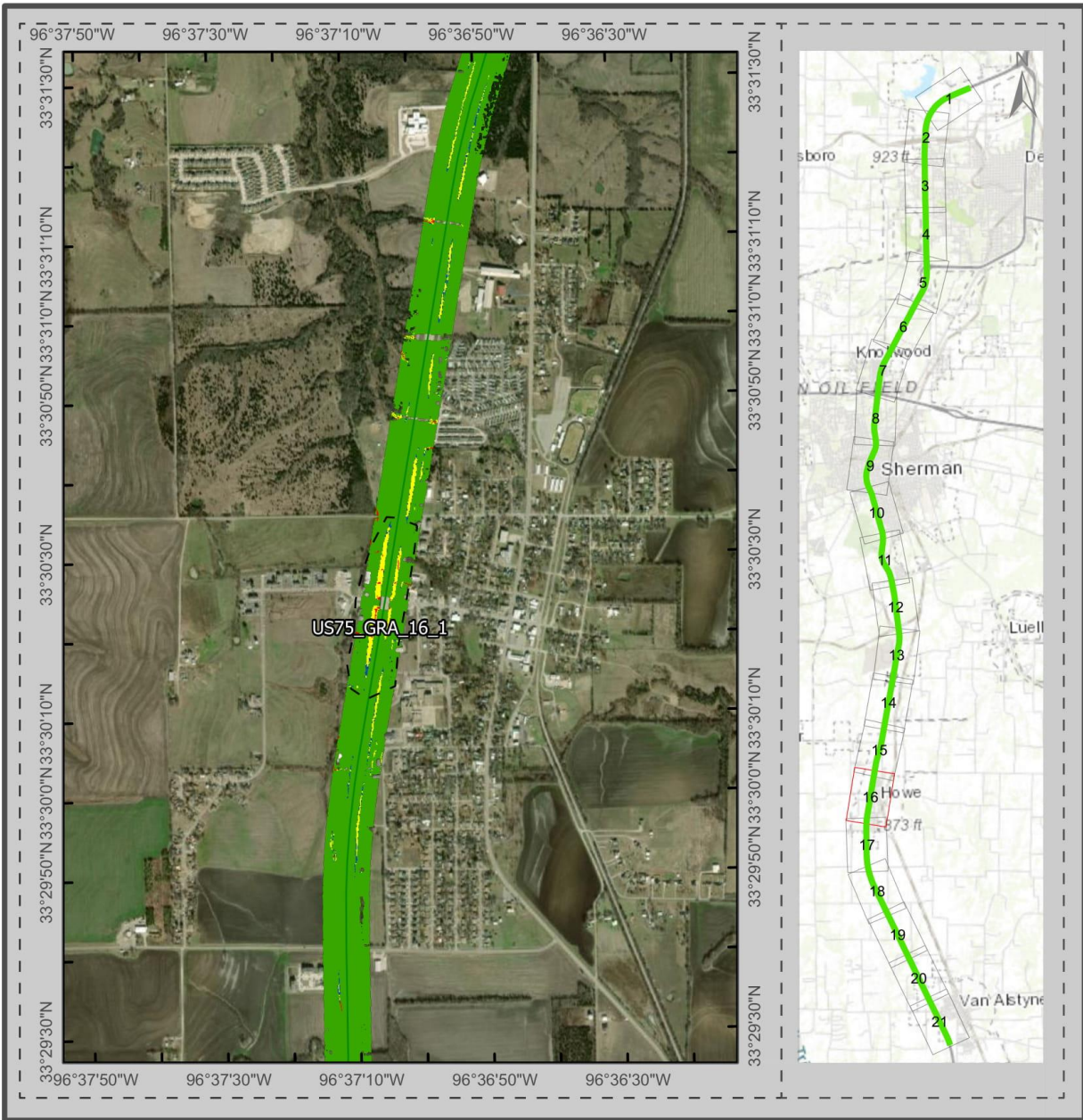


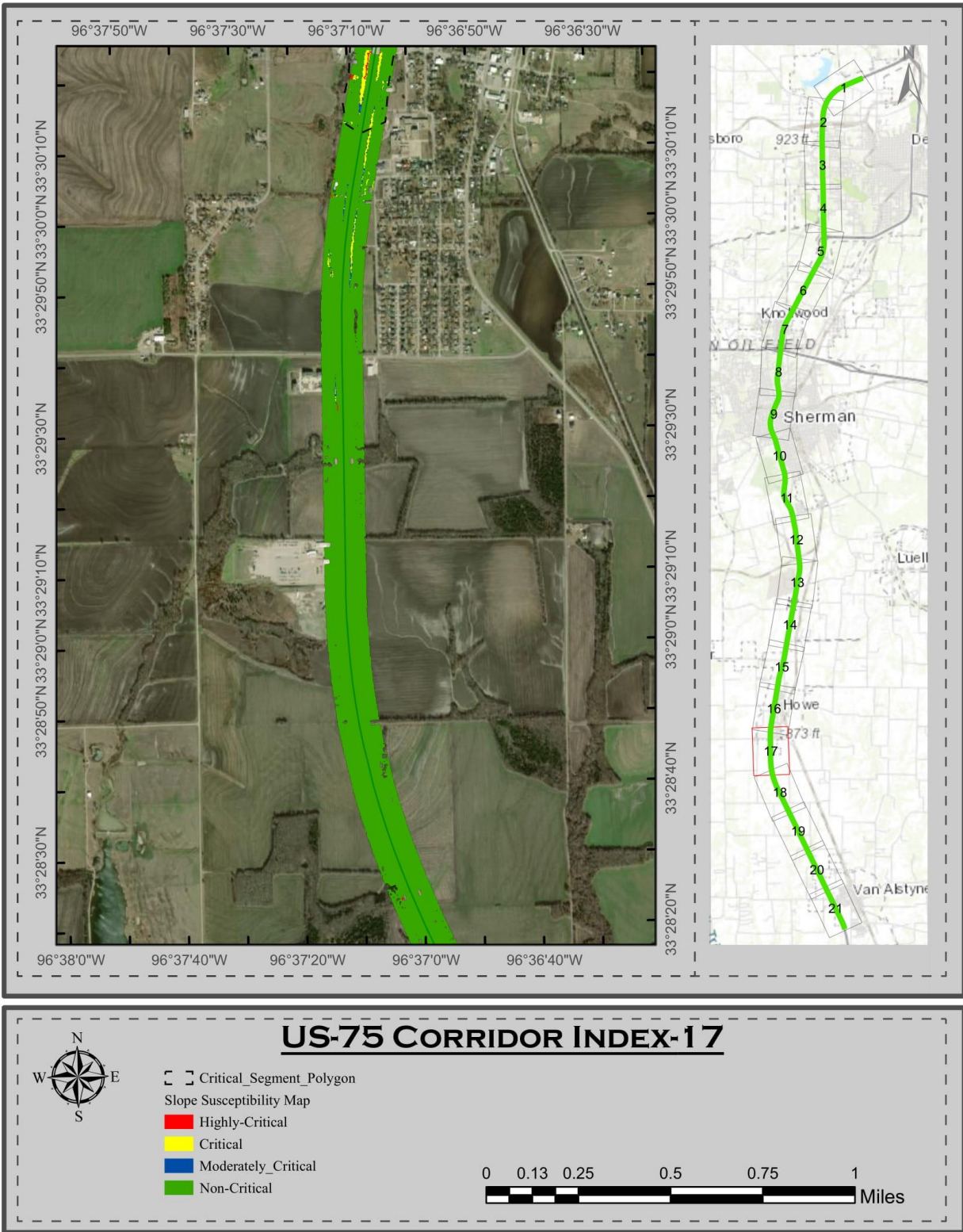




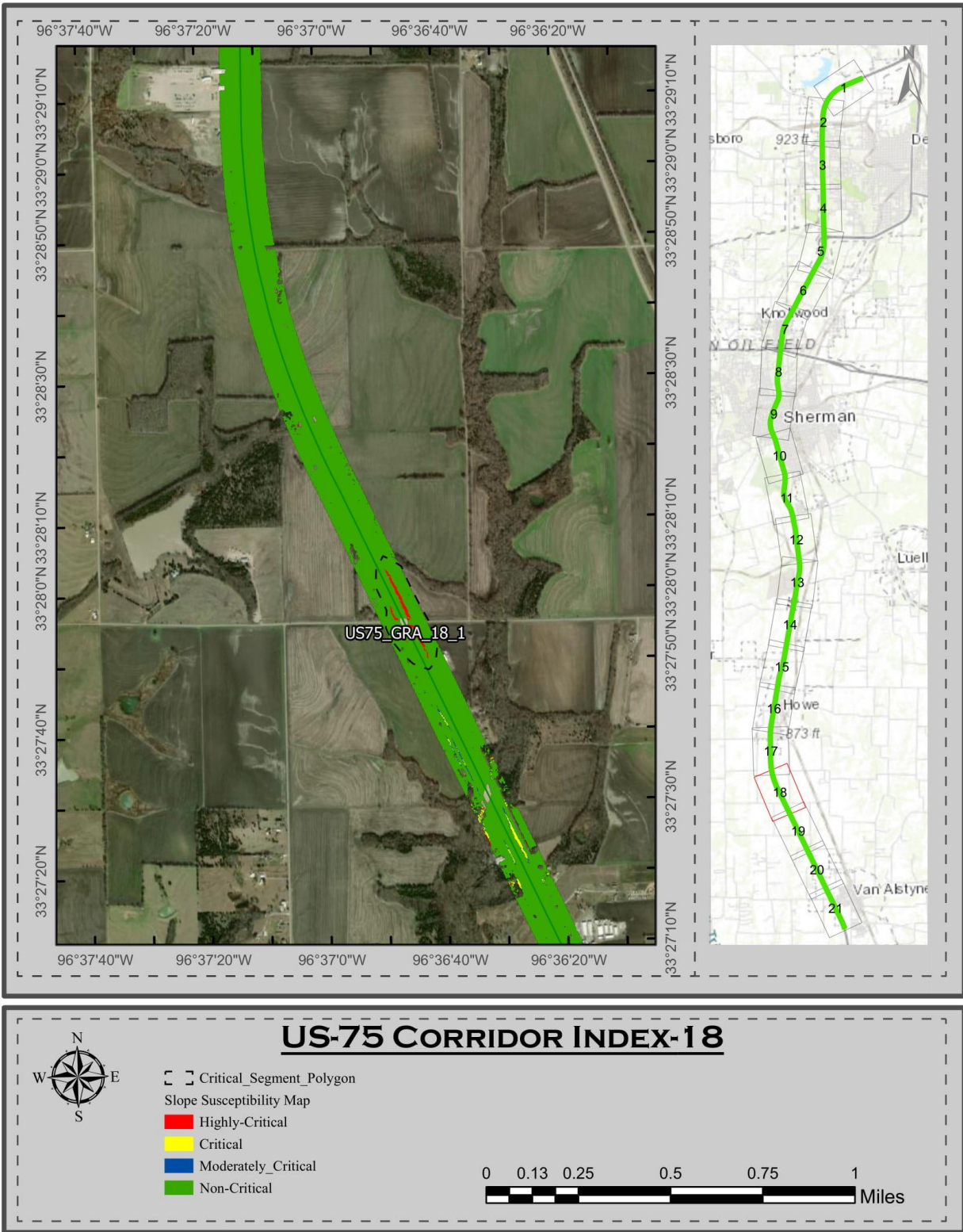


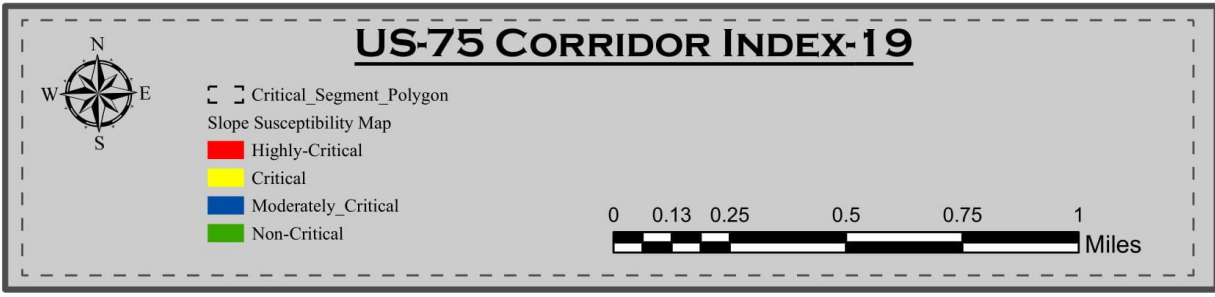


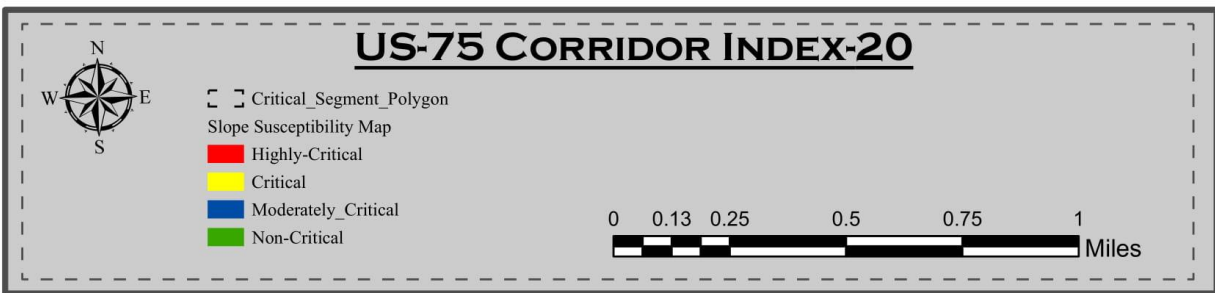
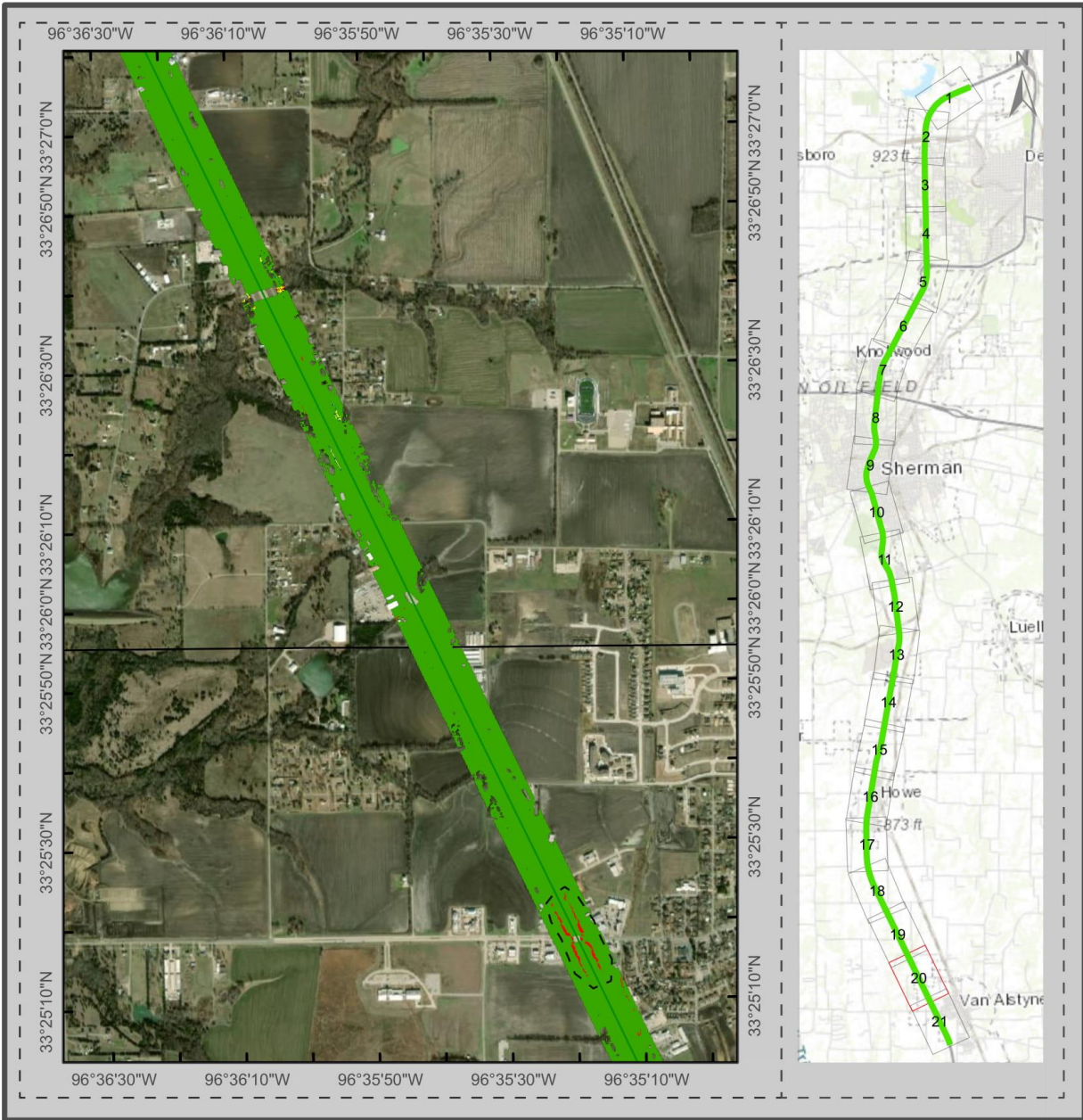


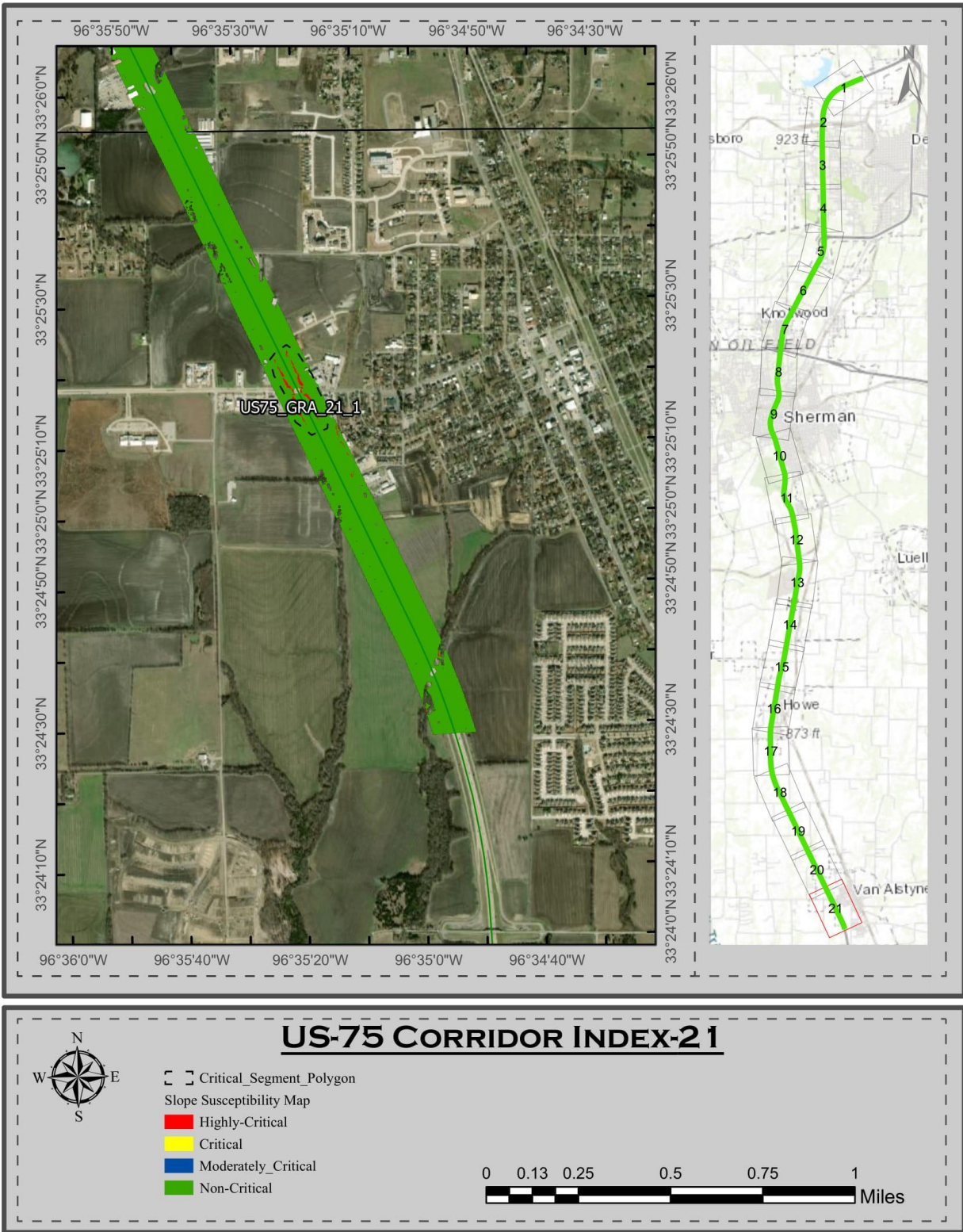




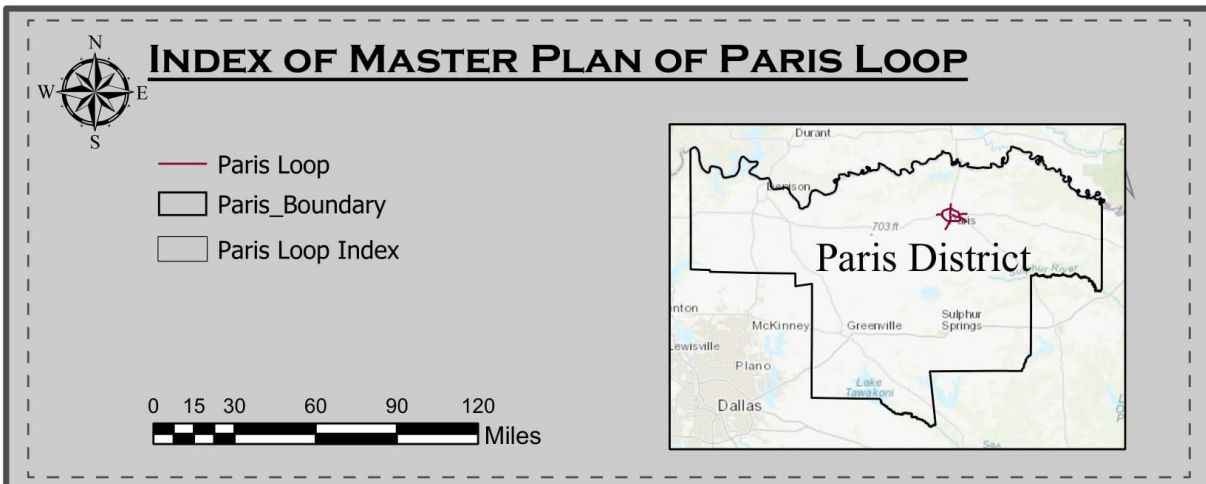
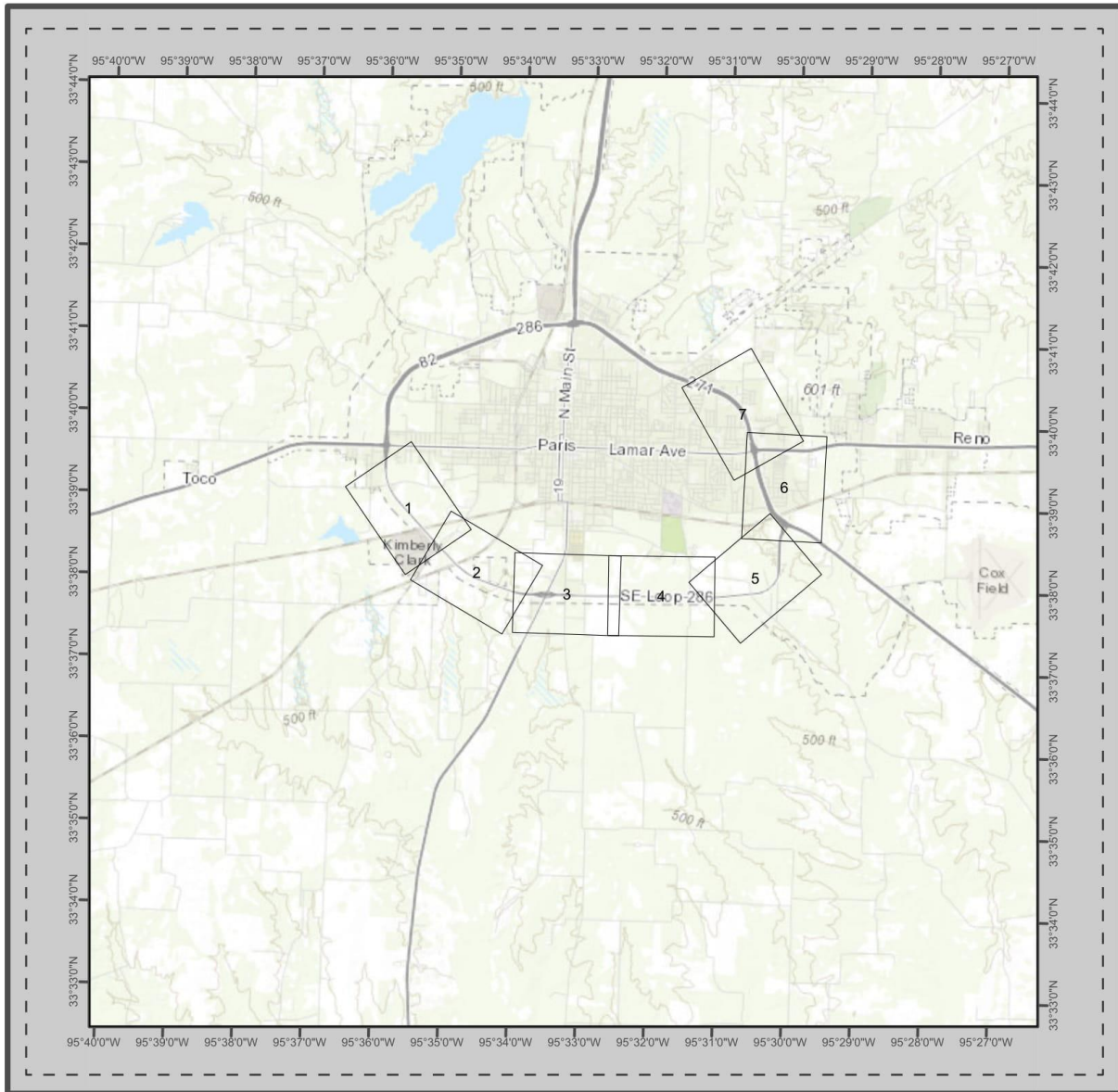


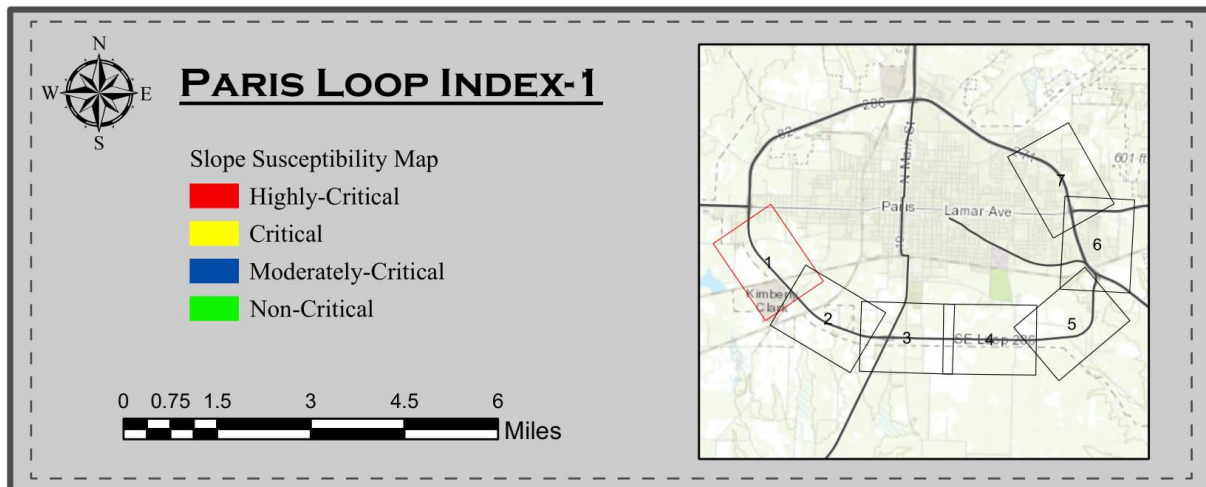
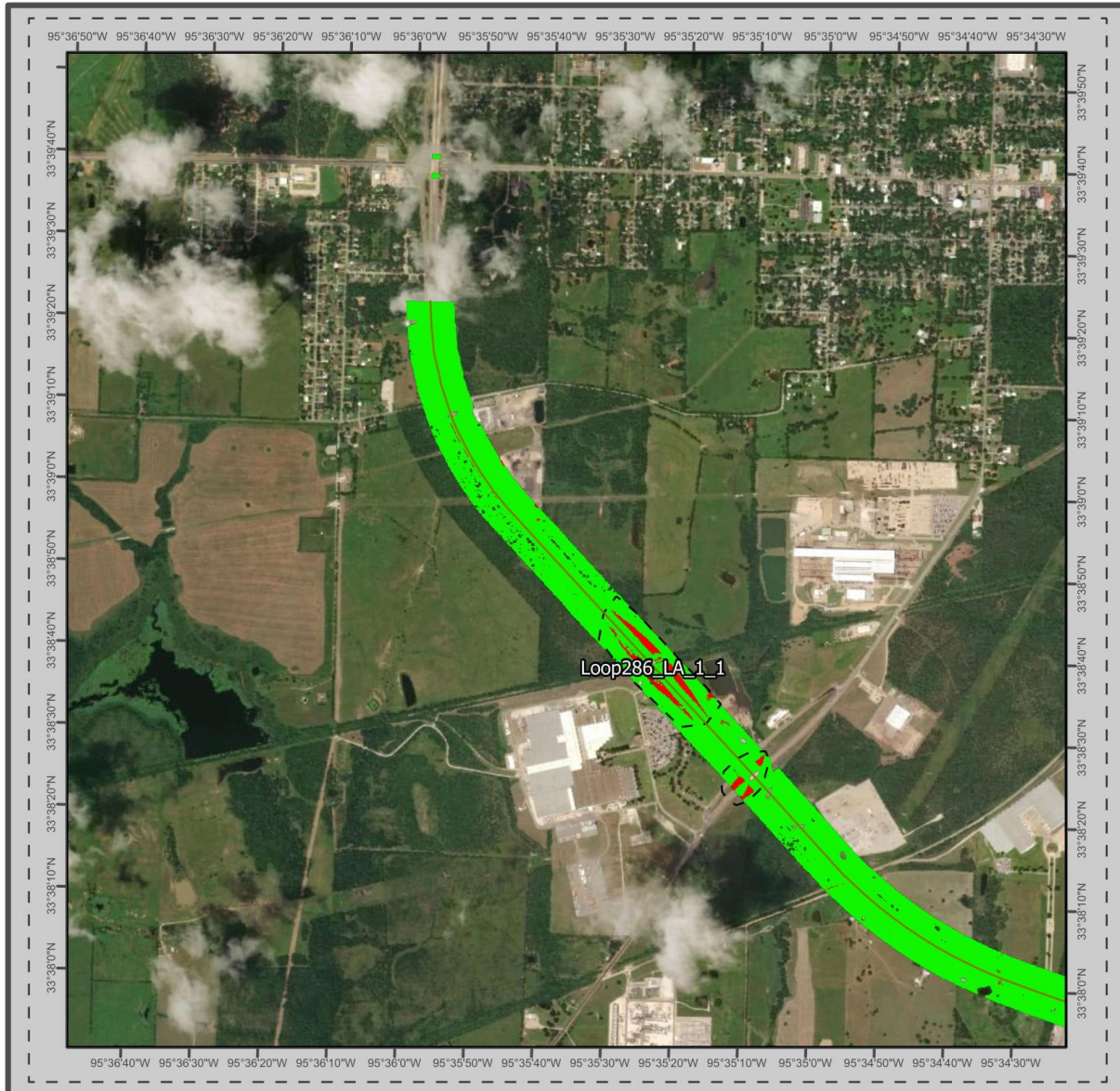


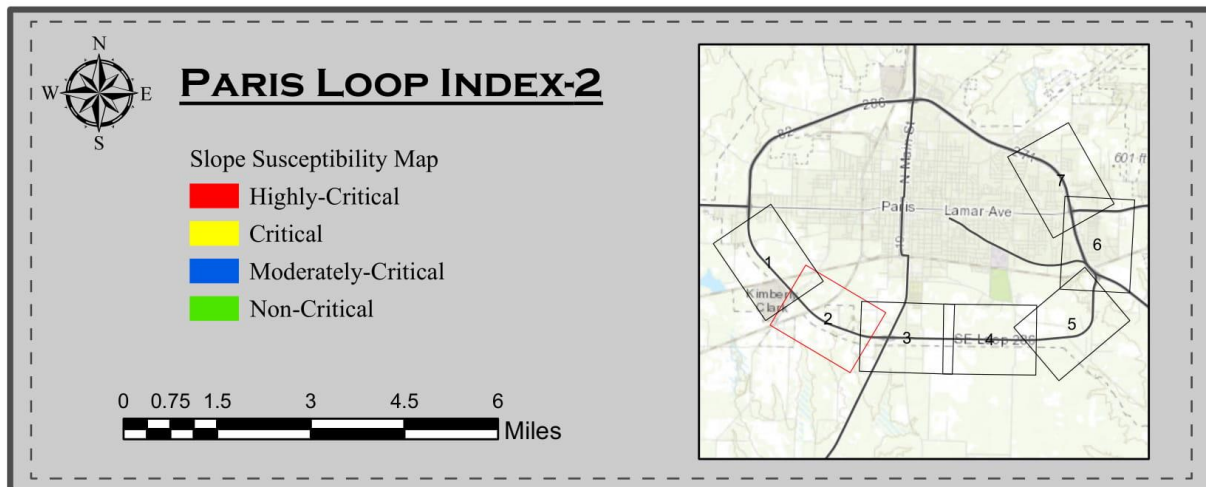


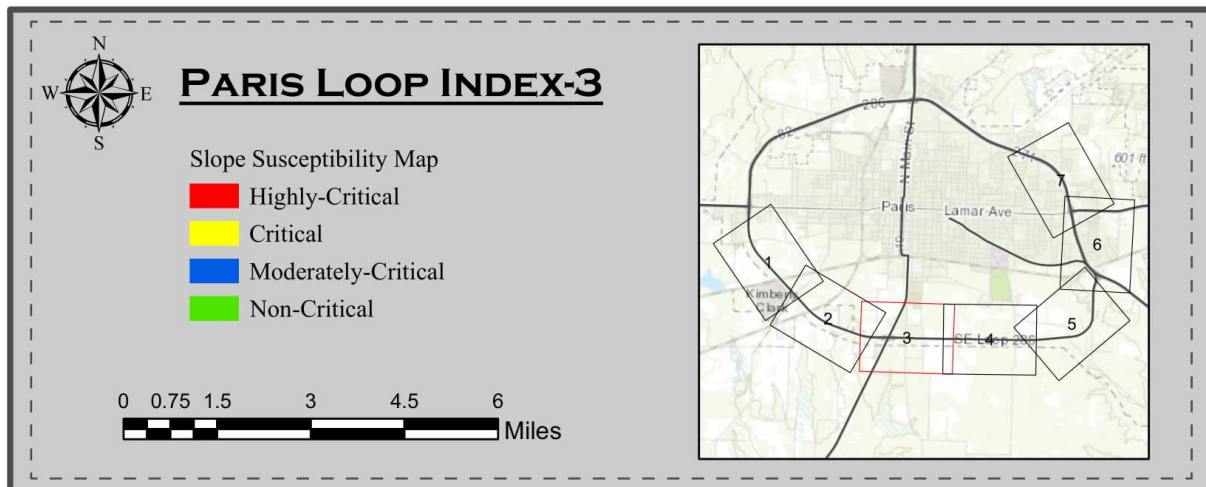
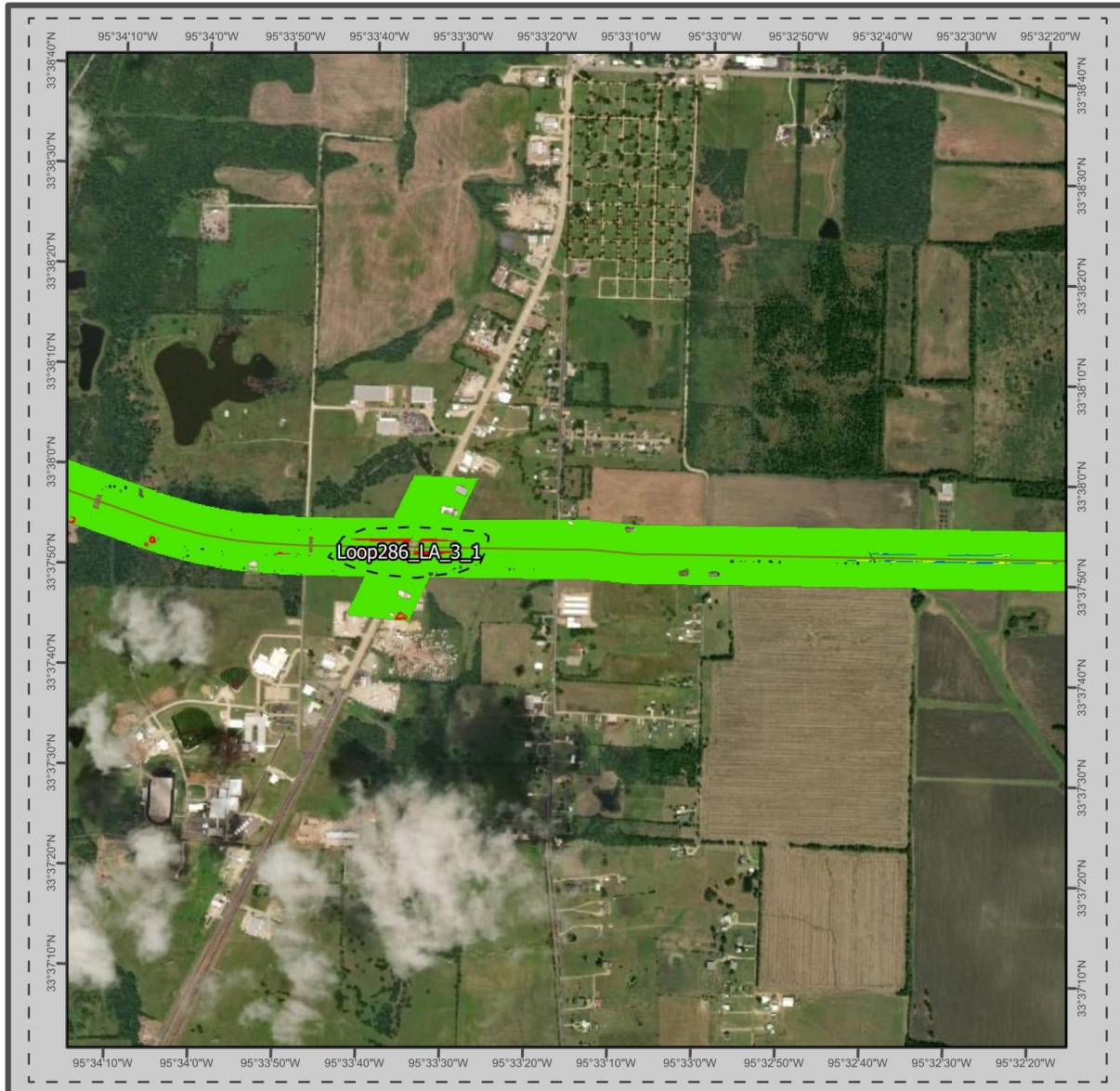


### Map Book of Critical Segments for Loop 286

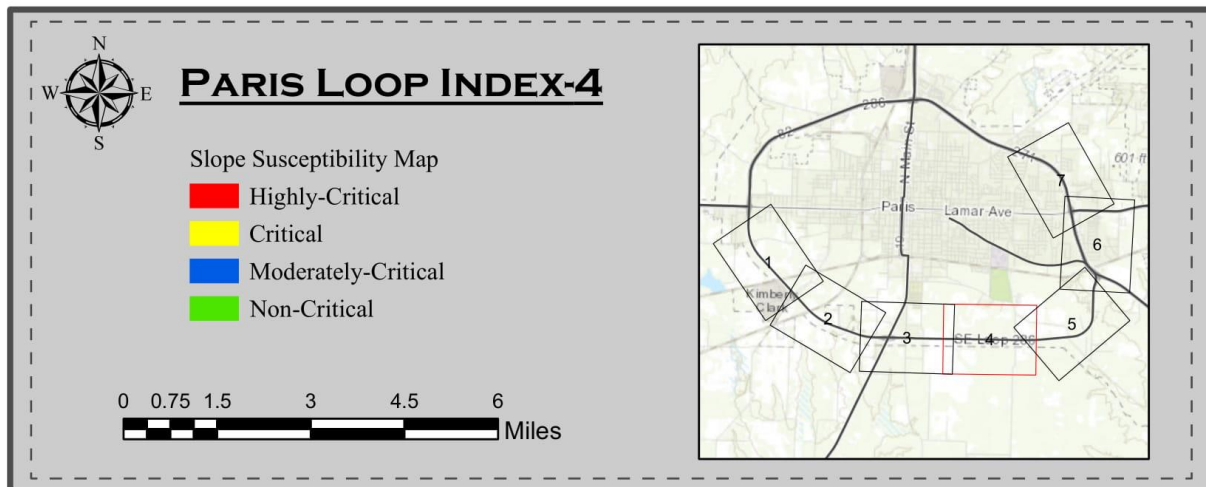


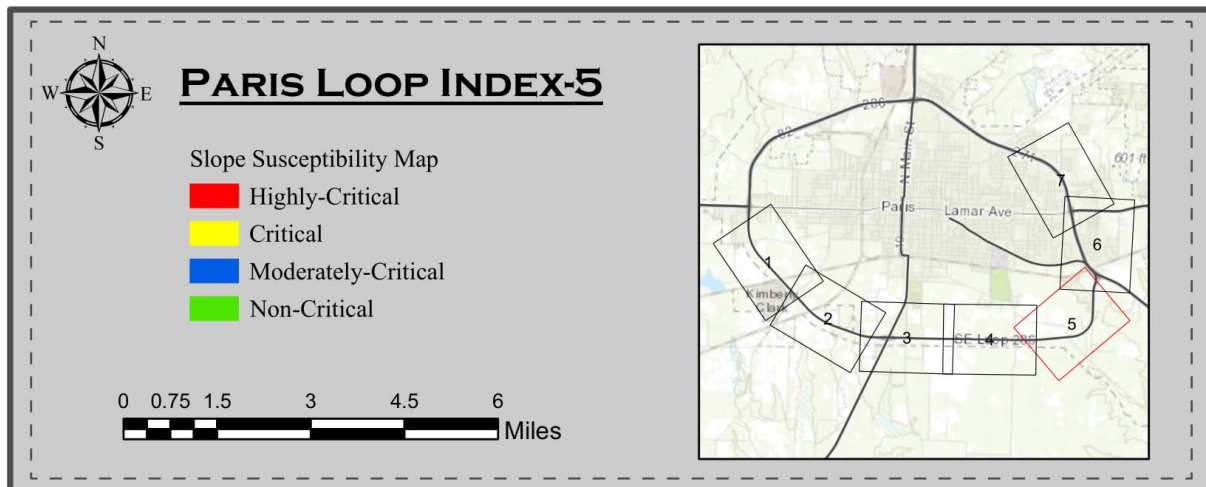
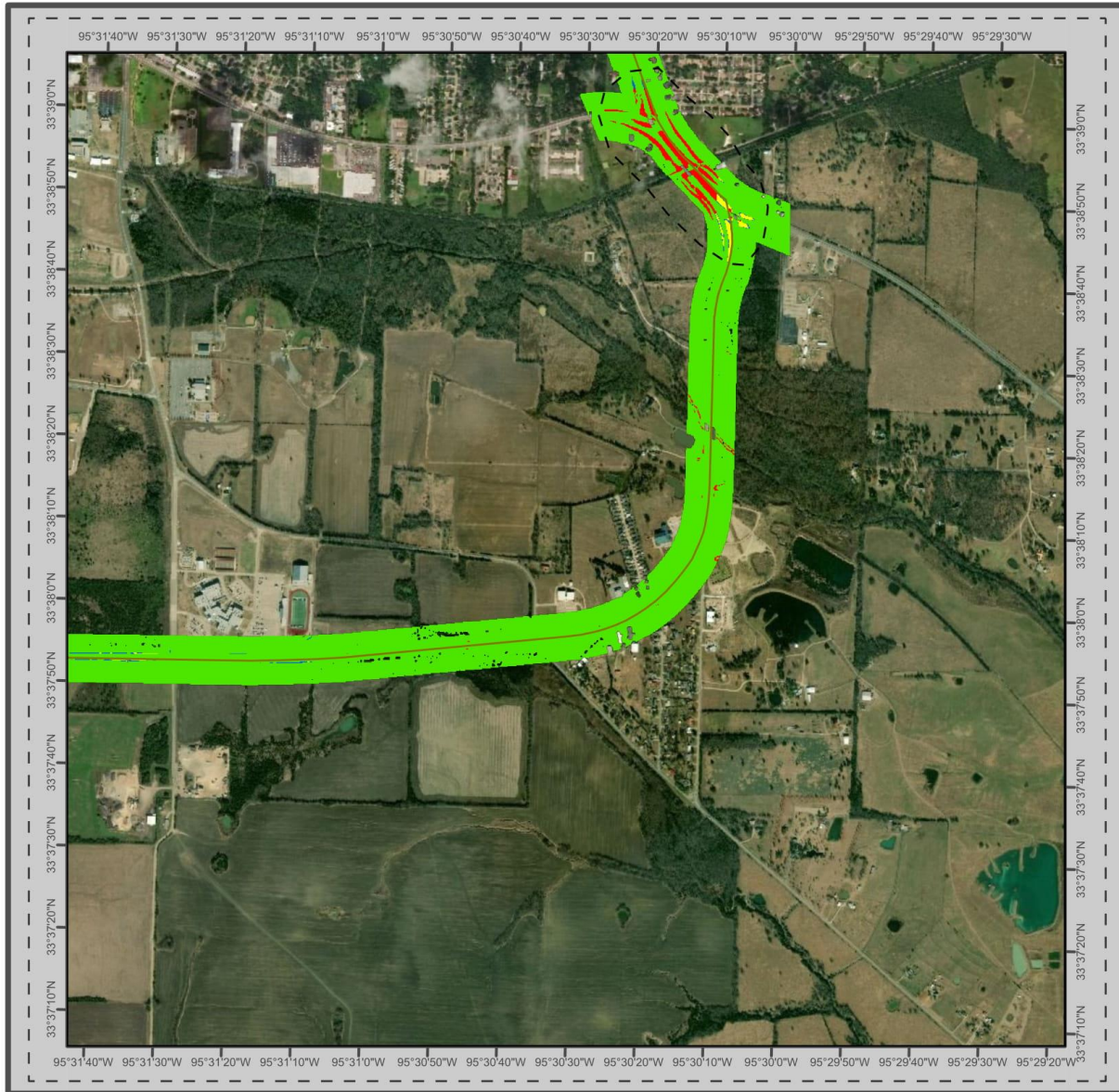


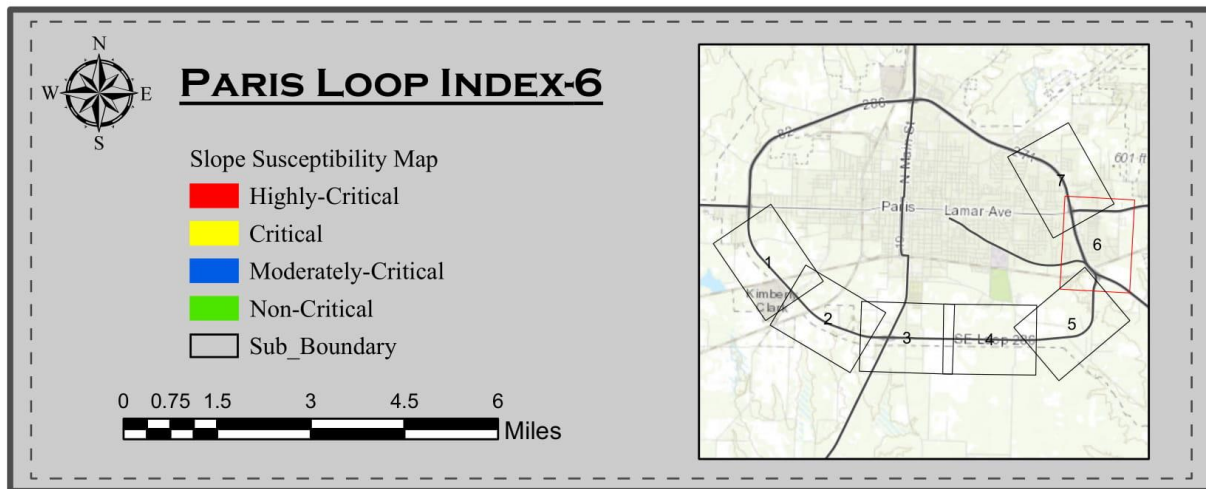
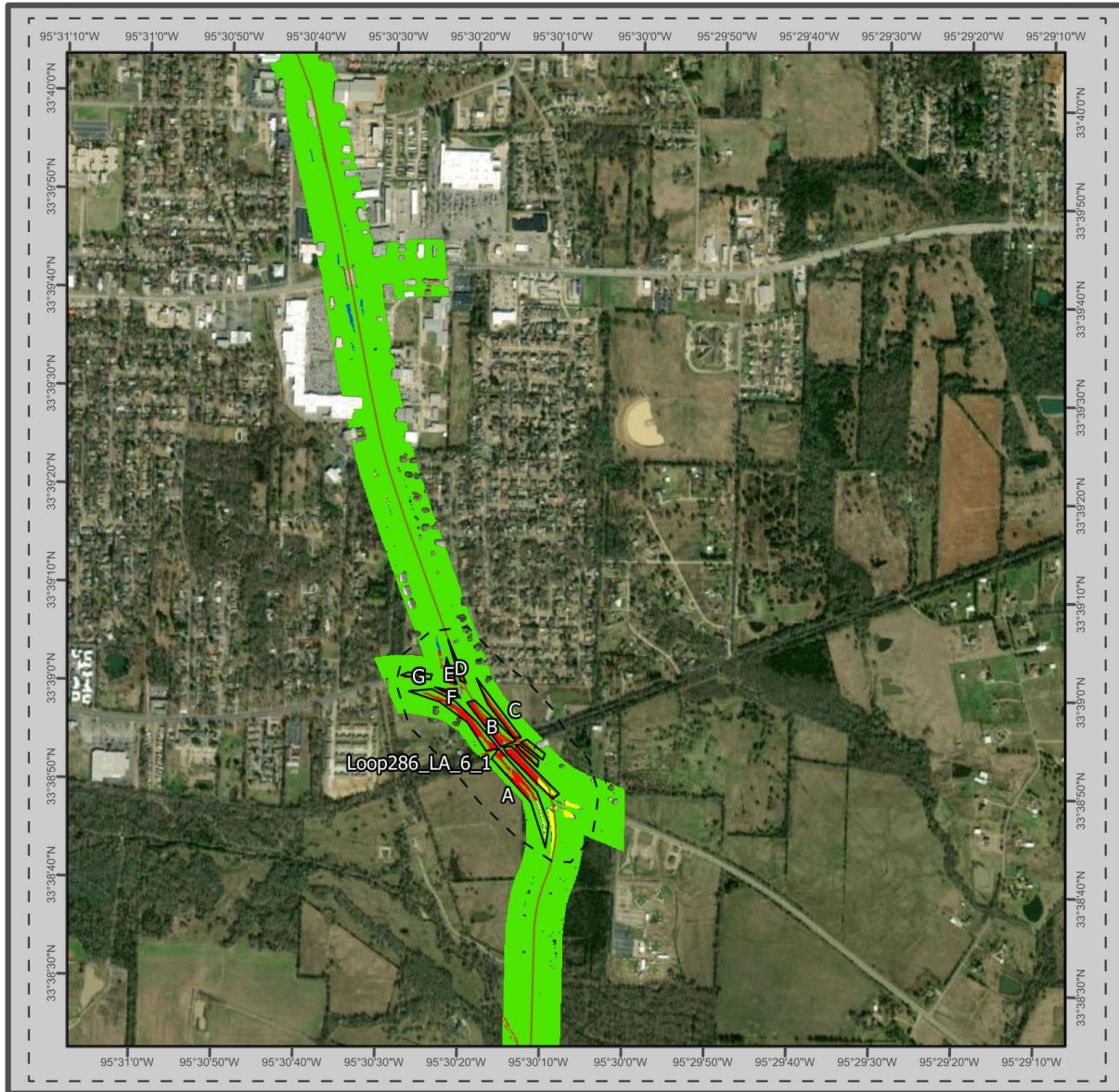


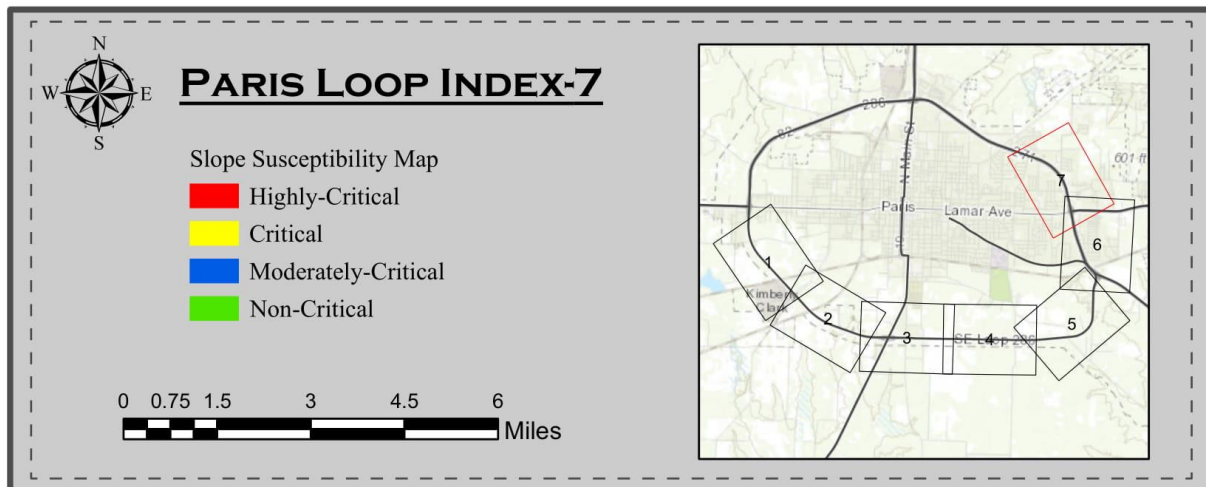












### 9.3.2. Google Earth Street View Images of Critical Slope Segments

The critical slope segments along the corridors were identified in the maps included in Section 9.3.1. It is essential to assess the vegetation and water management system of critical slope segments to develop the slope repair and maintenance plan. Google Earth street view images of all the highly critical slope segments along the US 75 and Loop 286 were collected to assess the present condition of critical slope segments. Google Earth street view images of each critical segment in US 75 and Loop 286 are presented in this section.

#### *Google Earth Street View Images of Critical Segments along US 75*

The Google Earth street view images for each critical segment in the US 75 highway corridor (Figure 9.4) are presented in this section. Critical segments along one side of the corridor have been presented with only one image. Critical segments on both sides along the corridor have been presented with two google images; the first image represents the right side (RT) of the corridor, and the second image represents the left side (LT) of the corridor.

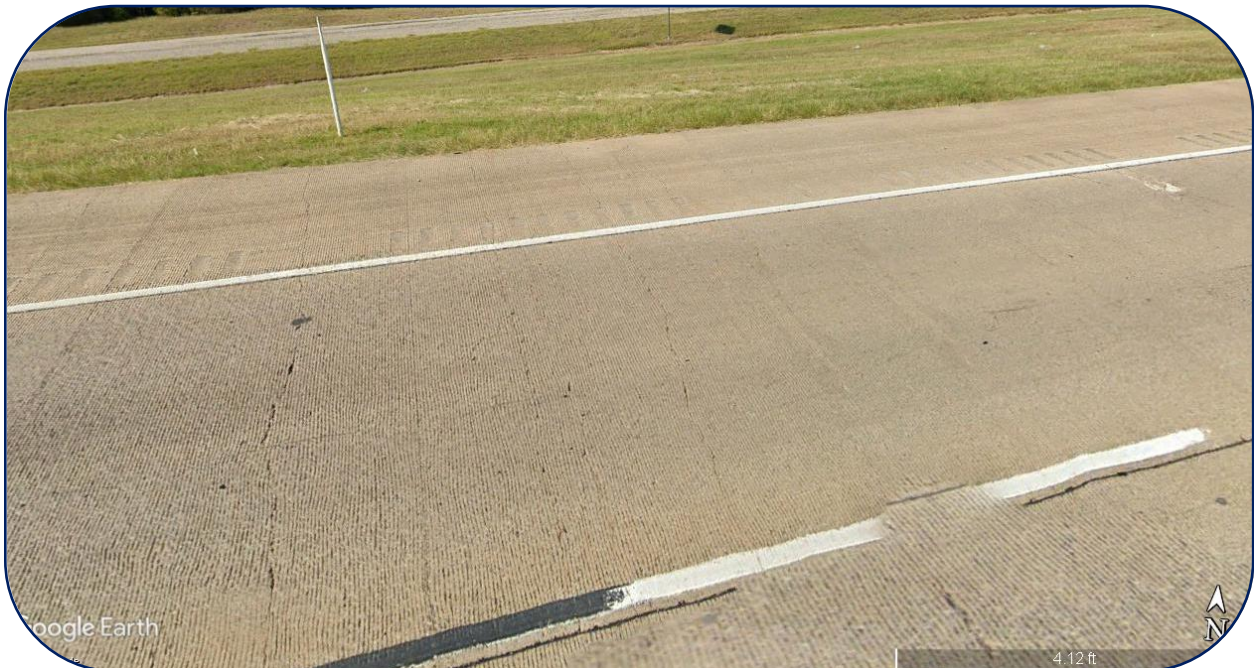


**Figure 9.4** US 75 corridor in Paris district

**US75\_GRA\_1\_1**



**US75\_GRA\_1\_2**



**US75\_GRA\_1\_3**



**US75\_GRA\_2\_1**



US75\_GRA\_2\_2



US75\_GRA\_2\_3





US75\_GRA\_2\_5



US75\_GRA\_2\_6



US75\_GRA\_2\_7



US75\_GRA\_5\_1



**US75\_GRA\_5\_2**



**US75\_GRA\_6\_1**



US75\_GRA\_7\_1



US75\_GRA\_8\_1



**US75\_GRA\_8\_2**



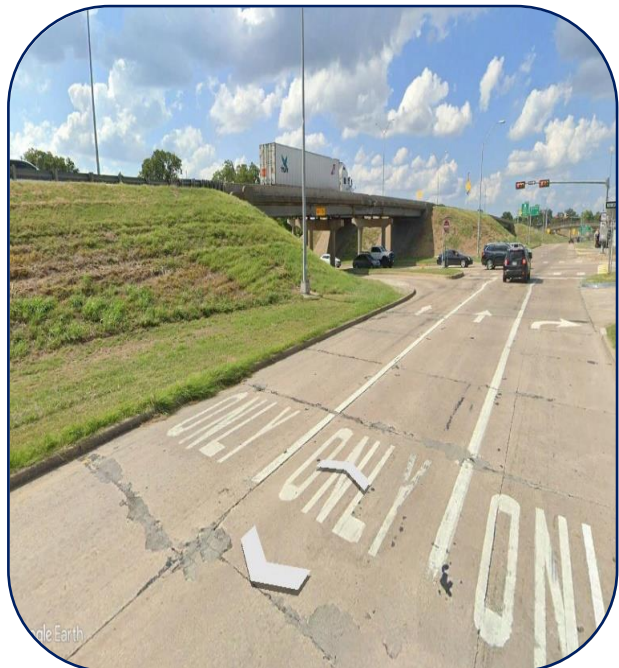
**US75\_GRA\_8\_3**



**US75\_GRA\_9\_1**



**US75\_GRA\_9\_2**



**US75\_GRA\_10\_1**



**US75\_GRA\_10\_2**



**US75\_GRA\_11\_1**



**US75\_GRA\_12\_1**





**US75\_GRA\_15\_1**



**US75\_GRA\_16\_1**



**US75\_GRA\_18\_1**



**US75\_GRA\_21\_1**



**Google Earth Street View Images of Critical Segments Along Loop 286**

This section includes the Google Earth street view images of critical segments along the southern segment of Loop 286 (Figure 9.5) in Lamar County of TxDOT Paris district.



**Figure 9.5** Map showing the southern segment of Loop 286 corridor in Paris district

**Loop286\_LA\_1\_1**



**Loop286\_LA\_2\_1**



**Loop286\_LA\_3\_1**



**Loop286\_LA\_6\_1\_A**



**Loop286\_LA\_6\_1\_B**



**Loop286\_LA\_6\_1\_C**



**Loop286\_LA\_6\_1\_D**



**Loop286\_LA\_6\_1\_E**



**Loop286\_LA\_6\_1\_F**



**Loop286\_LA\_6\_1\_G**





#### **9.4. MAINTENANCE SCHEDULE**

The maintenance schedule was developed for repair and maintenance of critical slope segments along the US 75 and Loop 286 corridors. The critical slope segments were prioritized based on four criteria: proximity to bridges, proximity to intersections, proximity to road carriageway, and traffic interruption. The prioritization criteria were assigned values of 0 or 1 for all critical slope segments. For example, the slopes that are within 50 ft from bridges and intersections were assigned a value of 1, whereas the slopes, which are not located close to bridges and intersections, were assigned a value of 0. Similarly, the slopes that directly support the road carriageway were assigned a value of 1. Otherwise, a value of zero was assigned. Also, slopes that cause significant disruption to traffic in case of emergency slope repair due to inadequate right of way were assigned a value of 1. The average value of prioritization criteria was determined for each critical slope segment. The critical slope segments were ranked based on the average value; the slope segment with the highest average was given top priority and scheduled for early maintenance. Table 9.1 and Table 9.2 show the maintenance schedule and prioritization schemes for critical slope segments of US 75 and Loop 286, respectively.

**Table 9.1** Maintenance schedule of critical slope segments along US 75 highway corridor

No	Proposed Schedule	Total Linear Length (in miles)	Designation	Location	Segment Length (in miles)	Proximity to Bridges	Proximity to Intersections	Proximity to Road	Traffic Interruption	Priority Index
1	2021	1.33	US75_GRA_9_1	N Sam Rayburn Fwy & W Washington St Intersection	0.44	1	1	1	1	1
2			US75_GRA_10_1	S Sam Rayburn Fwy	0.23	1	1	1	1	1
3			US75_GRA_10_2	S Sam Rayburn Fwy & W Park Ave Intersection	0.32	1	1	1	1	1
4			US75_GRA_8_1	N Sam Rayburn Fwy & E Buck Owens Fwy Intersection	0.1	1	1	1	1	1
5			US75_GRA_9_2	N Sam Rayburn Fwy & W Houston St Intersection, N Sam Rayburn Fwy & W Lamar St Intersection	0.23	1	1	1	1	1
6	2022	1.42	US75_GRA_16_1	S Collins Fwy & W Haning St Intersection	0.35	1	1	1	0	0.75
7			US75_GRA_2_6	Katy Memorial Expressway N	0.43	1	1	1	0	0.75
8			US75_GRA_2_7	Katy Memorial Expressway N	0.45	1	1	1	0	0.75
9			US75_GRA_21_1	S Henry Hynds Expy & W Van Alstyne Pkwy Intersection	0.19	1	1	1	0	0.75
10	2023	0.88	US75_GRA_18_1	US 75 N & Blythe Rd Intersection	0.26	1	1	1	0	0.75
11			US75_GRA_2_4	Katy Memorial Expressway N	0.19	1	0	1	1	0.75
12			US75_GRA_2_5	Katy Memorial Expressway N	0.16	1	0	1	1	0.75
13			US75_GRA_5_2	S US Highway 75 & Grayson Dr. Intersection	0.27	1	1	1	0	0.75
14	2024	0.93	US75_GRA_11_1	S Sam Rayburn Fwy & S Travis St Intersection	0.15	1	0	1	0	0.5

No	Proposed Schedule	Total Linear Length (in miles)	Designation	Location	Segment Length (in miles)	Proximity to Bridges	Proximity to Intersections	Proximity to Road	Traffic Interruption	Priority Index
15			US75_GRA_12_1	US 75 (Tyson Foods)	0.36	1	0	1	0	0.5
16			US75_GRA_15_1	US 75 & FM 902 Intersection	0.11	1	0	1	0	0.5
17			US75_GRA_2_1	Katy Memorial Expressway N	0.18	1	0	1	0	0.5
18			US75_GRA_2_2	Katy Memorial Expressway N	0.13	1	0	1	0	0.5
19	2025	1.3	US75_GRA_5_1	S US Highway 75 & Spur 504	0.017	1	0	1	0	0.5
20			US75_GRA_1_1	Katy Memorial Expressway N	0.32	0	0	1	0	0.25
21			US75_GRA_2_3	Katy Memorial Expressway N	0.06	0	0	1	0	0.25
22			US75_GRA_6_1	US 75 N & Fallon Dr Intersection	0.07	0	0	1	0	0.25
23			US75_GRA_7_1	N Sam Rayburn Fwy	0.09	0	0	1	0	0.25
24			US75_GRA_8_2	N Sam Rayburn Fwy	0.2	0	0	1	0	0.25
25			US75_GRA_8_3	N Sam Rayburn Fwy	0.44	0	0	1	0	0.25
26			US75_GRA_1_2	Katy Memorial Expressway N	0.12	0	0	0	1	0.25

**Table 9.2** Maintenance schedule of critical slope segments along Loop 286

No	Proposed Schedule	Total Linear Length (in miles)	Designation	Location	Segment Length (in miles)	Proximity to Bridges	Proximity to Intersections	Proximity to Road	Traffic Interruption	Priority Index
1	2021	1.14	Loop286_LA_6_1_A	Texas Loop 286 SE & Clarksville St	0.40	1	1	1	1	1
2			Loop286_LA_6_1_B	Texas Loop 286 SE & Clarksville St	0.26	1	1	1	1	1
3			Loop286_LA_6_1_C	Texas Loop 286 SE & Clarksville St	0.21	1	1	1	1	1
4			Loop286_LA_6_1_D	Texas Loop 286 SE & Clarksville St	0.09	1	1	1	1	1
5			Loop286_LA_6_1_E	Texas Loop 286 SE & Clarksville St	0.06	1	1	1	1	1
6			Loop286_LA_6_1_F	Texas Loop 286 SE & Clarksville St	0.07	1	1	1	1	1
7			Loop286_LA_6_1_G	Texas Loop 286 SE & Clarksville St	0.06	1	1	1	1	1
8	2022	0.60	Loop286_LA_3_1	Texas SW Loop 286 & S Church St	0.20	1	1	1	0	0.75
9			Loop286_LA_2_1	Texas SW Loop 286 & 19 <sup>th</sup> St. SW	0.06	1	0	1	1	0.75
10			Loop286_LA_1_1	Texas Lake Trl SW Loop286	0.34	1	0	0	1	0.5

## **9.5. LIST OF REPAIR METHODS AND THEIR ORDER OF MAGNITUDE COSTS**

This section includes a list of repair methods applicable for the repair and maintenance of critical slope segments of the US 75 corridors and Loop 286 along with their order of magnitude costs.

The slope maintenance and repair methods considered in the development of this master plan include the planting of vegetation, water management system geosynthetic, slope flattening, soil substitution, and retaining wall. The researchers considered the slope angle, soil type, and right of way for determining the range of slope repair methods applicable to the repair of the critical slope segments. The Google Earth street view images were used to inspect the condition of vegetation and water management system in the critical slope segments. In slopes with sparse or no vegetation, the order of magnitude cost was determined for the restoration of vegetation. For slopes with drainage problems, the order of magnitude cost for establishing a water management system was determined. Table 9.3 and Table 9.4 shows the list of repair methods for each of the critical slope segments along the US 75 and Loop 286 corridors with the order of magnitude costs. The capital cost is the order of magnitude cost for the implementation of each repair method. The maintenance cost is only applicable to vegetation and is the order of cost estimate for vegetative watering.

**Table 9.3** Order of magnitude cost estimate for repair and maintenance of critical slope segments in US 75 Corridor

S.NO.	Corridor Name	County	Map Index	Segment	Location	TxDOT Reference Marker Number	Displacement in miles	Distance from Origin in miles	Direction	Segment Length (in miles)	Designation	List of Related Proactive Rehabilitation Maintenance Solutions	Order of Magnitude Costs	
													Capital Cost <sup>1</sup>	Maintenance Cost <sup>2</sup>
1	US75	Grayson	1	1	Katy Memorial Expressway N	194	1.5	1.5	LT	0.3	US75_GRA_1_1	Vegetation	\$69,400	\$24,400
												Gabion Wall	\$503,900	\$0
												Geosynthetics Slope Protection	\$106,400	\$0
												Soil Substitution	\$396,000	\$0
2	US75	Grayson	1	2	Katy Memorial Expressway N	194	1.8	1.8	RT	0.1	US75_GRA_1_2	Vegetation	\$23,500	\$8,300
												Geosynthetics Slope Protection	\$36,100	\$0
												Soil Substitution	\$127,100	\$0
												Slope Flattening	\$286,000	\$0
3	US75	Grayson	1	3	Katy Memorial Expressway N	194	1.9	2.0	RT	0.35	US75_GRA_1_3	Vegetation	\$96,400	\$33,900
												Gabion Wall	\$547,800	\$0
												Geosynthetics Slope Protection	\$147,700	\$0
												Soil Substitution	\$564,400	\$0
												Slope Flattening	\$1,226,900	\$0

S.NO.	Corridor Name	County	Map Index	Segment	Location	TxDOT Reference Marker Number	Displacement in miles	Distance from Origin in miles	Direction	Segment Length (in miles)	Designation	List of Related Proactive Rehabilitation Maintenance Solutions	Order of Magnitude Costs	
													Capital Cost <sup>1</sup>	Maintenance Cost <sup>2</sup>
4	US75	Grayson	2	1	Katy Memorial Expressway N	196	0.2	3.1	RT	0.18	US75_GRA_2_1	Vegetation	\$24,900	\$8,800
												Gabion Wall	\$280,400	\$0
												Geosynthetics Slope Protection	\$38,100	\$0
												Soil Substitution	\$139,100	\$0
												Slope Flattening	\$258,800	\$0
5	US75	Grayson	2	2	Katy Memorial Expressway N	196	0.3	3.2	LT	0.13	US75_GRA_2_2	Vegetation	\$18,000	\$6,300
												Gabion Wall	\$200,400	\$0
												Geosynthetics Slope Protection	\$27,500	\$0
												Soil Substitution	\$101,800	\$0
6	US75	Grayson	2	3	Katy Memorial Expressway N	196	0.4	3.4	LT	0.06	US75_GRA_2_3	Vegetation	\$5,500	\$2,000
												Gabion Wall	\$87,800	\$0
												Geosynthetics Slope Protection	\$8,400	\$0
												Soil Substitution	\$31,100	\$0
												Water Management	\$8,900	\$0

S.NO.	Corridor Name	County	Map Index	Segment	Location	TxDOT Reference Marker Number	Displacement in miles	Distance from Origin in miles	Direction	Segment Length (in miles)	Designation	List of Related Proactive Rehabilitation Maintenance Solutions	Order of Magnitude Costs	
													Capital Cost <sup>1</sup>	Maintenance Cost <sup>2</sup>
7	US75	Grayson	2	4	Katy Memorial Expressway N	196	0.6	3.5	LT	0.19	US75_GRA_2_4	Vegetation	\$45,500	\$16,000
												Gabion Wall	\$292,600	\$0
												Geosynthetics Slope Protection	\$69,700	\$0
												Soil Substitution	\$261,400	\$0
8	US75	Grayson	2	5	Katy Memorial Expressway N	196	0.6	3.5	RT	0.16	US75_GRA_2_5	Vegetation	\$30,100	\$10,600
												Gabion Wall	\$258,200	\$0
												Geosynthetics Slope Protection	\$46,000	\$0
												Soil Substitution	\$166,500	\$0
												Slope Flattening	\$361,400	\$0
9	US75	Grayson	2	6	Katy Memorial Expressway N	196	1.3	4.2	LT	0.43	US75_GRA_2_6	Vegetation	\$79,000	\$27,800
												Gabion Wall	\$679,400	\$0
												Geosynthetics Slope Protection	\$121,100	\$0
												Soil Substitution	\$436,000	\$0
												Slope Flattening	\$980,200	\$0
10	US75	Grayson	2	7	Katy Memorial Expressway N	196	1.3	4.2	RT	0.45	US75_GRA_2_7	Vegetation	\$88,800	\$31,200



S.NO.	Corridor Name	County	Map Index	Segment	Location	TxDOT Reference Marker Number	Displacement in miles	Distance from Origin in miles	Direction	Segment Length (in miles)	Designation	List of Related Proactive Rehabilitation Maintenance Solutions	Order of Magnitude Costs	
													Capital Cost <sup>1</sup>	Maintenance Cost <sup>2</sup>
												Gabion Wall	\$708,700	\$0
												Geosynthetics Slope Protection	\$136,000	\$0
												Soil Substitution	\$487,000	\$0
												Slope Flattening	\$992,000	\$0
												Water Management	\$71,800	\$0
11	US75	Grayson	5	1	S US Highway 75 & Spur 503	200	0.3	7.2	LT/RT	0.02	US75_GRA_5_1	Vegetation	\$10,700	\$3,800
												Gabion Wall	\$79,500	\$0
												Geosynthetics Slope Protection	\$16,400	\$0
												Soil Substitution	\$59,400	\$0
12	US75	Grayson	5	2	S US Highway 75 & Grayson Dr. Intersection	200	1.2	8.1	LT/RT	0.27	US75_GRA_5_2	Vegetation	\$147,100	\$51,600
												Gabion Wall	\$838,900	\$0
												Geosynthetics Slope Protection	\$225,300	\$0
												Soil Substitution	\$825,700	\$0
												Slope Flattening	\$1,653,700	\$0

S.NO.	Corridor Name	County	Map Index	Segment	Location	TxDOT Reference Marker Number	Displacement in miles	Distance from Origin in miles	Direction	Segment Length (in miles)	Designation	List of Related Proactive Rehabilitation Maintenance Solutions	Order of Magnitude Costs	
													Capital Cost <sup>1</sup>	Maintenance Cost <sup>2</sup>
13	US75	Grayson	6	1	US 75 N & Fallon Dr Intersection	202	0.7	9.6	LT/RT	0.07	US75_GRA_6_1	Vegetation	\$28,600	\$10,100
												Gabion Wall	\$212,900	\$0
												Geosynthetics Slope Protection	\$43,800	\$0
												Soil Substitution	\$162,800	\$0
												Water Management	\$21,600	\$0
14	US75	Grayson	7	1	N Sam Rayburn Fwy	202	1.7	10.6	LT	0.09	US75_GRA_7_1	Vegetation	\$8,700	\$3,100
												Gabion Wall	\$140,800	\$0
												Geosynthetics Slope Protection	\$13,900	\$0
												Soil Substitution	\$50,600	\$0
												Slope Flattening	\$102,000	\$0
15	US75	Grayson	8	1	N Sam Rayburn Fwy & E Buck Owens Fwy Intersection	204	0.19	11.1	LT/RT	0.10	US75_GRA_8_1	Vegetation	\$45,300	\$15,900
												Gabion Wall	\$316,100	\$0
												Geosynthetics Slope Protection	\$69,300	\$0
												Soil Substitution	\$256,700	\$0

S.NO.	Corridor Name	County	Map Index	Segment	Location	TxDOT Reference Marker Number	Displacement in miles	Distance from Origin in miles	Direction	Segment Length (in miles)	Designation	List of Related Proactive Rehabilitation Maintenance Solutions	Order of Magnitude Costs	
													Capital Cost <sup>1</sup>	Maintenance Cost <sup>2</sup>
												Water Management	\$32,000	\$0.00
16	US75	Grayson	8	2	N Sam Rayburn Fwy	204	0.4	11.3	RT	0.20	US75_GRA_8_2	Vegetation	\$22,200	\$7,800
												Gabion Wall	\$309,500	\$0
												Geosynthetics Slope Protection	\$34,000	\$0
												Soil Substitution	\$125,100	\$0
												Water Management	\$31,400	\$0
17	US75	Grayson	8	3	N Sam Rayburn Fwy	204	0.4	11.3	LT	0.44	US75_GRA_8_3	Vegetation	\$83,700	\$29,400
												Gabion Wall	\$688,000	\$0
												Geosynthetics Slope Protection	\$128,200	\$0
												Soil Substitution	\$467,700	\$0
												Slope Flattening	\$956,800	\$0
												Water Management	\$69,700	\$0
18	US75	Grayson	9	1	N Sam Rayburn Fwy & W	206	0.06	13.0	LT/RT	0.44	US75_GRA_9_1	Vegetation	\$129,000	\$45,300
												Gabion Wall	\$1,386,200	\$0.00

S.NO.	Corridor Name	County	Map Index	Segment	Location	TxDOT Reference Marker Number	Displacement in miles	Distance from Origin in miles	Direction	Segment Length (in miles)	Designation	List of Related Proactive Rehabilitation Maintenance Solutions	Order of Magnitude Costs	
													Capital Cost <sup>1</sup>	Maintenance Cost <sup>2</sup>
					Washington St Intersection							Geosynthetics Slope Protection	\$197,600	\$0
												Soil Substitution	\$696,000	\$0
												Slope Flattening	\$805,700	\$0
19	US75	Grayson	9	2	N Sam Rayburn Fwy & W Houston St Intersection, N Sam Rayburn Fwy & W Lamar St Intersection	206	0.6	13.4	LT/RT	0.23	US75_GRA_9_2	Vegetation	\$82,700	\$29,100
												Gabion Wall	\$733,700	\$0
												Geosynthetics Slope Protection	126,700	\$0
												Soil Substitution	\$459,200	\$0
												Slope Flattening	\$981,800	\$0
20	US75	Grayson	10	1	S Sam Rayburn Fwy	206	1.0	13.9	LT/RT	0.23	US75_GRA_10_1	Vegetation	\$71,800	\$25,200
												Gabion Wall	\$729,300	\$0
												Geosynthetics Slope Protection	\$110,000	\$0
												Soil Substitution	\$399,500	\$0
												Slope Flattening	\$830,600	\$0
21	US75	Grayson	10	2	S Sam Rayburn Fwy & W Park Ave Intersection	206	1.9	14.9	LT/RT	0.32	US75_GRA_10_2	Vegetation	\$96,000	\$33,700
												Gabion Wall	\$1,012,600	\$0.00

S.NO.	Corridor Name	County	Map Index	Segment	Location	TxDOT Reference Marker Number	Displacement in miles	Distance from Origin in miles	Direction	Segment Length (in miles)	Designation	List of Related Proactive Rehabilitation Maintenance Solutions	Order of Magnitude Costs	
													Capital Cost <sup>1</sup>	Maintenance Cost <sup>2</sup>
												Geosynthetics Slope Protection	\$147,100	\$0
												Soil Substitution	\$529,700	\$0
												Slope Flattening	\$1,167,100	\$0
												Water Management	\$102,500	\$0
22	US75	Grayson	11	1	S Sam Rayburn Fwy & S Travis St Intersection	208	1.0	15.9	LT	0.15	US75_GRA_11_1	Vegetation	\$23,600	\$8,300
												Gabion Wall	\$238,900	\$0
												Geosynthetics Slope Protection	\$36,100	\$0
												Soil Substitution	\$132,100	\$0
												Slope Flattening	\$256,800	\$0
23	US75	Grayson	12	1	US 75 (Tyson Foods)	210	0.8	17.7	LT/RT	0.36	US75_GRA_12_1	Vegetation	\$132,100	\$46,400
												Gabion Wall	\$1,136,200	\$0
												Geosynthetics Slope Protection	\$202,400	\$0
												Soil Substitution	\$729,200	\$0
												Slope Flattening	\$1,639,400	\$0
												Water Management	\$57,500	\$0

S.NO.	Corridor Name	County	Map Index	Segment	Location	TxDOT Reference Marker Number	Displacement in miles	Distance from Origin in miles	Direction	Segment Length (in miles)	Designation	List of Related Proactive Rehabilitation Maintenance Solutions	Order of Magnitude Costs	
													Capital Cost <sup>1</sup>	Maintenance Cost <sup>2</sup>
24	US75	Grayson	15	1	US 75 & FM 902 Intersection	214	0.1	21.0	LT/RT	0.11	US75_GRA_15_1	Vegetation	\$25,900	\$9,100
												Gabion Wall	\$344,500	\$0
												Geosynthetics Slope Protection	\$39,700	\$0
												Soil Substitution	\$143,100	\$0
												Slope Flattening	\$1,795,200	\$0
												Water Management	\$34,900	\$0
25	US75	Grayson	16	1	S Collins Fwy & W Haning St Intersection	214	1.5	22.4	LT/RT	0.35	US75_GRA_16_1	Vegetation	\$147,900	\$51,900
												Gabion Wall	\$1,102,000	\$0
												Geosynthetics Slope Protection	\$226,500	\$0
												Soil Substitution	\$820,600	\$0
												Slope Flattening	\$1,795,200	\$0
												Water Management	\$111,600	\$0
26	US75	Grayson	18	1	US 75 N & Blythe Rd Intersection	218	0.5	25.3	LT/RT	0.27	US75_GRA_18_1	Vegetation	\$105,800	\$37,200
												Gabion Wall	\$844,800	\$0
												Geosynthetics Slope Protection	\$162,100	\$0

S.NO.	Corridor Name	County	Map Index	Segment	Location	TxDOT Reference Marker Number	Displacement in miles	Distance from Origin in miles	Direction	Segment Length (in miles)	Designation	List of Related Proactive Rehabilitation Maintenance Solutions	Order of Magnitude Costs	
													Capital Cost <sup>1</sup>	Maintenance Cost <sup>2</sup>
27	US75	Grayson	21	1	S Henry Hynds Expy & W Van Alstyne Pkwy Intersection	220	1.9	28.7	LT/RT	0.19	US75_GRA_21_1	Soil Substitution	\$303,800	\$0.00
												Water Management	\$85,500	\$0.00
												Vegetation	\$78,100	\$27,400
												Gabion Wall	\$597,600	\$0
												Geosynthetics Slope Protection	\$119,600	\$0
												Soil Substitution	\$446,400	\$0
Water Management	\$60,500	\$0												

**Note:**

<sup>1</sup>Capital cost of:

- slope repair with *vegetation* includes the cost of two components: vegetation (block sodding) and vegetative watering
- slope repair with *gabions* include the cost of three components: excavation, 2 gabions of 3' x 3' cross-section and 1 gabion of 3' x 3' cross-section, and crushed drainage stone
- slope repair with *geosynthetics* slope protection include the cost of four components: geosynthetics material, backfill, vegetation (block sodding), and vegetative watering
- slope repair with *slope flattening* include the cost of five components: excavation, backfill, compaction, vegetation (block sodding), and vegetative watering
- slope repair with *soil substitution* include the cost of five components: excavation, backfill soil, compaction, vegetation (block sodding), and vegetative watering
- *water management* include the cost of installing TxDOT Type II curb and Gutter

<sup>2</sup>Maintenance cost of:

- *vegetation* includes the cost of vegetative watering

**Table 9.4** Order of magnitude cost estimate for repair and maintenance of critical slope segments in Loop 286

S.NO	Corridor Name	County	Map Index	Segment	Location	TxDOT Reference Marker Number	Displacement in miles	Distance from Origin in miles	Direction	Segment Length (in miles)	Designation	List of Related Proactive Rehabilitation Maintenance Solutions	Order of Magnitude Costs	
													Capital Cost <sup>1</sup>	Maintenance Cost <sup>2</sup>
1	Loop 286	Lamar	1	1	Texas Lake Trl SW Loop286	652	0.871	1.177	RT/LT	0.34	Loop286_LA_1_1	Vegetation	\$268,400	\$94,200
												Gabion Wall	\$1,064,100	\$0.00
												Geosynthetics Slope Protection	\$411,200	\$0
												Soil Substitution	\$1,537,100	\$0
2	Loop 286	Lamar	2	1	Texas SW Loop 286 & 19th St. SW	652	1.357	1.663	RT/LT	0.0598	Loop286_LA_2_1	Vegetation	\$36,900	\$13,000
												Gabion Wall	\$187,400	\$0
												Geosynthetics Slope Protection	\$56,500	\$13,000
												Soil Substitution	\$207,100	\$0
3	Loop 286	Lamar	3	1	Texas SW Loop 286 & S Church St	654	0.977	3.27	RT/LT	0.201	Loop286_LA_3_1	Vegetation	\$49,500	\$17,400
												Gabion Wall	\$629,000	\$0
												Geosynthetics Slope Protection	\$75,900	\$0
												Soil Substitution	\$214,400	\$0
4	Loop 286	Lamar	6	1	Texas Loop 286 SE & Clarksville St	660	0	7.448	LT	0.403	Loop286_LA_6_1_A	Vegetation	\$91,000	\$32,000
												Gabion Wall	\$630,800	\$0
												Geosynthetics Slope Protection	\$139,400	\$0



S.NO	Corridor Name	County	Map Index	Segment	Location	TxDOT Reference Marker Number	Displacement in miles	Distance from Origin in miles	Direction	Segment Length (in miles)	Designation	List of Related Proactive Rehabilitation Maintenance Solutions	Order of Magnitude Costs	
													Capital Cost <sup>1</sup>	Maintenance Cost <sup>2</sup>
												Soil Substitution	\$523,900	\$0
5	Loop 286	Lamar	6	1	Texas Loop 286 SE & Clarksville St	660	0	7.448	RT	0.259	Loop286_LA_6_1_B	Vegetation	\$99,200	\$34,800
												Gabion Wall	\$405,500	\$0
												Geosynthetics Slope Protection	\$152,000	\$0
												Soil Substitution	\$569,000	\$0
6	Loop 286	Lamar	6	1	Texas Loop 286 SE & Clarksville St	660	0	7.448	RT	0.21	Loop286_LA_6_1_C	Vegetation	\$32,200	\$11,300
												Gabion Wall	\$328,700	\$0
												Geosynthetics Slope Protection	\$49,400	\$0
												Soil Substitution	\$184,600	\$0
7	Loop 286	Lamar	6	1	Texas Loop 286 SE & Clarksville St	660	0	7.448	LT	0.0908	Loop286_LA_6_1_D	Vegetation	\$19,300	\$6,800
												Gabion Wall	\$142,000	\$0
												Geosynthetics Slope Protection	\$29,600	\$0
												Soil Substitution	\$108,300	\$0
8	Loop 286	Lamar	6	1	Texas Loop 286 SE & Clarksville St	660	0	7.448	LT	0.058	Loop286_LA_6_1_E	Vegetation	\$9,800	\$3,500
												Gabion Wall	\$90,700	\$0
												Geosynthetics Slope Protection	\$14,900	\$0

S.NO	Corridor Name	County	Map Index	Segment	Location	TxDOT Reference Marker Number	Displacement in miles	Distance from Origin in miles	Direction	Segment Length (in miles)	Designation	List of Related Proactive Rehabilitation Maintenance Solutions	Order of Magnitude Costs	
													Capital Cost <sup>1</sup>	Maintenance Cost <sup>2</sup>
												Soil Substitution	\$51,200	\$0
9	Loop 286	Lamar	6	1	Texas Loop 286 SE & Clarksville St	660	0	7.448	LT	0.066	Loop286_LA_6_1_F	Vegetation	\$16,200	\$5,700
												Gabion Wall	\$103,200	\$0
												Geosynthetics Slope Protection	\$24,800	\$0
												Soil Substitution	\$85,500	\$0
10	Loop 286	Lamar	6	1	Texas Loop 286 SE & Clarksville St	660	0	7.448	RT	0.057	Loop286_LA_6_1_G	Vegetation	\$800	\$600
												Geosynthetics Slope Protection	\$6,200	\$0

**Note:**

<sup>1</sup>Capital cost of:

- slope repair with *vegetation* includes cost of two components: vegetation (block sodding) and vegetative watering
- slope repair with *gabions* include the cost of three components: excavation, 2 gabions of 3' x 3' cross-section and 1 gabion of 3' x 3' cross-section, and crushed drainage stone
- slope repair with *geosynthetics* slope protection include the cost of four components: geosynthetics material, backfill, vegetation (block sodding), and vegetative watering
- slope repair with *slope flattening* include the cost of five components: excavation, backfill, compaction, vegetation (block sodding), and vegetative watering
- slope repair with *soil substitution* include the cost of five components: excavation, backfill soil, compaction, vegetation (block sodding), and vegetative watering
- *water management* include the cost of installing TxDOT Type II curb and Gutter

<sup>2</sup>Maintenance cost of:

- *vegetation* includes the cost of vegetative watering

## CHAPTER 10 SUMMARY AND CONCLUSION

In this project, a Slope Repair and Maintenance Management System (SRMMS) was developed to identify critical slopes along highway corridors for facilitating proactive slope maintenance decisions in the TxDOT Paris district. Spatial data entities, such as soil properties, slope angles, precipitation, vegetation, and general features (e.g., Paris district past slope failures, Paris district boundary, Paris district connectivity corridors), were collected and stored in a geodatabase.

A physically-based geotechnical model was used to determine the minimum duration of rainfall required to initiate the slope instability. Spatial data entities stored in the geodatabase were used as inputs to the physically-based geotechnical model. Based on the minimum duration of rainfall required to trigger the slope instabilities, color-coded slope failure susceptibility maps were prepared: Highly critical (< 3 days), Critical (3-10 days), Moderately critical (10-45 days), and Non-critical (>45 days). The slope failure susceptibility maps were calibrated to consider the effect of landcover on slope stability and validated using the past slope failures.

A map-based interface was developed to facilitate the visualization of the collected spatial data and the slope failure susceptibility maps. The map-based interface was created using the ArcGIS online platform. The spatial data entities are published in the University of Texas at Arlington (UTA) ArcGIS online account. The published data entities are displayed in the map-based interface. The map-based interface is hosted in the UTA cloud. A multi-criteria decision support system was developed to provide a ranked list of potential slope repair methods to facilitate the selection of repair methods. The multi-criteria decision support system was integrated with the map-based interface of the slope repair and maintenance management system. This system does not force the engineers to select a repair method but supports the selection by providing a ranked list of repair methods. Finally, a repair and maintenance master plan was prepared for the critical slope segments along US 75 and Loop 286 corridors in the TxDOT Paris district. The order of magnitude cost estimate and maintenance schedule were prepared for the proactive maintenance of the critical slope segments.

It is expected that the Slope Repair and Maintenance Management System (SRMMS) will be useful for local engineers and managers for planning and carrying out proactive slope maintenance works. The implementation of the system is currently limited to the TxDOT Paris district. The

system, if extended to other TxDOT districts, shall help the state and local officials to effectively identify the critical slope segments and plan mitigation works to avoid costly damages.

---

**REFERENCES**

- Abdullah, M. N., Osman, N., & Ali, F. H. (2011). Soil-root shear strength properties of some slope plants. *Sains Malaysiana*, 40(10), 1065-1073.
- Abrams, T. G., & Wright, S. G. (1972). *A survey of earth slope failures and remedial measures in Texas* (No. 161-1).
- Ali, N., Farshchi, I., Mu'azu, M. A., & Rees, S. W. (2012). Soil-root interaction and effects on slope stability analysis. *Electronic Journal of Geotechnical Engineering*, 17, 319-328.
- Arellano, D., Stark, T. D., Horvath, J. S., & Leshchinsky, D. (2011). Guidelines for geofoam applications in slope stability projects. *Preliminary Draft Final Rep., NCHRP Project No. 24-11 (02)*.
- Azadeh, A., Kor, H., & Hatefi, S. M. (2011). A hybrid genetic algorithm-TOPSIS-computer simulation approach for optimum operator assignment in cellular manufacturing systems. *Journal of the Chinese Institute of Engineers*, 34(1), 57-74.
- B.P. Bhatt, K.D. Awasthi, B.P. Heyojoo, T. Silwal, G. Kafle, Using Geographic Information System and Analytical Hierarchy Process in Landslide Hazard Zonation, *Applied Ecology and Environmental Sciences*, 1(2), 2013, pp. 14 – 22.
- Baeza, C., & Corominas, J. (2001). Assessment of shallow landslide susceptibility by means of multivariate statistical techniques. *Earth Surface Processes and Landforms: The Journal of the British Geomorphological Research Group*, 26(12), 1251-1263.
- Baum, R. L., Savage, W. Z., & Godt, J. W. (2002). TRIGRS—a Fortran program for transient rainfall infiltration and grid-based regional slope-stability analysis. *US geological survey open-file report*, 424, 38.
- Berti, M., & Simoni, A. (2010). Field evidence of pore pressure diffusion in clayey soils prone to landsliding. *Journal of Geophysical Research: Earth Surface*, 115(F3).
- BEVEN, K. J., & Kirkby, M. J. (1979). A physically based, variable contributing area model of basin hydrology/Un modèle à base physique de zone d'appel variable de l'hydrologie du bassin versant. *Hydrological Sciences Journal*, 24(1), 43-69.

- Bhattacharai, P., Tiwari, B., Marui, H., & Aoyama, K. (2004). Quantitative slope stability mapping with ArcGIS: prioritize highway maintenance. In *Proceedings of ESRI's 24th Annual International User's Conference, San Diego. ESRI.*
- Biddle, G. (2001). Tree root damage to buildings. In *Expansive Clay Soils and Vegetative Influence on Shallow Foundations* (pp. 1-23).
- Caine, N. (1980). The rainfall intensity-duration control of shallow landslides and debris flows. *Geografiska annaler: series A, physical geography*, 62(1-2), 23-27.
- Carrara, A. (1983). Multivariate models for landslide hazard evaluation. *Journal of the International Association for Mathematical Geology*, 15(3), 403-426.
- Carrara, A., Guzzetti, F., Cardinali, M., & Reichenbach, P. (1999). Use of GIS technology in the prediction and monitoring of landslide hazard. *Natural hazards*, 20(2-3), 117-135.
- Castellanos, B. A., Brandon, T. L., & VandenBerge, D. R. (2016). Use of fully softened shear strength in slope stability analysis. *Landslides*, 13(4), 697-709.
- Chau, K. T., Sze, Y. L., Fung, M. K., Wong, W. Y., Fong, E. L., & Chan, L. C. P. (2004). Landslide hazard analysis for Hong Kong using landslide inventory and GIS. *Computers & Geosciences*, 30(4), 429-443.
- Chauhan, A., & Vaish, R. (2012). Magnetic material selection using multiple attribute decision making approach. *Materials & Design (1980-2015)*, 36, 1-5.
- Chok, Y., Kaggwa, G., Jaksa, M., & Griffiths, D. (2004). Modeling the effects of vegetation on stability of slopes.
- Clerici, A., Perego, S., Tellini, C., & Vescovi, P. (2002). A procedure for landslide susceptibility zonation by the conditional analysis method. *Geomorphology*, 48(4), 349-364.
- Collin, J. G., Loehr, J. E., & Hung, C. J. (2008). Slope Maintenance and Slide Restoration Reference Manual for NHI Course 132081, prepared for FHWA. Report FHWA NHI-08-098.
- Coppin, N. J., & Richards, I. G. (Eds.). (1990). *Use of vegetation in civil engineering* (pp. 23-36). Butterworths: Ciria.

- Crosta, G. B., & Frattini, P. (2001, October). Rainfall thresholds for triggering soil slips and debris flow. In *Proceedings of the 2nd EGS Plinius Conference on Mediterranean Storms, edited by: Mugnai, A., Guzzetti, F., and Roth, G., Siena, Italy* (pp. 463-487).
- Das, B. M. (2010). *Geotechnical engineering handbook*. J. Ross Publishing.
- D'Odorico, P., Fagherazzi, S., & Rigon, R. (2005). Potential for landsliding: dependence on hyetograph characteristics. *Journal of Geophysical Research: Earth Surface*, 110(F1).
- Duncan, J. M., Wright, S. G., and Brandon, T. L. (2014). *Soil strength and slope stability*. John Wiley & Sons.
- Esmaeili, M., Nik, M. G., & Khayyer, F. (2013). Experimental and numerical study of micropiles to reinforce high railway embankments. *International Journal of Geomechanics*, 13(6), 729-744.
- Fall, M., Azzam, R., & Noubactep, C. (2006). A multi-method approach to study the stability of natural slopes and landslide susceptibility mapping. *Engineering geology*, 82(4), 241-263.
- Federal Geographic Data Committee (June 1998). *Content Standard for Digital Geospatial Metadata, Version 2.0, FGDC-STD-001-1998*
- Gamez, J. A., & Stark, T. D. (2014). a softened shear strength at low stresses for levee and embankment design. *Journal of Geotechnical and Geoenvironmental Engineering*, 140(9), 06014010.
- Greenwood, J. R., Morgan, R. P. C., Coppin, N. J., Vickers, A. W., & Norris, J. E. (2001). *Bioengineering: a field trial at Longham Wood Cutting*.
- Greenwood, J. R., Norris, J. E., & Wint, J. (2004). Assessing the contribution of vegetation to slope stability. *Proceedings of the ICE-Geotechnical Engineering*, 157(4), 199-207.
- Guzzetti, F., Carrara, A., Cardinali, M., & Reichenbach, P. (1999). Landslide hazard evaluation: a review of current techniques and their application in a multi-scale study, Central Italy. *Geomorphology*, 31(1-4), 181-216.
- Guzzetti, F., Mondini, A. C., Cardinali, M., Fiorucci, F., Santangelo, M., & Chang, K. T. (2012). Landslide inventory maps: New tools for an old problem. *Earth-Science Reviews*, 112(1-2), 42-66.

- Guzzetti, F., Peruccacci, S., Rossi, M., & Stark, C. P. (2008). The rainfall intensity–duration control of shallow landslides and debris flows: an update. *Landslides*, 5(1), 3-17.
- He, Y., & Beighley, R. E. (2008). GIS-based regional landslide susceptibility mapping: a case study in southern California. *Earth Surface Processes and Landforms*, 33(3), 380-393.
- Hidalgo, C. A., Vega, J. A., & Obando, M. P. (2018). Effect of the Rainfall Infiltration Processes on the Landslide Hazard Assessment of Unsaturated Soils in Tropical Mountainous Regions. *Engineering and Mathematical Topics in Rainfall*, 163.
- Hossain, J. (2013). Geohazard potential of rainfall induced slope failure on expansive clay.
- Hossain, S., Khan, S., & Kibria, G. (2017). *Sustainable Slope Stabilisation using Recycled Plastic Pins*. CRC Press.
- Huabin, W., Gangjun, L., Weiya, X., & Gonghui, W. (2005). GIS-based landslide hazard assessment: an overview. *Progress in Physical Geography*, 29(4), 548-567.
- Huang, J. (2008). Combining entropy weight and TOPSIS method for information system selection. In *2008 IEEE Conference on Cybernetics and Intelligent Systems* (pp. 1281-1284). IEEE.
- Huang, W., Shuai, B., Sun, Y., Wang, Y., & Antwi, E. (2018). Using entropy-TOPSIS method to evaluate urban rail transit system operation performance: The China case. *Transportation Research Part A: Policy and Practice*, 111, 292-303.
- Innes, J. L. (1983). Debris flows. *Progress in Physical Geography*, 7(4), 469-501.
- Iverson, R. M. (2000). Landslide triggering by rain infiltration. *Water resources research*, 36(7), 1897-1910.
- Jafari, N., & Puppala, A. (2018). Prediction and Rehabilitation of Highway Embankment Slope Failures in Changing Climate.
- Jee, D. H., & Kang, K. J. (2000). A method for optimal material selection aided with decision making theory. *Materials & Design*, 21(3), 199-206



- Kayyal, M. K., & Wright, S. G. (1991). *INVESTIGATION OF LONG-TERM STRENGTH PROPERTIES OF PARIS AND BEAUMONT CLAYS IN EARTH EMBANKMENTS. FINAL REPORT* (No. FHWA/TX-92+ 1195-2F).
- Khan, M. S., Hossain, S., & Kibria, G. (2017). Stabilisation using recycled plastic pins. *J. Perform. Constructed Facil*, 229-234.
- Khan, M. S., Hossain, S., Ahmed, A., & Faysal, M. (2017). Investigation of a shallow slope failure on expansive clay in Texas. *Engineering geology*, 219, 118-129.
- Lee, E. M. (2001). Geomorphological mapping. Geological Society, London, Engineering Geology Special Publications, 18(1), 53-56.
- Loehr, J. E., Bernhardt, K. S., Huaco, D. R., & Midwest Transportation Consortium. (2004). *Decision support for slope construction and repair activities: an asset management building block* (No. MTC Project 2000-03). Missouri. Department of Transportation.
- Lohnes, R. A., Kjartanson, B. H., & Barnes, A. (2001). *Regional approach to landslide interpretation and repair* (No. TR-430,).
- Mohseni, O., Anderson, C., Strong, M., Conway, R., Hathaway, C., Grosser, A., & Mielke, A. (2018). *Storm-Induced Slope Failure Susceptibility Mapping* (No. MN/RC 2018-05). Minnesota. Dept. of Transportation.
- Montgomery, D. R., & Dietrich, W. E. (1994). A physically based model for the topographic control on shallow landsliding. *Water resources research*, 30(4), 1153-1171.
- Morrissey, M. M., Wieczorek, G. F., & Morgan, B. A. (2001). *A comparative analysis of hazard models for predicting debris flows in Madison County, Virginia*. US Department of the Interior, US Geological Survey.
- Multi-Resolution Land Characteristics Consortium (2016). National Land Cover Database 2016 (NLCD2016) Legend, The U.S. Geological Survey (USGS), retrieved on June 20, 2019, available at <https://www.mrlc.gov/>
- Nandi, A., & Shakoor, A. (2010). A GIS-based landslide susceptibility evaluation using bivariate and multivariate statistical analyses. *Engineering Geology*, 110(1-2), 11-20.

- Neely, M. K., & RICE, R. M. (1990). Estimating risk of debris slides after timber harvest in northwestern California. *Bulletin of the Association of Engineering Geologists*, 27(3), 281-289.
- Nelson, M., Saftner, D., & Carranza-Torres, C. (2017, January). Slope Stabilization for Local Government Engineers in Minnesota. In *Congress on Technical Advancement 2017* (pp. 127-138).
- Nelson, S. A. (2013). Slope Stability, Triggering Events, Mass Movement Hazards. *Nat. Disasters*.
- NOAA/NWS/Office of Water Prediction (formerly Office of Hydrologic Development), Hydrometeorological Design Studies Center (September 26, 2018). Precipitation Frequency for Texas, USA – NOAA Atlas 14 Volume 11, retrieved on June 22, 2019, available at <https://hdsc.nws.noaa.gov/hdsc/pfds/>
- O'loughlin, E. M. (1986). Prediction of surface saturation zones in natural catchments by topographic analysis. *Water Resources Research*, 22(5), 794-804.
- Onyelowe Ken, C., & Okafor, F. O. (2006). A comparative review of soil modification methods.
- Overton, D. E., & Meadows, M. E. (2013). *Stormwater modeling*. Elsevier.
- Özer, A. T., Akay, O., Fox, G. A., Bartlett, S. F., & Arellano, D. (2014). A new method for remediation of sandy slopes susceptible to seepage flow using EPS-block geof foam. *Geotextiles and Geomembranes*, 42(2), 166-180.
- Pack, R. T., Tarboton, D. G., & Goodwin, C. N. (1998, September). The SINMAP approach to terrain stability mapping. In *8th congress of the international association of engineering geology, Vancouver, British Columbia, Canada* (Vol. 21, p. 25).
- Perry, J., Pedley, M., Brady, K., & Reid, M. (2003). Briefing: Embankment cuttings: condition appraisal and remedial treatment.
- Ramanathan, R. S. (2012). *Soil Slope Failure Investigation Management Systems* (Doctoral dissertation).
- Ray, R. L., & De Smedt, F. (2009). Slope stability analysis on a regional scale using GIS: a case study from Dhading, Nepal. *Environmental geology*, 57(7), 1603-1611.

- Ressel, D. (1979). Soil survey of Lamar and Delta counties, Texas.
- Roszkowska, E. (2011). Multi-criteria decision making models by applying the TOPSIS method to crisp and interval data. *Multiple Criteria Decision Making/University of Economics in Katowice*, 6, 200-230.
- Saaty, T. L. (1990). How to make a decision: the analytic hierarchy process. *European journal of operational research*, 48(1), 9-26.
- Saboya Jr, F., da Glória Alves, M., & Pinto, W. D. (2006). Assessment of failure susceptibility of soil slopes using fuzzy logic. *Engineering Geology*, 86(4), 211-224.
- Santacana, N., Baeza, B., Corominas, J., De Paz, A., & Marturiá, J. (2003). A GIS-based multivariate statistical analysis for shallow landslide susceptibility mapping in La Pobla de Lillet area (Eastern Pyrenees, Spain). *Natural hazards*, 30(3), 281-295.
- Seeley, M. W., & West, D. O. (1990). Approach to geologic hazard zoning for regional planning, Inyo National Forest, California and Nevada. *Bulletin of the Association of Engineering Geologists*, 27(1), 23-35.
- Shahabi, H., Ahmad, B. B., & Khezri, S. (2013). Evaluation and comparison of bivariate and multivariate statistical methods for landslide susceptibility mapping (case study: Zab basin). *Arabian journal of geosciences*, 6(10), 3885-3907.
- Shahandashti, M., Hossain, S., Khankarli, GH., Zahedzahedani, S.E., Abediniangerabi, B., and Nabaei, M. (2019). *Synthesis on Rapid Repair Methods for Embankment Slope Failure*. Report Number (FHWA/TX-18/0-6957-1). The University of Texas at Arlington, Arlington, Texas.
- Shanian, A., & Savadogo, O. (2006). TOPSIS multiple-criteria decision support analysis for material selection of metallic bipolar plates for polymer electrolyte fuel cell. *Journal of Power Sources*, 159(2), 1095-1104. doi:10.1016/j.jpowsour.2005.12.092
- Singh, H., Huat, B. B., & Jamaludin, S. (2008). Slope assessment systems: A review and evaluation of current techniques used for cut slopes in the mountainous terrain of West Malaysia. *Electronic Journal of Geotechnical Engineering*, 13, 1-24.

- Singh, H., Huat, B. B., & Jamaludin, S. (2008). Slope assessment systems: A review and evaluation of current techniques used for cut slopes in the mountainous terrain of West Malaysia. *Electronic Journal of Geotechnical Engineering*, 13, 1-24.
- Skempton, A. W. (1970). First-time slides in overconsolidated clays. *Geotechnique*, 20(3), 320-324.
- Skempton, A. W. (1977). "Slope Stability of cuttings in brown London clay." Proc., 9th Int. Conf. of Soil Mechanics and Foundations, Vol. 3, Springer, New York, 261–270.
- Skempton, A. W., & DeLory, F. A. (1984). Stability of natural slopes in London clay. In Selected Papers on Soil Mechanics (pp. 70-73). Thomas Telford Publishing.
- Smith, M. J., Paron, P., & Griffiths, J. S. (2011). *Geomorphological mapping: methods and applications* (Vol. 15). Elsevier.
- Stark, T. D., & Eid, H. T. (1997). Slope stability analyses in stiff fissured clays. *Journal of Geotechnical and Geoenvironmental Engineering*, 123(4), 335-343.
- Stark, T. D., & Hussain, M. (2012). Empirical correlations: drained shear strength for slope stability analyses. *Journal of Geotechnical and Geoenvironmental Engineering*, 139(6), 853-862.
- Stark, T. D., Choi, H., & McCone, S. (2005). Drained shear strength parameters for analysis of landslides. *Journal of Geotechnical and Geoenvironmental Engineering*, 131(5), 575-588.
- Stark, T. D., Choi, H., & McCone, S. (2005). Drained shear strength parameters for analysis of landslides. *Journal of Geotechnical and Geoenvironmental Engineering*, 131(5), 575-588.
- Texas Department of Transportation (April 01, 2016). TxDOT Survey Manual
- Texas Department of Transportation (July 2010). TxDOT Data Architecture (Version 4.2)
- Texas Department of Transportation (July 31, 2018). TxDOT\_Statewide\_Connectivity\_Corridors, retrieved on June 20, 2019, available at <http://gis-txdot.opendata.arcgis.com>
- Titi, H. H., & Helwany, S. (2007). Investigation of vertical members to resist surficial slope instabilities (No. WHRP 07-03). Wisconsin. Dept. of Transportation. Bureau of Technical Services.

- Tuttle, R. W., Ralston, D. C., Sotir, R. B., Gray, D. H., Adams, C. A., Saele, L. M., & Reckendorf, F. F. (1992). Soil bioengineering for Upland slope protection and erosion reduction: Chapter 18. Department of Agriculture, Washington (EUA).
- USDA/NRCS - National Geospatial Center of Excellence (2011). 1981-2010 Annual Average Precipitation by State, retrieved on June 22, 2019, available at <https://datagateway.nrcs.usda.gov>
- Van Westen, C. J., Rengers, N., Terlien, M. T. J., & Soeters, R. (1997). Prediction of the occurrence of slope instability phenomenon through GIS-based hazard zonation. *Geologische Rundschau*, 86(2), 404-414.
- White, D. J., Yang, H., Thompson, M. J., & Schaefer, V. R. (2005). Innovative solutions for slope stability reinforcement and characterization: Vol. I.
- Whitworth, M., Anderson, I., & Hunter, G. (2011). Geomorphological assessment of complex landslide systems using field reconnaissance and terrestrial laser scanning. In *Developments in Earth Surface Processes* (Vol. 15, pp. 459-474). Elsevier.
- Wright, S. G., Zornberg, J. G., & Aguetant, J. E. (2007). *The fully softened shear strength of high plasticity clays* (No. FHWA/TX-07/0-5202-3).
- Wu, J. Y., Huang, K., & Sungkar, M. (2017). Remediation of slope failure by compacted soil-cement fill. *Journal of Performance of Constructed Facilities*, 31(4), 04017022.
- Yalcin A, Reis S, Aydinoglu AC, Yomralioglu T (2011) A GIS-based comparative study of frequency ratio, analytical hierarchy process, bivariate statistics and logistics regression methods for landslide susceptibility mapping in Trabzon, NE Turkey. *Catena* 85(3):274–287
- Zavadskas, E. K., Turskis, Z., & Kildienė, S. (2014). State of art surveys of overviews on MCDM/MADM methods. *Technological and economic development of economy*, 20(1), 165-179.
- Zhang, S., Zhao, L., Delgado-Tellez, R., & Bao, H. (2018). A physics-based probabilistic forecasting model for rainfall-induced shallow landslides at regional scale. *Natural Hazards and Earth System Sciences*, 18(3), 969-982.

- Zimmermann, M., Bichsel, M., & Kienholz, H. (1986). Mountain hazards mapping in the Khumbu Himal, Nepal. *Mountain Research and Development*, 29-40.
- Zou, Z. H., Yi, Y., & Sun, J. N. (2006). Entropy method for determination of weight of evaluating indicators in fuzzy synthetic evaluation for water quality assessment. *Journal of Environmental sciences*, 18(5), 1020-1023.
- Zuazo, V. H. D., & Pleguezuelo, C. R. R. (2009). Soil-erosion and runoff prevention by plant covers: a review. In *Sustainable agriculture* (pp. 785-811). Springer, Dordrecht.